SEMMELWEIS EGYETEM

DOKTORI ISKOLA

Ph.D. értekezések

3173.

PATTHY ÁGOSTON JÓZSEF

Neuromorfológia és sejtbiológia

című program

Programvezető: Dr. Alpár Alán, egyetemi tanár

Témavezető: Dr. Alpár Alán, egyetemi tanár

CANNABINOID RECEPTOR TYPE 1 IN THE HUMAN FOETAL BRAIN AND ITS CHANGES IN DOWN'S SYNDROME

PhD thesis

Ágoston Patthy, MD

János Szentágothai Doctoral School of Neurosciences

Semmelweis University

Supervisor:	Alán Alpár, MD, D.Sc
Official reviewers:	András Birinyi, med. habil. Tamás Marton, MD, Ph.D
Head of the Complex Examination Committee:	Árpád Dobolyi, D.Sc
Members of the Complex Examination Committee:	Erik Hrabovszky, MD, D.Sc Tibor Kovács, MD, med. habil.

Budapest
2024

Table of Contents

List of Abbreviations

Δ^9-THC - Δ^9–tetrahydrocannabinol

2-AG - 2-arachidonoyl glycerol

ABHD 6/12 - alpha/beta hydrolase 6 or 12

AC - adenylyl cyclase

AEA - anandamide

ALS - amyotrophic lateral sclerosis

BDNF - brain-derived neurotrophic factor

BRCA1 - breast cancer type 1 susceptibility protein

BSA - bovine serum albumin

cAMP - cyclic adenosine monophosphate

CB_1R - cannabinoid receptor type 1

CB_2R - cannabinoid receptor type 2

CCK - cholecystokinin

CNS - central nervous system

CP - cortical plate

Cy - carbocyanine

DAB - 3,3-diaminobenzidine-tetrahydrochloride

DAG - diacylglycerol

DAGL α/β - diacylglycerol lipase alpha or beta

DCC - deleted in colorectal cancer

DIV - day *in vitro*

DS - Down's syndrome

DSE - depolarization induced suppression of excitation

DSI - depolarization induced suppression of inhibition

eCB - endocannabinoid

ECS - endocannabinoid system

ERK1/2 - extracellular signal-regulated kinase 1/2

FAAH - fatty acid amide hydrolase

FGF-2 - fibroblast growth factor-2

FGFR - fibroblast growth factor receptor

GABA - gamma-aminobutyric acid

$G_{i/o}$ - inhibitory G proteins

GIRKs - G-protein-coupled inwardly rectifying potassium channels

GPCRs - G protein-coupled receptors

GPR55 - G protein-coupled receptor 55

HRP - horseradish peroxidase

ID - intellectual disability

iNAT - Ca^{2+}-independent N-acyltransferase

IP3 - inositol 1,4,5-trisphosphate

iPSCs - induced pluripotent stem cells

IQ - intelligence quotient

IZ - intermediate zone

JNK - c-Jun N-terminal kinase

JNK1 - c-Jun N-terminal kinase 1

LTD - eCB mediated long-term depression

MAGL - monoacylglycerol lipase

MAPK - mitogen-activated protein kinase

MRI - magnetic resonance imaging

MSE - metabotropic suppression of excitation

MSI - metabotropic suppression of inhibition

NAPE - N-acyl-phosphatidylethanolamine

NAPE-PLD - N-acyl-phosphatidylethanolamine-specific phospholipase D

NAT - N-acyltransferase

NDS - normal donkey serum

NeuN - neuronal nuclear protein

NGF - nerve growth factor

NM II - non-muscle myosin II

P2 - postnatal day 2

PB - phosphate buffer

PIP2 - phosphatidylinositol 4,5-bisphosphate

pkA - protein kinase A

PLC - phospholipase C

PPARγ - peroxisome proliferator-activated receptor gamma

REST - repressor element-1 silencing transcription factor

Rho - Ras homolog family member

ROCK - Rho-associated, coiled coil-containing kinase

ROI - region of interest

s.e.m. - standard error of mean

SCG10 - Superior cervical ganglion 10 or stathmin-2

SVZ - subventricular zone

TrkA - tropomyosin receptor kinase A

TrkB - tropomyosin receptor kinase B

TRPV1 - transient receptor potential cation channel subfamily V member 1

VGCCs - voltage-gated calcium channels

VZ - ventricular zone

1. Introduction

1.1. The endocannabinoid system. Cannabinoid receptor type 1 and its enzymatic machinery

The development of the central nervous system (CNS), the formation of proper connections between neurons and the establishment of neural circuitries in the prenatal brain are regulated by the coordinated operation of multiple factors and signaling systems, acting in sensitive time windows. In the past few decades several ligand-receptor families involved in these processes have been characterized, often with distant functions in the postnatal brain. Signaling modules that play pivotal role during brain development by controlling cellular positioning, axonal pathfinding and presynaptic differentiation may also play key roles in tuning synaptic activity at mature synapses [1].

Amongst these signaling units, the endocannabinoid system (ECS) gained significant attention due to its growing prospects as potential pharmacological target in treating various forms of neurological disorders and its vulnerability to illicit (plant-derived or synthetic) drugs [2, 3]. Historically, the identification of the major psychoactive constituent of the plant *Cannabis sativa*, Δ^9-tetrahydrocannabinol (Δ^9-THC, an exogenous cannabinoid) [4] initiated the consecutive discoveries of the three main components of the ECS: first, the cannabinoid receptors, next their endogenous cannabinoid ligands (termed endocannabinoids) and subsequently the metabolic apparatus responsible for the biosynthesis and degradation of these compounds [3, 5].

Endocannabinoids (eCBs) are small bioactive lipids, with N-arachidonoyl ethanolamine or anandamide (AEA) and 2-arachidonoyl glycerol (2-AG) being the most studied and pharmacologically best characterized molecules [6-8]. Both compounds are derivatives of arachidonic acid [9]. In addition to 2-AG and AEA, various other structurally related molecules (e.g., N-arachidonoyl dopamine) were shown to produce endocannabinoid-like effects [10] and even peptides (e.g., hemopressin) interacting with cannabinoid receptors have been identified [11]. 2-AG is thought to behave as a full agonist at both cannabinoid receptor type 1 (CB_1R) and type 2 (CB_2R) with moderate affinity, whereas AEA is a CB_1R-selective partial agonist with high affinity [12]. Apart from their actions on 'classical' cannabinoid receptors, both 2-AG and AEA are capable of modulating several other ion channels, transmembrane and nuclear receptors (e.g., transient receptor potential cation channel subfamily V member 1 (TRPV1), G protein coupled-receptor 55 (GPR55),

peroxisome proliferator-activated receptor gamma (PPARγ)), allowing for many interactions between the ECS and other signaling systems [13].

Regarding the production of these eCBs, the prevailing view is that the dominant form of synthesis is 'on demand', meaning that eCBs exist as phospholipid precursors in the inner leaflet of the cell membrane and upon a certain signal (e.g. a rise in intracellular calcium, activation of G proteins) the activated enzymatic machinery release the eCBs in a very accurate spatial and temporal manner [14]. In spite of the similarities in origin and structure, the main synthetic and degradation pathways of 2-AG and AEA are different. The canonical pathway for 2-AG biosynthesis starts with the hydrolysis of phosphatidylinositol 4,5-bisphosphate (PIP2) by phospholipase C (PLC), resulting in the formation of inositol 1,4,5-trisphosphate (IP3) and diacylglycerol (DAG) [15, 16]. Subsequently, diacylglycerol lipase alpha or beta (DAGL α/β) creates 2-AG by removing the acyl group in the 1 position from DAG [16]. The most relevant biosynthetic pathway of AEA begins with the formation of N-acyl-phosphatidylethanolamine (NAPE) by Ca^{2+}-dependent or independent N-acyltransferases (NAT/iNAT), followed by the hydrolysis of NAPE by a NAPE-specific phospholipase D (NAPE-PLD) [17]. Several alternative synthetic pathways exist with varying degrees of importance in different tissues and developmental stages. It should be noted that the level of 2-AG in the developing CNS is generally about 1000 times higher than the level of AEA (the magnitude of the concentrations are nmol/g for 2-AG and pmol/g for AEA, respectively) although there may be differences between brain areas [18, 19].

The exact mechanisms underlying the intracellular, transmembrane and extracellular transport of eCBs are not yet fully understood and are the subject of extensive research. To date, there are two main theories on the membrane transport of eCBs: simple diffusion (based upon the observations that uncharged signal lipids can spread across and within biological membranes, and the kinetics of eCB uptake seems to be non-saturable) and facilitated diffusion by a putative eCB membrane transporter (underpinned by the results that structural eCB analogs can inhibit eCB transport), although other mechanisms, like synuclein dependent vesicular exocytosis, have also been described [20, 21]. The possibility that eCBs act by volumetric diffusion means that eCB signals could have a substantial impact during intrauterine brain development, when neuronal polarisation and morphogenesis rest on a >1,000-fold expansion of the membrane surface in each

neuroblast and when the brain is yet devoid of astroglial or oligodendroglial limiting cellular barriers [6]. Despite the incomplete glial map of the prenatal brain, diffusible lipids can instead be spatially confined by recruitment of the enzymatic machinery that limits their availability [22, 23].

Endocannabinoid signaling can be terminated by hydrolysis or oxidation. In the CNS, the hydrolysis of 2-AG into arachidonic acid and glycerol is catalyzed primarily by the enzyme monoacylglycerol lipase (MAGL), which is responsible for the degradation of about 85% of 2-AG. The remaining 15% of brain 2-AG hydrolase activity is mainly attributed to the enzymes alpha/beta hydrolase 6 and 12 (ABHD6/12). Termination of AEA action is primarily carried out by the enzyme fatty acid amide hydrolase (FAAH), resulting in arachidonic acid and ethanolamine [24]. Oxidation by eicosanoid pathway enzymes like cyclooxygenase-2 or lipoxygenases serves as an additional mechanism to cease eCB signaling [25].

The best characterized cannabinoid receptors are cannabinoid receptor type 1 (CB_1R) and type 2 (CB_2R) [26, 27]. Both receptors belong to the superfamily of seven-transmembrane domain, G protein-coupled receptors (GPCRs). Based on shared cannabinoid ligands, the orphan GPCR GPR55 has emerged as a putative cannabinoid receptor 'type 3' [28].

CB_1R is encoded by the gene *CNR1*, located on the long arm of human chromosome 6. Though controversy exists, some polymorphisms of the *CNR1* gene have been associated with certain neuropsychiatric illnesses, such as hebephrenic schizophrenia or childhood attention deficit/hyperactivity disorder. In humans, the full-length CB_1R consists of 472 amino-acids, however two different isoforms with shorter N-terminus, resulting from alternative splicing, have also been described [29-32]. The CB_1R is considered as one of the most abundant GPCR in the adult brain, expressed in many areas at different levels [33]. Thanks to the numerous immunohistochemical, autoradiographic and in situ hybridization studies, we have a detailed map about the anatomical distribution of the CB_1R in the mature CNS [33-35]. High level of expression can be observed in the allocortical areas including the hippocampal formation, entorhinal cortex, amygdaloid complex and the olfactory bulb [36]. Neocortical areas are also enriched in CB_1Rs, especially in the associational cortical regions of the frontal lobe and the cingulate gyrus; primary cortical regions (e.g. primary visual, primary motor cortex) show lower densities of CB_1Rs [37]. At the population level, both in the allo- and neocortical areas, the majority

of the CB_1Rs are located on the axon terminals of cholecystokinin (CCK) expressing gamma-aminobutyric acidergic (GABAergic) interneurons [38]. To a lesser extent, yet at functionally important level, CB_1Rs are present on other neuron populations, like glutamatergic pyramidal neurons [39]. In the cerebellum, the molecular layer exhibits the greatest protein expression, corresponding to the axon terminals of the parallel fibers, climbing fibers and basket cells [40]. Amongst the basal ganglia, particularly high level of expession can be found in the globus pallidus and the substantia nigra pars reticulata. Structures with relatively low levels of CB_1Rs include the thalamus, hypothalamus, brainstem (apart from structures related to emesis, e.g., the area postrema) and the spinal cord (except for regions associated with analgesia) [41]. Despite the low CB_1R density in the hypothalamus, hypothalamic CB_1Rs are strongly coupled to G proteins [42] to efficiently regulate multiple neuroendocrine processes, including the stress response and reproductive function [43, 44].

During the foetal life period, although in smaller quantities, CB_1Rs can already be found in the hippocampus, neocortex, basal ganglia and cerebellum [6, 45]. However, during prenatal development functional CB_1Rs are transiently expressed in white matter areas that show little or no expression in the adult CNS. These structures involve the internal capsule, corpus callosum, hippocampal fimbria, fornix, anterior commissure, stria terminalis, the corticofugal axons coursing in the intermediate zone (IZ) of the developing cortex and even the pyramidal tract [45, 46]. Initially, it was suggested that these receptors are expressed on glial cells (astrocytes, oligodendrocytes), but later it was proven that white matter area CB_1Rs are mainly localized to the axons of projection neurons, more precisely to the axolemma and to intra-axonal endosomal organelles [47]. Thus, a striking difference is that postnatally the major neuronal population expressing CB_1Rs are GABAergic interneurons, whereas prenatally axons of glutamatergic projection neurons carry a significant amount of CB_1R. This difference in localisation highlights the divergent roles of the ECS in the mature and developing CNS.

In the adult CNS, neuronal CB_1Rs are primarily coupled to inhibitory G proteins ($G_{i/o}$), and upon agonist ligand binding engage signaling pathways associated with $G_{i/o}$ [48]. Receptor activation leads to the inhibition of the enzyme adenylyl cyclase (AC) thus decreasing the intracellular formation of cyclic adenosine monophosphate (cAMP) and the activity of protein kinase A (pkA). CB_1R stimulation, likely via the βγ subunits of the

heterotrimeric G protein, also leads to the activation of G-protein-coupled inwardly rectifying potassium channels (GIRKs) and to the suppression of calcium influx via the inhibition of several types of voltage-gated calcium channels (VGCCs). These signaling events seem to be crucial in the eCB mediated control of synaptic plasticity in the mature CNS (see below) [48, 49]. Depending on the cell type and stimulation conditions, 'atypical' coupling with other G-protein subtypes occur. In cultured striatal neurons, when activated simultaneously with D_2 dopamine receptors, CB_1R triggered cAMP production by coupling to G_s proteins [50]. In hippocampal astrocytes a $G_{q/11}$ coupled form has been reported, and its activation led to an increase in intracellular Ca^{2+} levels in a PLC dependent manner and triggered astrocytic glutamate release [51]. Under developmental circumstances, neuronal CB_1Rs can couple to $G_{12/13}$ proteins with particular impact on cytoskeletal stability and neuronal morphology. In cultured embryonic hippocampal neurons CB_1R activation led to the contraction of the actomyosin cytoskeleton triggering the retraction of the actin-rich growth cone of the distal axon segment. The underlying signaling pathway downstream of the CB_1R and heterotrimeric $G_{12/13}$ proteins involved a Rho-GTPase, the Rho-associated, coiled coil-containing kinase (ROCK), and ultimately the motor protein with actin filament cross-linking properties, non-muscle myosin II (NM II)[52].

Members of the mitogen-activated protein kinase (MAPK) family, such as the extracellular signal-regulated kinase 1/2 (ERK 1/2), p38 MAPK and c-Jun N-terminal kinase (JNK) are often associated with cannabinoid signalling, as CB_1R stimulation is followed by ERK 1/2, p38 MAPK and JNK activation in multiple cell types [53]. From a neurodevelopmental perspective, the CB_1R triggered JNK signalling has become the subject of particular interest, due to its direct influence on neuritogenesis. Following CB_1R stimulation, the phosphorylation of JNK1 (the brain specific JNK isoform) negatively regulates the availability of the microtubule-binding protein Superior cervical ganglion 10 (SCG10)/stathmin-2, as JNK1 promotes the proteosomal degradation of SCG10 [54, 55]. SCG10 is a neuron specific protein expressed only during axonal growth and guidance, and its main function to provide microtubule 'dynamic instability', a property indispensable for continuous microtubule reorganization and thus for neurite elongation and directional growth [56]. The developmental interplay between the CB_1R and SCG10 is further supported by their anatomical co-distribution and close proximity

in developing corticofugal projections [55]. It seems clear from the aforementioned molecular pathways, that during foetal development CB_1R signalling can affect both the filamentous-actin and the microtubule networks, the major polymers that compose the cytoskeleton.

Another aspect of CB_1R signalling that is relevant to the development of the nervous system, is its interplay with growth factor and neurotrophin signalling at multiple levels. In cerebellar granule neurons, brain-derived neurotrophic factor (BDNF) increases the expression of CB_1R transcripts and neuronal sensitivity to eCBs [57]. Reciprocally, CB_1R knockout mice show decreased BDNF levels in the hippocampus [58]. In addition, CB_1Rs are able to trans-activate multiple growth factor receptors with tyrosine kinase activity; among these, the Src kinase-dependent tropomyosin receptor kinase B (TrkB) receptor transactivation seems particularly interesting, as it may infulance the migration of CCK-expressing interneurons and thus proper interneuron placement during corticogenesis [59]. CB_1R can also be a downstream effector of neurotrophin signalling: in cerebellar granule neurons, activation of the fibroblast growth factor receptor (FGFR) by N-cadherin/fibroblast growth factor-2 (FGF-2) promote neurite outgrowth via DAGL activation, 2-AG generation and cell-autonomous action on CB_1Rs [60].

Finally it should be noted that several molecular interactions between the ECS and other ligand/receptor families known to be involved in axonal growth and guidance have been identified. In the developing visual system, CB_1Rs can limit the availability of the adhesion molecule deleted in colorectal cancer (DCC) – a receptor for the axonal guidance molecule netrin-1 – impacting growth cone behavior [61]. Likewise, during cortical development, eCBs can configure Slit2/Robo1 signalling to modulate axonal patterns, as 2-AG increases the amount of Robo1 expressed on the axonal growth cone via the CB_1R and also the level of its ligand Slit2 – a chemorepellent protein produced by oligodendroglia – via the CB_2R [62].

1.2. Physiological functions of the ECS and the CB_1R in the mature and developing brain

The evolutionarily conserved ECS is a widespread homeostatic regulatory system, present in various tissues and involved in numerous physiological and pathological processes. A functional ECS is operative throughout the whole ontogenesis, already in

the preimplantation embryo and the pregnant uterus [63]. Given the psychoactive effects of phytocannabinoids and the characterization of the ’brain cannabinoid receptor’ CB_1R in 1990 [64], the main line of cannabinoid research focused on the neuromodulatory effects of the ECS, although several studies pointed out the significance of ’peripheral’ cannabinoid actions [65].

The physiological roles of the ECS and the CB_1R in the mature CNS are relatively well characterized. Through so-called retrograde signalling, they regulate transient and long-lasting forms of synaptic plasticity. During retrograde transmission, eCBs synthesized by the postsynaptic neuron travel ’backwards’ in the synapse to stimulate presynaptic CB_1Rs. Three basic forms of retrograde eCB signalling mediated synaptic plasticity have been described. These are termed (i) depolarization induced suppression of inhibition / excitation (DSI/DSE), (ii) metabotropic suppression of inhibition / excitation (MSI/MSE) and (iii) eCB mediated long-term depression (LTD) [1, 66]. In DSI/DSE, the depolarization of the postsynaptic neuron induces eCB production that stimulates presynaptic CB_1Rs on inhibitory or excitatory afferents, leading to a decrease in inhibitory (DSI) or excitatory (DSE) neurotransmission. MSI/MSE indicates similar processes, with the difference that here eCB formation is triggered by the activation of postsynaptic $G_{q/11}$-linked receptors (e.g., group I metabotropic glutamate receptors). 2-AG seems to be the primary eCB required for retrograde signalling, synthesized by postsynaptic, membrane-bound DAGLα. The reduction in presynaptic neurotransmitter release following CB_1R stimulation is mainly attributed to the $G_{i/o}$ mediated inhibition of VGCCs and activation of GIRKs, resulting in the suppression of presynaptic calcium influx. 2-AG action is largely terminated by presynaptic MAGLs. DSI/DSE and MSI/MSE are considered to be different forms of eCB-mediated ’short term depression’, where the decrease in the excitatory or inhibitory neurotransmitter release typically lasts less then a minute. In eCB mediated LTD, which can occur during repetitive, low-frequency stimulation of excitatory synapses, the decrease in neurotransmitter release can last more than an hour. Here, for long term plasticity, the principal mechanism requires $G_{i/o}$ mediated AC inhibition, and thus the downregulation of the cAMP/pkA pathway [48, 67].

Non-retrograde forms of eCB mediated synaptic plasticity have also been observed. In the process termed ’slow self inhibition’, repetitive depolarization of a neuron facilitates

2-AG production, which activates CB_1Rs on the same cell, that by opening GIRK channels hyperpolarizes the membrane potential and inhibits neuronal firing. In this case, 2-AG acts in an autocrine fashion, at the site of its own formation [68, 69]. In summary, a fundamental and extensively studied physiological function of the ECS in the adult CNS is the regulation of neuronal excitability and the strength of synaptic connections.

In addition to its neuromodulatory role at established adult synapses, research over the past 20 years has identified the ECS and the CB_1R as a key signalling unit involved in the development of the CNS. eCBs influence brain development at multiple levels as they participate in almost every developmental step during the formation of the cerebral cortex **(Fig. 1)**. These include neural stem cell proliferation in the progenitor zones **(Fig. 1A**), neuron versus glia fate decision **(Fig. 1B**), migration of the neural cell progeny to their final positions **(Fig. 1C**) and once they reached the proper location in the developing cortex, neuronal polarisation, axonal growth, pathfinding and fasciculation **(Fig. 1D, E**) [70]. The widespread nature of eCB action throughout corticogenesis implicates that during foetal life, manipulation of the ECS through exogenous cannabinoids (e.g., maternal cannabis smoking during pregnancy) could have a detrimental impact on the developing brain, and may predispose the affected offspring to neuropsychiatric illnesses [2].

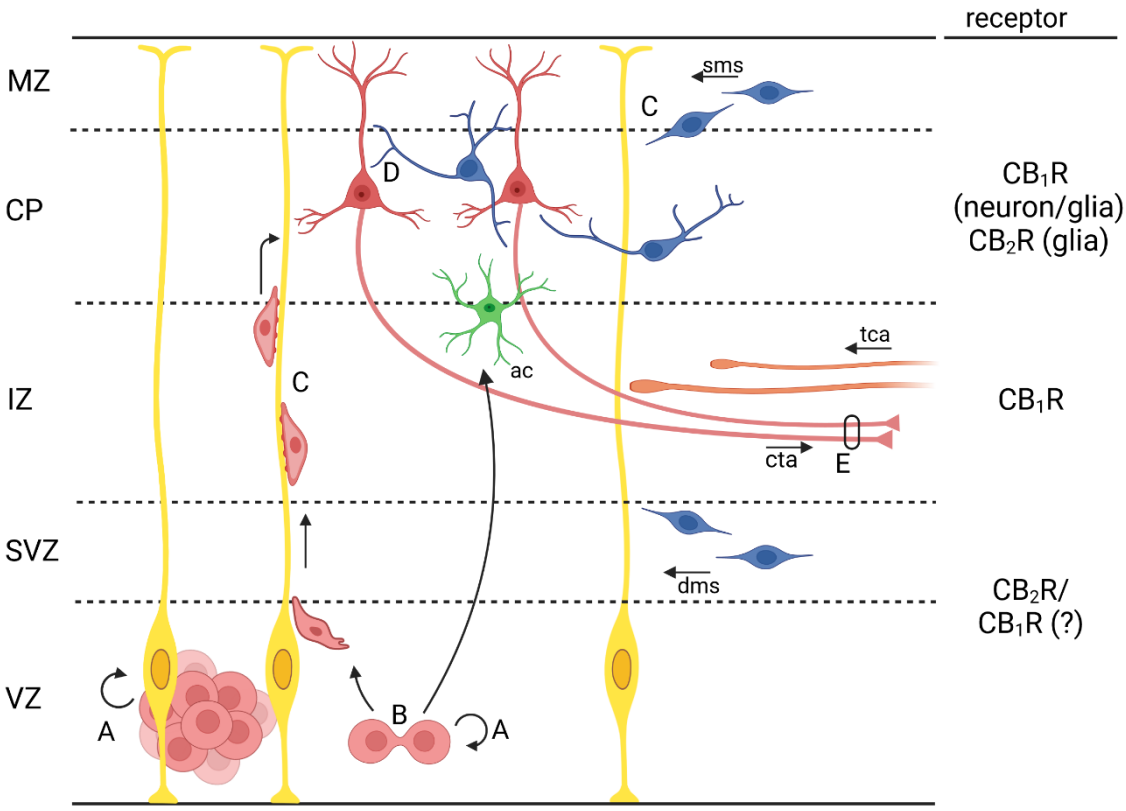

Figure 1. The widespread nature of endocannabinoid actions through corticogenesis. Modified after Harkany et al. 2008 [1]. During the development of the cerebral cortex, eCB signals regulate neural progenitor proliferation **(A)** [71-73] and lineage commitment **(B)** [74] in the cortical proliferative zones. Here, based on recent findings, CB_2R appears to be the primary cannabinoid receptor [75]. Upon neuronal commitment, up-regulation of CB_1R expression occurs, which is indispensable for the proper migration of both radially migrating postmitotic pyramidal cells and tangentially migrating immature interneurons **(C)** [59, 72, 76]. Finally, eCBs through the CB_1R control the postsynaptic target selection of both intracortical and long-range axons, as well as the formation of axon bundles, termed fasciculation **(D, E)** [52, 72, 77, 78]. *Abbreviations*: MZ, marginal zone; CP, cortical plate; IZ, intermediate zone; SVZ, subventricular zone; VZ, ventricular zone; sms/dms, superficial/deep migratory stream; ac, astrocyte; tca, thalamocortical axons; cta, corticothalamic axons; CB_1R/CB_2R, cannabinoid receptor type 1/type 2.

The effect of eCBs and the CB_1R on the number, division rate and lineage commitment of neural stem cells was examined both *in vitro* and *in vivo*. In rodent models, cultured embryonic neural progenitor cells have the ability to produce eCBs, express the CB_1R and the AEA inactivating enzyme FAAH. Pharmacological CB_1R stimulation enhances progenitor proliferation and neurosphere generation likely via the sequential activation of $G_{i/o}$ proteins and ERK signaling. Consistently, application of the CB_1R inverse agonist rimonabant lead to a decrease in progenitor proliferation [71, 73]. CB_1R knock-out mice show decreased progenitor proliferation in the ventricular zone (VZ) and subventricular zone (SVZ) of the developing cortex, while elevated eCB levels in FAAH knock-out mice significantly increase the proliferation of VZ/SVZ progenitors [72]. Interestingly, in another series of experiments, *in vitro* CB_1R activation on postnatal mouse neural progenitor cells promoted not only progenitor proliferation but differentiation into astroglial cells as well, and accordingly, hippocampal astrogliogenesis was impaired in CB_1R-deficient mice and enhanced in FAAH-deficient mice *in vivo* [74]. In human foetal brains, CB_1R expression was observed in the SVZ during early-mid gestation [45, 79]. These results suggest that eCBs regulate the neural progenitor cell pool expansion and differentiation in a CB_1R-dependent manner. However, neural progenitors often co-express CB_1Rs and CB_2Rs, and growing evidence indicates a predominant CB_2R expression in the SVZ of the cerebral cortex. Similarly to the CB_1R, CB_2R agonists stimulate progenitor cell proliferation, while CB_2R antagonists inhibit the proliferation of neural stem cells [75, 80]. On these basis, the CB_2R is increasingly recognized as the primary cannabinoid receptor responsible for the proliferation-promoting effect of eCBs. This notion is further supported by a recent ultrastructural analysis of the embryonic mouse and rhesus macaque cerebral cortex, that did not find credible CB_1R immunolabeling in proliferating VZ/SVZ cells [81]. Nevertheless, there is a consensus view that upon commitment to a neuronal fate, CB_1R levels become up-regulated (at the expense of CB_2Rs) [75], and modulate the directional motility for both neurons and subsequently their navigating neurites.

Postmitotic projection neurons, generated in the pallial VZ and SVZ undergo radial migration to occupy their proper position in the developing cortical plate (CP). Immature interneurons, originating from the germinative zones of the pallium and subpallium (ganglionic eminence) reach their final location by radial and tangential migration. Both

population of migrating neurons are enriched in CB_1Rs, as they contain numerous CB_1R-positive intracellular vesicles [81]. CB_1Rs turn out to be strictly required for proper migration rate and appropriate neuronal placement in the developing cortex. *In vitro*, eCBs 2-AG and AEA behave as chemoattractant cues for both newborn pyramidal neurons and interneurons, by acting through CB_1Rs [59, 76]. In organotypic cultures, application of the synthetic CB_1R agonist HU-210 or the FAAH inhibitor URB597 promotes radial cell migration from the VZ/SVZ to the superficial cortical layers, while FAAH overexpression leads to the opposite outcome. *In vivo*, CB_1R-knockout mice display a cortical migration arrest, as pyramidal cell progenitors populate the deeper cortical layers when compared to wild-type littermates examined on the same postnatal day [72]. Similarly, acute knock-down of the CB_1R selectively in radially migrating neurons (by *in utero* electroporation of siRNAs) results in reduced colonization of the embryonic CP and cell accumulation in the IZ and the VZ/SVZ. Remarkably, transient *in utero* CB_1R siRNA electroporation induces long-lasting cortical malformations (subcortical pyramidal neuron accumulation even in the late postnatal age) and increase seizure susceptibility in adulthood. An identified molecular mechanism behind the CB_1R-elicited promigratory effect is the modulation of the cytoskeleton-regulating small GTPase RhoA, as CB_1R signaling promotes the proteasomal degradation of this protein in newborn pyramidal neurons [76]. Proper interneuron placement also seems to be influenced by eCB actions: in rats, prenatal exposition to Δ^9-THC (a partial CB_1R agonist) causes aberrant patterning of CCK/CB_1R-expressing interneurons in the early postnatal hippocampus, likely by interfering with physiological eCB signals [59].

Once neuronal migration is complete and the immature neurons have reached their final location in the developing cortex, they start to form composite neuronal networks. Growing axons traverse an extremely complex tissue microenvironment, often over long distances, to reach their appropriate postsynaptic partner. At the tip of extending axons, there are actin-rich protuberances called growth cones. Growth cones are highly specialized and motile structures that explore and sense the attractive or repulsive cues distributed along a concentration gradient in the extracellular environment and use these navigational signals to determine the direction of growth and control axonal elongation [82]. Multiple identified axon guidance systems exist (e.g., Slits and their Robo receptors,

netrins and their DCC and UNC5 receptors, semaphorins and their neuropilin receptors [83]) and the ECS recently emerged as such a signaling unit.

As mentioned before, in the adult brain, CB_1R expression on glutamatergic axon terminals is relatively low compared to GABAergic terminals. In contrast, during cortical development, glutamatergic projection neurons express high levels of CB_1Rs distributed along the axon shafts and growth cones. This is reflected by the intense CB_1R immunoreactivity of developing fiber tracts, such as the corpus callosum, fimbria hippocampi, fornix or the individual corticofugal fibers traversing the IZ [72]. Postnatally, CB_1R expression of projection neurons gradually decreases [47]. Not only CB_1Rs but also the enzymatic machinery required for eCB metabolism is present on growing axons, as both the major 2-AG synthesizing enzyme DAGLα/β and the primary 2-AG degrading enzyme MAGL are expressed by corticofugal projections. The subcellular recruitment of these enzymes is mutually exclusive, with MAGL accumulating in the proximal, stabilising axon segment, while DAGLα/β accumulates in the distal, motile neurite segment, including the growth cone [22]. Remarkably, the spatial segregation of MAGL is tuned by neurotrophin signalling, as nerve growth factor (NGF) – acting through tropomyosin receptor kinase A (TrkA) and breast cancer type 1 susceptibility protein (BRCA1) – induces the proteasomal degradation of MAGL in the growth cone, making DAGLα/β generated 2-AG available for axonal CB_1Rs [84]. This subcellular distribution is substantially different from what is present in the mature CNS. Indeed, upon synapse formation, a molecular reconfiguration occurs, as DAGLs become selectively enriched in the somatodendritic compartment, while MAGLs assume a presynaptic position [75]. Thus, ECS components are well positioned to control neural circuit wiring during development, and retrograde signaling once proper synaptic connections are established.

The available *in vitro* data regarding the exact effect of CB_1R activation on axon outgrowth is somewhat controversial. Multiple studies reported repulsive growth cone turning and eventual collapse upon CB_1R stimulation in cortical neurons [61, 77]. However, it has also been described that in immature pyramidal cells AEA induces the elongation of a leading axon and inhibits axon branching in a CB_1R-dependent manner [72]. Similarly, MAGL inhibition (and thus elevation of 2-AG levels) promotes the elongation of the primary neurite of cortical neurons [22]. One possible explanation to

resolve the discrepancy is that in developing neural networks, 2-AG produced by axonal DAGLs activates CB_1Rs on the same axon (in an autocrine way) or on adjacent axons (in a paracrine way), leading to repeated cycles of repulsion-alternative pathfinding responses, ultimately resulting in net neurite elongation [75].

In vivo, complete or conditional CB_1R-knockout mice lacking CB_1Rs selectively in cortical glutamatergic neurons exhibit fasciculation deficits and impaired axonal targeting. Notably, in these animals, scattered, abnormally large axon bundles (fascicles) can be observed in the corpus callosum and in the corticothalamic and thalamocortical projections. Further, corticofugal axons fail to invade the dorsal striatum, and the number of misrouted thalamocortical axons is increased [72, 78]. Similarly, *in utero* intra-cerebroventricular injection of rat embryos with CB_1R antagonist increases the number of mistargeted corticofugal axons, as they also invade the cortical SVZ, a region from which corticofugal projections are usually excluded [52]. However, the exact functional consequences of these anatomical abnormalities remain to be determined.

Immature GABAergic interneurons also express CB_1Rs on their axons and axonal growth cones during late gestation, but GABAergic axons lack 2-AG synthesizing capacity. *In vitro* CB_1R stimulation elicits chemorepulsion and axonal growth cone collapse by the sequential signaling events of RhoA and ROCK activation, myosin light chain phosphorylation and actin cytoskeleton contraction. *In vivo*, genetic CB_1R ablation from GABAergic interneurons alters the distribution and density of inhibitory perisomatic terminals on pyramidal cells, reflecting impaired postsynaptic target selection [77].

Taken together, a growing body of *in vitro* and *in vivo* evidence supports that the ECS via CB_1Rs actively participates in the control of axon growth, intracortical and long-range axon patterning and bundle formation of axons with similar growth trajectories.

It is well known that prenatal cannabis exposure can increase the risk for drug seeking behavior, cognitive deficit, attention deficit, anxiety and depression among affected offspring [2]. Upon marijuana smoking during pregnancy, Δ^9-THC effectively passes through the placental barrier and could interfere with physiological eCB signaling in the developing brain, either as a partial agonist, or – in the presence of a full agonist like 2-AG – as a functional antagonist at CB_1Rs [23, 70]. In rodent models, prenatal exposure to Δ^9-THC leads to the redistribution of CB_1R-expressing inputs in both the neocortex and hippocampus and reshapes the coalescing of corticofugal axons (a phenotype

reminiscent of what is seen in CB_1R-knockout animals), while *in vitro*, Δ^9-THC diminishes neurite outgrowth in cortical neurons [55]. The Δ^9-THC induced wiring deficits can be traced back to the previously mentioned microtubule-binding protein SCG10/stathmin-2, a protein co-distributed with CB_1Rs in growth cone-like structures of corticofugal axons. In human foetal cortices exposed to cannabis *in utero*, SCG10 expression is significantly decreased, as Δ^9-THC triggers CB_1R-mediated rapid axonal breakdown of SCG10 through its phosphorylation by JNK1, and subsequent proteosomal degradation. The loss of SCG10 results in excess microtubule stability and tubulin aging, leading to axonal growth and guidance errors. These results raise the possibility that the increased incidence of neuropsychiatric disorders upon *in utero* cannabis exposure might also be due, at least in part, to CB_1R-mediated altered developmental synaptic organization [85].

1.3. Neurodevelopmental aspects of Down's syndrome, and the possible connection between the ECS and Down's syndrome

Down's syndrome (DS), caused by partial or complate triplication of human chromosome 21, is the most common genetically determined neurodevelopmental disorder, occuring in about 1 of every 800 live births [86]. DS is a complex, devastating disorder affecting multiple organ systems and can be associated with congenital cardiac and gastrointestinal malformations, craniofacial and skeletal anomalies and increased incidence of certain childhood leukemias. The most penetrant hallmark of DS is intellectual disability (ID), as all patients suffering from DS have some degree of ID, ranging from moderate to severe, with a median intelligence quotient (IQ) around 40. Deficits are prevailing in executive functioning (e.g., attention, planning and organization) and in short-term and long-term declarative memory [87, 88]. Epilepsy is also a highly prevalent comorbidity of DS [89].

According to the post-mortem and magnetic resonance imaging (MRI) analyses of brains affected by DS, DS patients exhibit an overall reduced brain size, particularly in the cerebral cortical hemispheres, hippocampal formation and cerebellum [90-92]. These anatomical changes are already present at birth, indicating an early onset during foetal development [93]. Indeed, the neuropathological consequences of DS can be observed in the neocortex, hippocampal region and cerebellum already in the second trimester. In

foeti with DS, cell proliferation in the neocortical germinal matrix is decreased and the total cell number of the forebrain is reduced [94, 95]. Neocortical areas show a higher percentage of astrocytes, together with an increased proportion of cells expressing GABAergic interneuron markers [96, 97]. In addition to the presumably defunct neurogenesis, the emergence of cortical lamination is delayed and desorganized, cortical pyramidal cells possess smaller dendritic arborizations and the cortical level of proteins marking dendritic spines and synaptosomal stuctures is significantly lower, indicating impaired circuit formation and synaptogenesis [98-100]. Many of the neocortical abnormalities can also be detected in the hippocampus and dentate gyrus: progenitor cell proliferation and total cell number are reduced and the proportion of cells with astrocytic and inhibitory interneuron phenotypes are higher [96, 101]. Impaired progenitor proliferation and hypocellularity are also evident in the developing cerebellum of foeti with DS [102]. In sum, based on the available data obtained from human foetal brain tissue, CNS development in DS is characterised by diminished neurogenesis, an imbalance of the projection neuron/interneuron ratio, dendritic deterioration and astrogliosis **(Fig. 2).**

To identify the mechanisms underlying the developmental changes in DS and to provide a tractable approach for designing and testing potential therapeutic strategies, multiple genetically heterogenous mouse models have been developed. Many of these mouse models take advantage of the homology between human chromosome 21 and the distal portion of mouse chromosome 16. The most widely used and therefore best characterized model of DS is the $Ts65Dn^{+/+}$ mouse, that carries and extra copy of a large part of the mouse chromosome 16, resulting in trisomy of around 90 conserved protein-coding gene orthologues to the human chromosome 21. Postnatally, $Ts65Dn^{+/+}$ mice exhibit several features and behavioural abnormalities associated with DS (e.g., cranifacial dysmorphology, learning and memory deficits), while prenatally, they recapitulate a number of neurodevelopmental phenotypes found in human studies [88, 103]. Examination of mouse models has revealed additional details about the pathological neurodevelopmental events that may be present in the human foetal DS brain as well **(Fig. 2)**.

In the dorsal telencephalic VZ of $Ts65Dn^{+/+}$ mice, the cell cycle duration is longer, leading to an overall reduced production of excitatory neurons. Moreover, the

commitment of the newly generated neurons is delayed and they do not migrate as quickly towards the superficial cortical layers as their euploid counterparts. The delayed differentiation and arrival of excitatory neurons also affects the development of axonal tracts in the white matter, mirrored by a thinner IZ when compared to euploid controls of the same age [87, 104]. In contrast to the under-production of excitatory neurons, the numbers of parvalbumin and somatostatin expressing interneurons in the neocortex and hippocampus are increased, resulting from the elevated precursor proliferation in the ganglionic eminence of the embryonic ventral telencephalon [105]. The functional consequence of the altered excitatory/inhibitory neuron ratio is the over-inhibiton of the $Ts65Dn^{+/+}$ forebrain. This developmentally established imbalance may be partly responsible for the cognitive dysfunction, as pharmacological blockade of inhibitory GABAergic neurotransmission in adult $Ts65Dn^{+/+}$ mice improves spatial orientation and related learning processes [106].

The alterations and delays in neurogenesis may set the stage for subsequent defects in synapse formation, or there is a possibility that intracortical and long-range axon patterning itself is also dysfunctional in trisomic state. In the Ts16 mouse model of DS (which is trisomic for the entire mouse chromosome 16) the arrival of the thalamocortical axons is hampered in the foetal neocortex [107]. In early postnatal $Ts65Dn^{+/+}$ mice, synaptic density is decreased in both the neocortex and the hippocampus, and the volume of the hippocampal commissure is significantly reduced [104, 108]. The latter differences could be explained by the lower cell numbers in the hippocampus, however *in vitro* developing hippocampal $Ts65Dn^{+/+}$ neurons display reduced axon length and number of branches per axon, as compared to neurons from their euploid littermates, suggesting that disrupted axon growth may contribute to the wiring deficits observed [108]. In support of this notion, two additional studies examining cultured neurons described reduced axon length associated with DS. One utilized induced pluripotent stem cells (iPSCs) derived from DS patients that have been differentiated into cortical GABAergic interneurons. These DS GABAergic interneurons showed decreased migration, reduced soma size, branches and neurite length *in vitro* and following their transplantation into the medial septum of mice, they exhibited impaired migration and substantially reduced axonal projection to the hippocampus (when compared to their euploid counterparts) [109]. The other employed cortical neuronal precursor cells from a human foetus with DS, and

reported a reduced average neurite length and grossly misshapen neurites in these neurons. What is particularly interesting, that in the same study, the down-regulation of repressor element-1 silencing transcription factor (REST)-regulated genes was identified, and amongst these STMN2 (the gene coding the SCG10 protein) was the topmost affected target, as STMN2/SCG10 mRNA was almost undetectable in the DS derived precursor cells [110]. This finding raises the possibility that SCG10 depletion is a key mechanism underlying axonal growth defects detected in DS. As previously mentioned, during foetal development, SCG10 expression is negatively regulated by the CB_1R and is sensitive to exogenous Δ^9-THC [55], which allows us to link DS affected molecular determinants to CB_1R regulated ones, at least in theory.

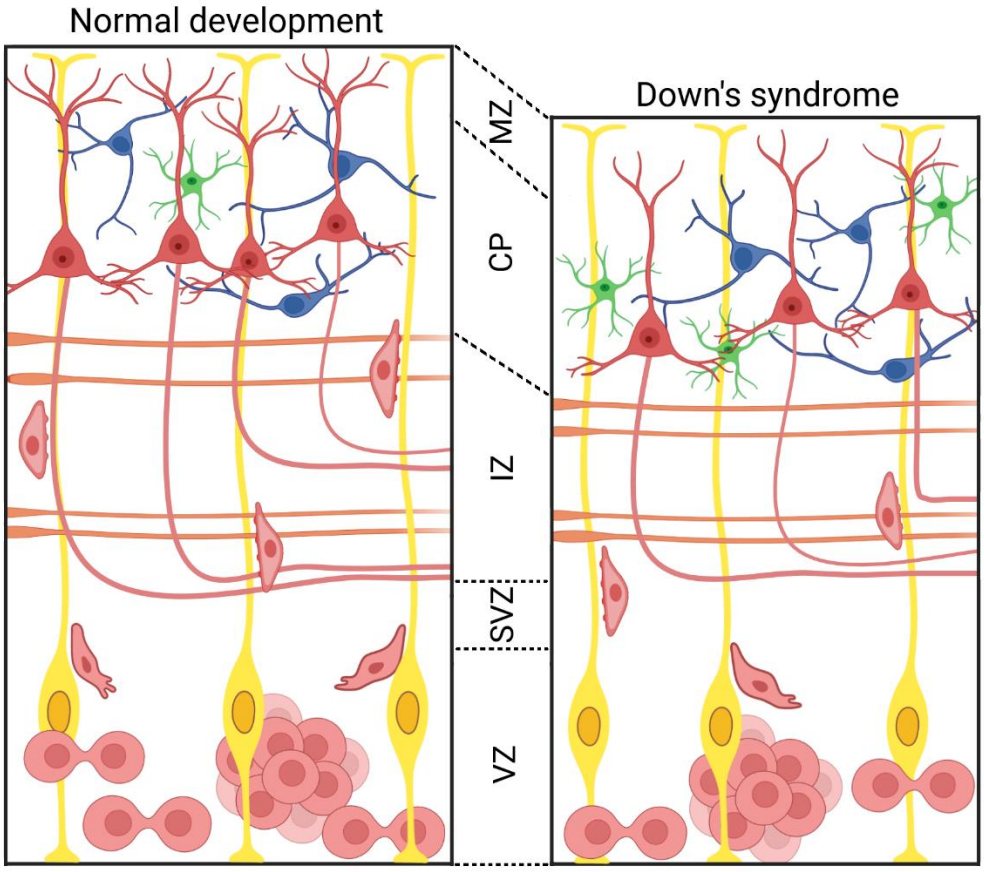

Figure 2. Developmental abnormalities during corticogenesis in Down's syndrome, based on human histopathology studies and mouse models. Modified after Haydar et al. 2012 [87]. Neocortical proliferative zones exhibit reduced cell proliferation, which, together with the increased production of interneurons in the ganglionic eminence, leads to an altered ratio of excitatory/inhibitory neurons [94, 105]. Newly generated neurons in the dorsal telencephalon show slower migration and delayed arrival, resulting in a thinner intermediate zone containing the descending and ascending cortical axon tracts [104]. Additionally, cortical pyramidal cells possess smaller dendritic arborizations and cortical synapse formation is defective [99, 100, 104]. *In vitro* results suggest that axonal growth errors may contribute to the wiring deficits observed [108-110]. Neocortical areas also display a higher percentage of astrocytes [96, 97]. *Abbreviations:* MZ, marginal zone; CP, cortical plate; IZ, intermediate zone; SVZ, subventricular zone; VZ, ventricular zone.

Despite the widespread roles of the ECS in the mature and developing nervous system, little is known about whether errant eCB signaling contributes to the pathogenesis of developmental brain disorders or if its changes are instead secondary to the evolving pattern of structural synaptic deficits. To date, only a handful of studies investigated the possible relationship between the ECS and DS, and most of these studies utilized adult mice models or in one case, human brain tissue of elderly DS subjects. In the *post-mortem* brain samples of aged DS patients, CB_1R expression was enhanced in the hippocampal formation [111], and this phenotype seems to be recapitulated by $Ts65Dn^{+/+}$ mice. More precisely, in the dorsal hippocampus of male adult $Ts65Dn^{+/+}$ mice, CB_1R expression was upregulated in GABAergic neurons, whereas it was downregulated in glutamatergic neurons [112]. In spite of the decreased CB_1R expression in hippocampal pyramidal neurons, CB_1R function was found to be increased at hippocampal excitatory terminals of young-adult $Ts65Dn^{+/+}$ mice, as CB_1R agonist WIN55,212-2 produced an enhanced inhibitory effect on the amplitude of evoked excitatory postsynaptic currents in trisomic mice compared to controls [113]. These CB_1R-related alterations could substantially aggravate the previously mentioned, developmentally established imbalance of excitatory/inhibitory neuronal circuit activity and contribute to the intellectual disability in DS. Accordingly, genetic ablation or pharmacological inhibition of the CB_1R improved cognitive performance and hippocampal synaptic plasticity in $Ts65Dn^{+/+}$ mice [113]. Based on these findings, some authors consider the CB_1R as a potential therapeutic target to mitigate cognitive deficits associated with DS, for which there is no effective treatment yet in the clinical practice.

2. Objectives

Available studies examined the involvement of the ECS in the pathobiology of DS in the light of its neuromodulatory function at adult synapses, but failed to consider the various roles of eCB signaling during the development of the CNS. Many of the diverse neurodevelopmental processes regulated by the ECS and the CB_1R appear to be pathological in DS (e.g., neurogenesis, neuronal migration, neurite growth), thus it is reasonable to hypothesize that dysfunctional eCB signaling may contribute to the developmental abnormalities observed. However, until now no relevant research has been made in this field and the participation of the ECS in DS brain development remain to be elucidated.

Therefore, the main goal of our study was to clarify whether the neuroarchitectural impairments in DS are associated with the alterations of the ECS during brain morphogenesis. To address this question, we first systematically mapped the distribution of CB_1R expression in human foetal brains with DS and in age-matched controls. We focused on brain areas known to be profoundly affected by DS: the developing neocortex, hippocampus, cerebellum and white matter tracts. Our work also aimed to provide the first detailed neuromorphological description of CB_1R expression in different brain regions during the development of the human telencephalon, as the available human data in this field is also limited. During our analysis, we sought to answer the following questions:

1. What is the morphological appearance of CB_1R^+ profiles during development and does it differ between DS and control foetal brains?
2. Is there a difference during development in the temporal appearance (and disappearance) of CB_1R^+ profiles between DS and control foetal brains?
3. Is there a quantitative difference in the expression of CB_1R^+ profiles in distinct brain areas between DS and age-matched control foetal brains?

Guided by our human neuropathological results, in the second part of our study we aimed to resolve whether CB_1R-driven molecular pathways related to neuritogenesis are affected by DS. To approach this issue, we performed *in vitro* neuropharmacology on cortical neuron cultures derived from neonatal $Ts65Dn^{+/+}$ and wild-type littermate mice, and focused on the expression of the microtubule-binding protein SCG10, which was

previously shown to be down-regulated in human foetal neuronal precursor cells with trisomy 21 [110]. During our experiments, we sought to answer the following questions:

4. Is there a difference in the subcellular distribution of the SCG10 protein between $Ts65Dn^{+/+}$ and wild-type cortical neurons?
5. How does the stimulation of CB_1Rs affect SCG10 protein availability in $Ts65Dn^{+/+}$ cortical neurons compared to wild-type cortical neurons?
6. Does CB_1R stimulation leads to a different neurite growth response in $Ts65Dn^{+/+}$ cortical neurons?

3. Methods

3.1. Human foetal tissue

We have used foetal brain samples to establish the distribution map of CB_1R of the developing human brain. For this, we made use of tissue samples which were collected by the Brain Bank of the Institute of Neurology at the Medical University of Vienna in Austria. In total, 13 male and 14 female foetal brains between gestational weeks 14–40 were processed. The sex for further 3 brains remained unknown. All these samples were acquired from abortions (spontaneous or medically-induced) without neurological disease, genetic disorders or head injury. Subsequent sampling revealed no *post-mortem* autolysis or chromosomal aberration. A further extended neuropathological investigation excluded nervous system malformations, hypoxic/ischemic encephalopathy, intraventricular haemorrhage, hydrocephalus, meningitis or ventriculitis. We acknowledged these tissue samples as controls with normal brain development.

In parallel, we diagrammed the development of CB_1Rs in foeti with Down's syndrome. For this, tissue samples from further 23 brains were used, of which 10 were males, 8 were females and no sex were identified in further 5 cases.

The acquisition and processing of brain samples were in accordance with the Declaration of Helsinki and our own institutional guidelines, including the approval for histopathology by the Human Ethical Committee of the Medical University of Vienna (No.104/2009). Anonymity of samples during investigations was maintained according to the Ethical Policy of Semmelweis University.

3.2. Preparation of brain tissues, histochemistry

Brain samples were immersion fixed in formalin and subsequently embedded in paraffin. The tissue blocks were cut at 3 μm thickness and the sections were mounted onto pre-coated glass slides (StarFrost). The samples were then deparaffinized and rehydrated, pre-treated in low-pH EnVision FLEX at 98 °C for 20 minutes (PTLink; Dako) to retrieve antigens. Sections were then incubated with a polyclonal anti-CB_1R antibody made in rabbit (gift from Ken Mackie, 1:1,000 [22]) and subsequently with a biotinylated anti-rabbit secondary antibody produced in donkey (K5007, ThermoFisher). To visualize

antibody binding, immunoprecipitation was completed by using the DAKO EnVision detection kit including peroxidase/3,3-diaminobenzidine-tetrahydrochloride (DAB; Agilent). We investigated a positive control to validate the specificity of the applied anti-CB_1R antibody: corticospinal and corticobulbar tracts contain a large amount of CB_1Rs in mammals [76]. Indeed, the axons of these tracts showed strong immunolabelling in the medulla oblongata (**Fig. 3A, A'**). To optimize orientation, sections were counterstained with haematoxylin, dehydrated in an ascending gradient of ethanol, cleared with xylene, and coverslipped with Consil-Mount (Shandon; ThermoFisher) (**Fig. 3B**).

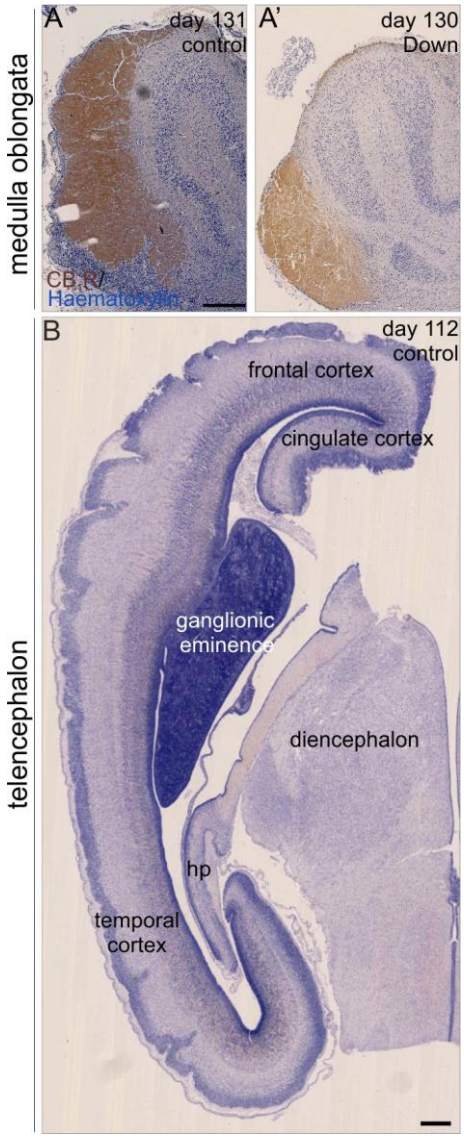

Figure 3. A, A'. CB_1R^+ pyramidal tract axons in the medulla oblongata of control and Down's syndrome subjects. **B.** Overview of a foetal forebrain section indicating the regions studied. *Abbreviations*: CB_1R, cannabinoid receptor type 1; hp, hippocampus. *Scale bars* = 1 mm. (Published in *Neuropathology and Applied Neurobiology*, 2023).

3.3. Imaging and quantification

For light microscopical investigations, representative images containing the region of interest (ROI) were automatically captured on a slide-scanner (Nikon) and exported from stored images using the NanoZoomer 2.0 plug-in (Hamamatsu). On these bright field microscopical images we performed a semi-quantitative analysis of CB_1R^+ varicosities. Their relative density was classified as: 0, +, ++, +++ or ++++. For this, CB_1R^+ varicosities were counted in regions of interest and normalized to equivalent surface areas (500 μm^2, n = 10/area/section) using the NanoZoomer 2.0 toolbox (**Fig. 4**).

For confocal laser scanning microscopy, human samples were deparaffinated, rehydrated, washed in phosphate buffer (0.1M PB; pH 7.4), and pre-treated with 0.3% Triton X-100 (Sigma; in 0.1M PB) at 22–24 °C for 2 hours to enhance antibody penetration. To suppress non-specific immunoreactivity, we incubated our samples in a mixture of 5% (wt/vol) normal donkey serum (NDS; Jackson ImmunoResearch), 2% (wt/vol) bovine serum albumin (BSA; Sigma) and 0.3% Triton X-100 in 0.1M PB at 22–24 °C for 90 minutes. Sections were then exposed to a mixture of mouse anti-neuronal nuclear protein (NeuN) and rabbit anti-CB_1R antibodies (**Table 1**) diluted in 0.1M PB, to which 0.1% NDS and 0.3% Triton X-100 had been added, at 4 °C for 72 hours. Immunoreactivities were revealed by carbocyanine (Cy) 3- or 5-tagged secondary antibodies raised in donkey (1:200; Jackson) and applied at 22–24 °C for 2 hours. Nuclei were counterstained with Hoechst 33,421 (1:10,000; Sigma). Sections were dehydrated in an ascending gradient of ethanol, cleared with xylene, and coverslipped with DePeX (ACM, Fluka). Images were captured on an LSM780 confocal laser-scanning microscope (Zeiss) with optical zoom ranging from 1–3x when using a 40x (Plan-Apochromat 40×/1.40) objective and the pinhole set to 0.5–0.7 µm ('optical thickness').

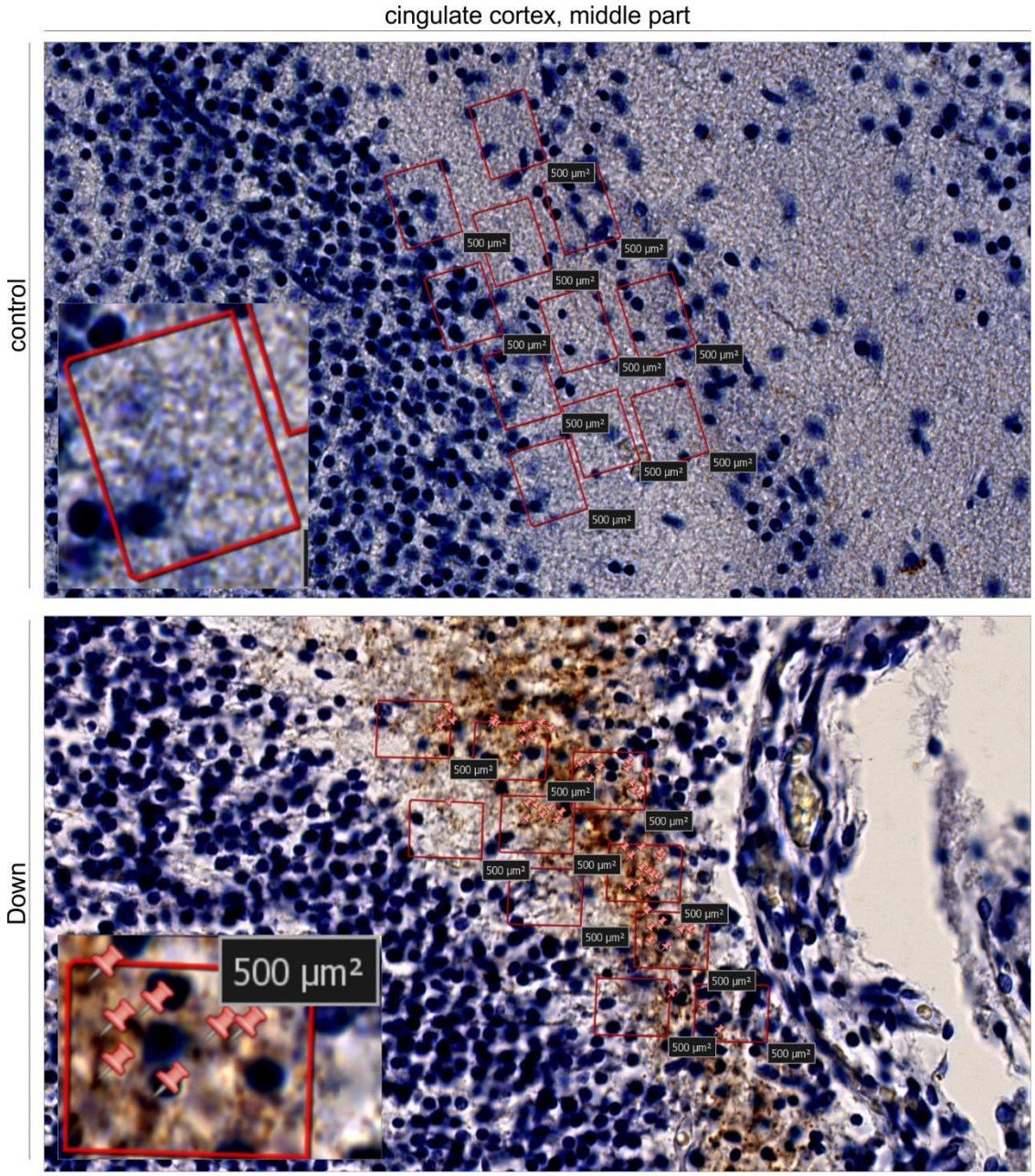

Figure 4. Quantification of CB_1R^+ profiles. The NanoZoomer 2.0 toolbox was used to manually count CB_1R^+ profiles in 500 μm^2 fields (n = 10/area/section). Inserts in overview images show high resolution magnification with pins indicating the profiles counted. The above image pairs show the middle part of the cingulate gyrus in the early second trimester (similar quantifications were carried out in the ventral and dorsal parts of the cingulate gyrus, as well as in the temporal and frontal cortices at the subventricular zone/intermediate zone border).

Table 1. List of markers used for immunolabelling.

Marker	Source	Host	IH dilution	WB dilution	Reference
acetylated tubulin	Abcam	Mouse, mc[1]	n.a	1:1,000	this study
SCG10/stathmin-2	NOVUS Biologicals	Rabbit, pc[2]	1:1,000	n.a.	Tortoriello *et al.*, 2014 [55]
GAPDH	Abcam	Mouse, mc[1]	n.a.	1:10,000	Tortoriello *et al.*, 2014 [55]
CB_1R	K. Mackie	rabbit, pc[2]	1:1,000	n.a.	Tortoriello *et al.*, 2014 [55]
β-III-tubulin	Sigma-Aldrich	Mouse, mc[1]	1:1,000	n.a.	Pintér *et al.*, 2020 [114]
NeuN	Merck	Mouse, mc[1]	1:100	n.a.	Tortoriello *et al.*, 2014 [55]

[1]monoclonal antibody, [2]polyclonal antibody

3.4. In vitro neuropharmacology in dissociated cortical cultures of neonatal mice

On postnatal day 2 (P2), whole neocortices were dissected from wild-type and littermate $Ts65Dn^{+/+}$ mice brains, the latter being the most common model of Down's syndrome [103, 113]. Brain tissue was dissociated enzymatically and plated for Western blotting or for immunohistochemistry. Cells were maintained in DMEM/F12 (1:1) containing B27 supplement [2% (vol/vol)], L-glutamine (2 mM), penicillin (100 U/mL), and streptomycin (100 μg/mL) (all from Invitrogen).

For Western blotting, dissociated cells were plated at a density of 200,000 cells/well in 6-well plates. On day 2 *in vitro* (DIV), neurons were stimulated by WIN55,212-2 (500 nM, Tocris) for 30 minutes (control cultures received no vehicle treatment) and lyzed immediately afterwards (*see below*). For immunohistochemistry, neurons were treated with WIN55,212-2 (500 nM) for 30 minutes on the second day and kept alive for another day in maintenance medium (DMEM/F12/B27). Subsequently, the coverslips were removed from the wells and immersion-fixed in ice-cold 4% paraformaldehyde (in 0.05M PB). This experiment was planned and carried out to test if $Ts650Dn^{+/+}$ neurons could overcome WIN55,212-2-induced growth arrest, as is known for wild-type neurons [55, 77, 84].

3.5. Western blotting

Neurons acquired from the 6-well plates were collected and homogenized by sonication in TNE buffer containing 0.5% Triton X-100 (Sigma), 1% octyl-β-D-glucopyranoside (Calbiochem), 5 mM NaF, 100 μM Na_3VO_4, and a mixture of protease inhibitors (Complete^{TM}; Roche). Cell debris and nuclei were pelleted by centrifugation (800× *g* at 4 °C for 10 minutes). Bradford's colorimetric method [115] was used to measure protein concentration. Samples were then diluted to a final protein concentration of 2 μg/μL, denatured in 5x Laemmli buffer, and analysed by SDS-PAGE on 8% or 10% (vol/vol) resolving gels. After transfer onto Immobilon-FL PVDF membranes (Millipore) the membrane-bound proteins were blocked in 3% (wt/vol) BSA and 0.5% Tween-20 diluted in TRIS-buffered saline (for 1.5 hours), and subsequently exposed to primary antibodies (**Table 1**) at 4 °C overnight. Signals were detected by using appropriate combinations of horseradish peroxidase (HRP)-conjugated secondary antibodies from goat, rabbit, or mouse hosts (Jackson; 1:10,000; 2h). Images were acquired and their analysis performed on a Bio-Rad XRS$^+$ imaging platform.

3.6. Immunocytochemistry and imaging of in vitro samples

Coverslips were immersed in 0.1M PB (pH 7.4) and pre-treated with 0.3% Triton X-100 (Sigma; in PB) at 22–24 °C for 1 hour to enhance the antibody penetration [55, 114] (**Table 1**). Non-specific immunoreactivity was suppressed by incubating the coverslips in a mixture of 5% (wt/vol) NDS (Jackson), 2% (wt/vol) BSA (Sigma) and 0.3% Triton X-100 in 0.1M PB at 22–24 °C for another hour. Coverslips were then exposed to mouse anti-β-III-tubulin and rabbit anti-SCG10 primary antibodies diluted in 0.1M PB, to which 0.1% NDS and 0.3% Triton X-100 had been added, at 4 °C for 72 hours. Immunoreactivities were revealed by carbocyanine (Cy) 2- or 3-tagged secondary antibodies raised in donkey (1:200; Jackson), and applied at 22–24 °C for 2 hours. Nuclei were counterstained by Hoechst 33,421 (1:10,000; Sigma). Coverslips were drop-dried and mounted onto fluorescence-free glass slides with glycerol/gelatin (GG-1; Sigma). Images were captured on an LSM780 confocal laser-scanning microscope (Zeiss) with optical zoom ranging from 1–3x when using a 40x (Plan-Apochromat 40×/1.40) objective

and the pinhole set to 0.5–0.7 μm ('optical thickness'). Emission spectra for the dyes were limited to 450-480 nm (Hoechst 33,421), 505–530 nm (Cy2) and 560–610 nm (Cy3).

3.7. Statistics

Data were expressed as means ± standard error of mean (s.e.m.). Morphological parameters were statistically compared between control (n = 3) and Down's syndrome (n = 3) subjects in equivalent age groups using two-tailed, paired Student's t-tests with gestational age being the intrinsic variable for pairing (GraphPad Prism). A two-tailed Student's t-test for independent samples was used to test pharmacological and genetic variables *in vitro*. A p value of < 0.05 was taken as indicative of statistical differences. Multi-panel figures were assembled in CorelDraw X7 (Corel Corp.). The cohort available allowed us to investigate sex-specific differences only between gestational days 121-160. Applying the 5 unit scale (0, +, ++, +++, ++++; see first paragraph of 3.3. section), we used ordinal logistic regression models to investigate the interaction between Down's syndrome status and sex.

4. Results

4.1. Diagram of CB_1Rs in the foetal brain and their delayed appearance in Down's syndrome

CB_1R^+ profiles appeared as a meshwork of fine-calibre axonal fibres and varicosities in most of the investigated brain regions. We first determined their distribution in cortical areas, hippocampal subfields, and the cerebellum across the three trimesters of pregnancy in our control samples and then compared the findings with those in Down's syndrome foetal brains. Our principal discovery is that CB_1R^+ fibres in foeti with Down's syndrome appear with a month delay but persist throughout pregnancy. The delayed appearance of CB_1R^+ axons and varicosities in foeti with Down's syndrome as late as the fourth month of pregnancy contrasts the early and transient presence of CB_1R^+ axons coincident with their active growth processes in control foeti.

4.2. CB_1R expression shows a disturbed and delayed development in Down's syndrome in the 2nd trimester

Our earliest samples allowed us to trace the development of CB_1R expression in the second trimester. In control brains, a dense bundle of CB_1R^+ fibres appeared at the border between the cortical subventricular (SVZ) and intermediate zones (IZ), which was typically distinguishable in the temporal cortex, between days 98-120 (**Fig. 5A, A_1**). In contrast, immunoreactive fibres were less and weakly visible in age-matched Down's syndrome samples in the corresponding regions (**Fig. 5A', A_1', C**, **Table 2**). Frontal cortices showed similar CB_1R development in control brains and was equally reduced and delayed in Down's syndrome at the same intrauterine age (**Fig. 5B, B', C**, **Table 2**). We identified similar differences between control and Down's syndrome samples within a phylogenetically more ancient cortical region: although axons and dendrites were more difficult to distinguish, allocortical hippocampi were also rich in fine CB_1R^+ immunoreactive fibres in control subjects during the 4th month of gestation, which contrasted those in Down's syndrome (**Fig. 6A-A_1'**, **Table 3**). Likewise, axons passing through the fornix, likely corresponding to hippocampal efferents arising from the subiculum, showed CB_1R-imunoreactivity in control but not in Down's syndrome cases

(**Fig. 6A, A'**). In contrast, CB_1R^+ axons entered the cingulate gyrus, even its dorsal part in Down's syndrome but not in control foeti (**Fig. 6B, B', C**).

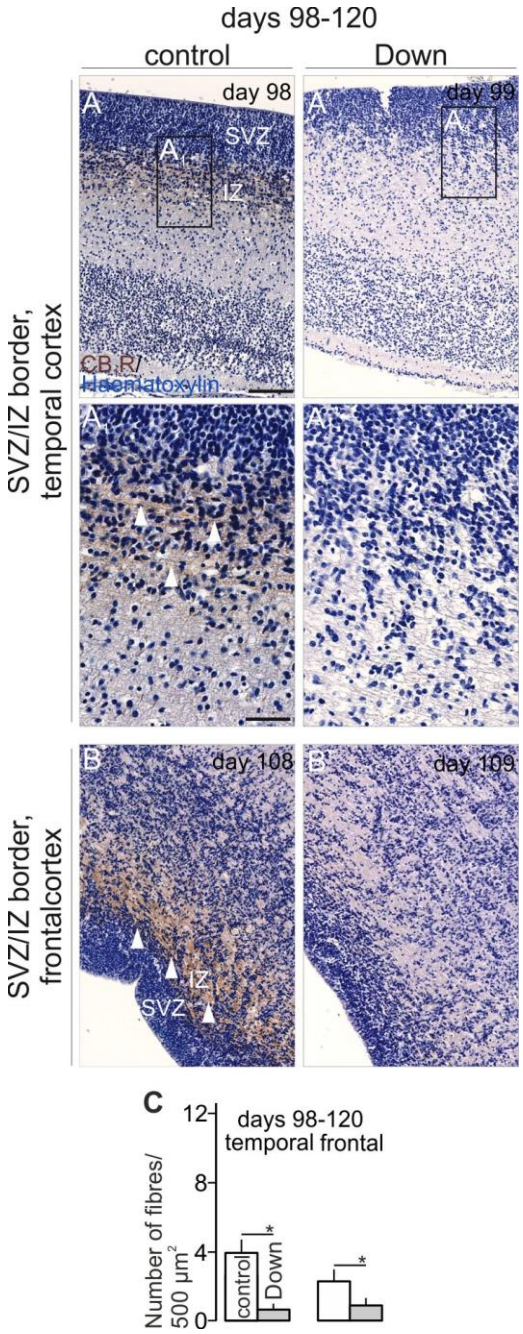

Figure 5. Axonal CB_1Rs in the neocortex in Down syndrome – days 98-120. A-A_1'. CB_1R^+ fibres in the SVZ/IZ zone of the temporal cortex in control but not in Down's syndrome subjects (*arrowheads* point to CB_1R^+ axons). **B, B'.** CB_1R^+ fibres in the SVZ/IZ zone of the frontal cortex in control but not in Down syndrome subjects (*arrowheads*). **C.** The density of CB_1R^+ fibres was lower in temporal and frontal cortices of subjects with Down's syndrome between days 98-120, as compared to age-matched

controls. *Abbreviations:* CB_1R, cannabinoid receptor type 1; SVZ, subventricular zone; IZ, intermediate zone. *Scale bar* = 300 µm (A), 100 µm (A_1). (Published in *Neuropathology and Applied Neurobiology*, 2023).

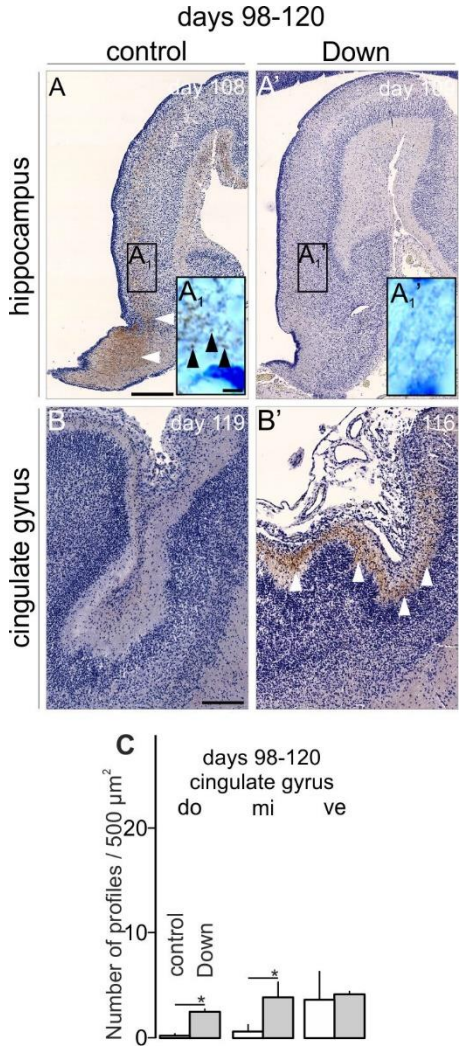

Figure 6. Axonal CB_1Rs in the hippocampus in Down's syndrome – days 98-120. A-A_1'. In control subjects, hippocampal CB_1R^+ fibres appear in the Ammon's horn (*black arrowheads* in A_1) and in the fornix (*white arrowheads* in A). Poor immunolabeling was noted in Down's syndrome subjects. **B, B'.** In the cingulate gyrus, CB_1R^+ fibres appeared in Down's syndrome (*white arrowheads* in B') but scarcely in control subjects. **C.** In the dorsal and middle parts of the cingulate gyrus, CB_1R^+ fibre density was higher in Down's syndrome relative to control between days 98-120. *Abbreviations*: do, dorsal; mi, middle; ve, ventral. *Scale bars* = 1 mm (A, B), 3 µm (A_1). (Published in *Neuropathology and Applied Neurobiology*, 2023).

Between gestational days 121-160, the distribution of CB_1Rs changed in both control and Down's syndrome subjects. CB_1R-immunoreactivity weakened in control brains. Conversely, in the temporal cortex of Down's syndrome foetal brains, CB_1R^+ processes first appeared adjacent to the cortical proliferative zone (at the SVZ/IZ boundary) around day 135 (**Fig. 7A, A'**, **Table 2**). Actually, we identified CB_1R^+ fibres at a higher density in Down's syndrome at this age, and considered them as ectopic and likely transient, relative to controls (**Fig. 7A$_1$-A'$_2$, D**, **Table 2**). CB_1R^+ immunoreactivity of periventricular processes in Down's syndrome remained more pronounced than those in age-matched controls, at least until day 160 (**Fig. 7B, B'**, **Table 2**). The distribution of CB_1R^+ profiles were largely identical in frontal and temporal cortices (**Fig. 7C, C', D**, **Table 2**). Typically, CB_1R^+ processes often carried pearl-lace-like swellings, which we considered as nascent varicosities instead of mature synapses. CB_1R-immunoreactivity did not overlap with NeuN-immunoreactivity; instead, we typically observed CB_1R^+ varicosities among or around $NeuN^+$ cell bodies (**Fig. 8A-A''**), which argues for their axonal identity. We traced developmental changes also in the archicortex: in control hippocampi, CB_1R^+ varicose structures became more numerous in the Ammon's horn around day 140 (**Fig. 9A, A$_1$, A$_2$**, **Table 3**) and occurred more often in the suprapyramidal layers, including the strata radiatum and lacunosomoleculare, in Down's syndrome cases (**Fig. 9A, A$_1$', A$_2$'**, **Table 3**). In the cingulate gyrus of control samples, numerous CB_1R^+ fibres were detected by day 130. However, the immunoreactivity in the equivalent structure of Down's syndrome cases had again a more expressed (although statistically not significant) labelling (**Fig. 9B, B', C**).

The sex of the embryos had no significant effect on the CB_1R^+ label intensity either in neo- or in allocortex (temporal cortex: $W = 2.05$, $p = 0.153$, frontal cortex: $W = 2.81$, $p = 0.094$, fimbriae/fornix: $W_{3,149} = 0.002$, $p = 0.962$, pyramidal layer of the hippocampus: $W = 2.36$, $p = 0.127$, molecular layer of the hippocampus: $W = 0.435$, $p = 0.509$, dentate gyrus: $W = 0.83$, $p = 0.362$).

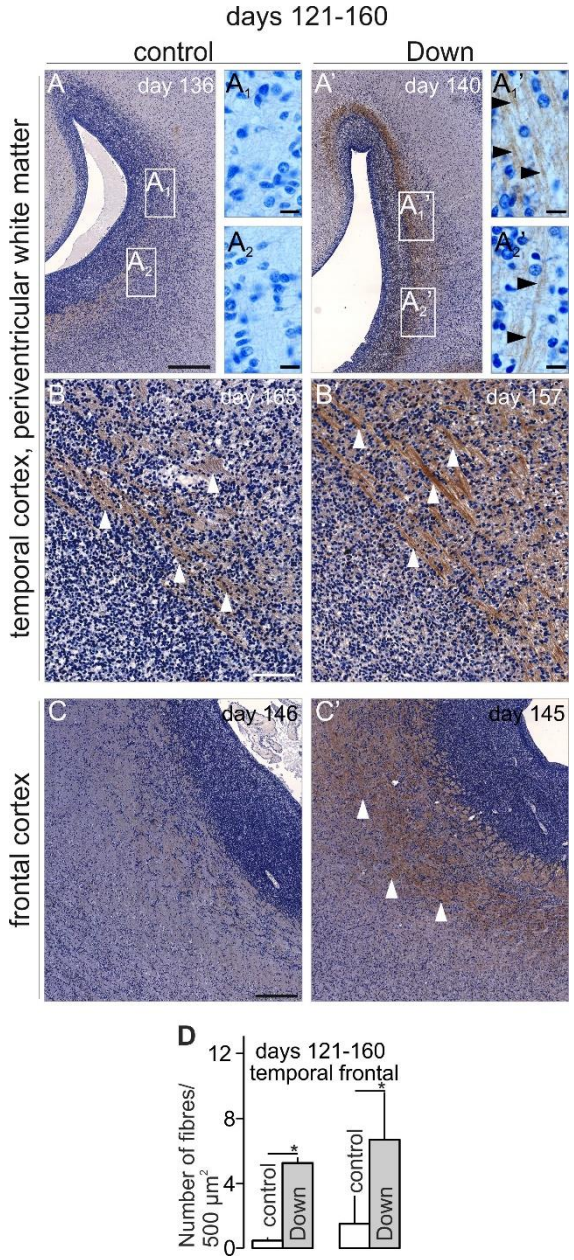

Figure 7. Axonal CB_1Rs in the neocortex in Down syndrome – days 121-160. A-B'. Between days 121-160, CB_1R^+ processes dominated in Down's syndrome vs. control subjects in the periventricular temporal cortex (*white arrowheads* in B and B'). **C, C'.** CB_1R^+ axonal bundles in Down's syndrome but not in control frontal cortices (*white arrowheads* in C'). **D.** CB_1R^+ density of subjects with Down's syndrome exceeded that of control subjects in the temporal and in frontal cortex between days 121-160. *Scale bar* = 1 mm (A, C), 300 µm (B), 3 µm (A_1). (Published in *Neuropathology and Applied Neurobiology*, 2023).

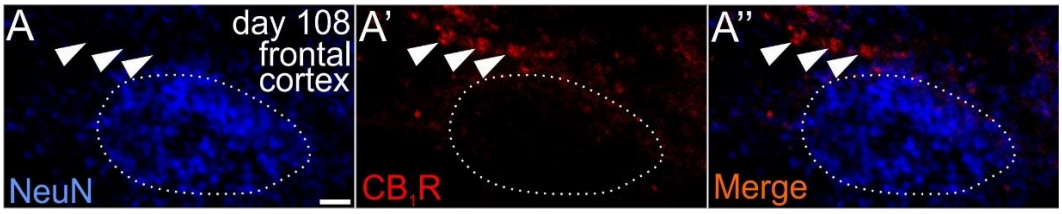

Figure 8. Relation of CB_1R-immunoreactivity to neuronal somata. A-A''. CB_1R^+ profiles typically appeared extrasomatically and contacted $NeuN^+$ cell bodies (*white arrowheads*). *Abbreviations:* CB_1R, cannabinoid receptor type 1; NeuN, neuronal nuclear protein. *Scale bar* = 3 µm (A). (Published in *Neuropathology and Applied Neurobiology*, 2023).

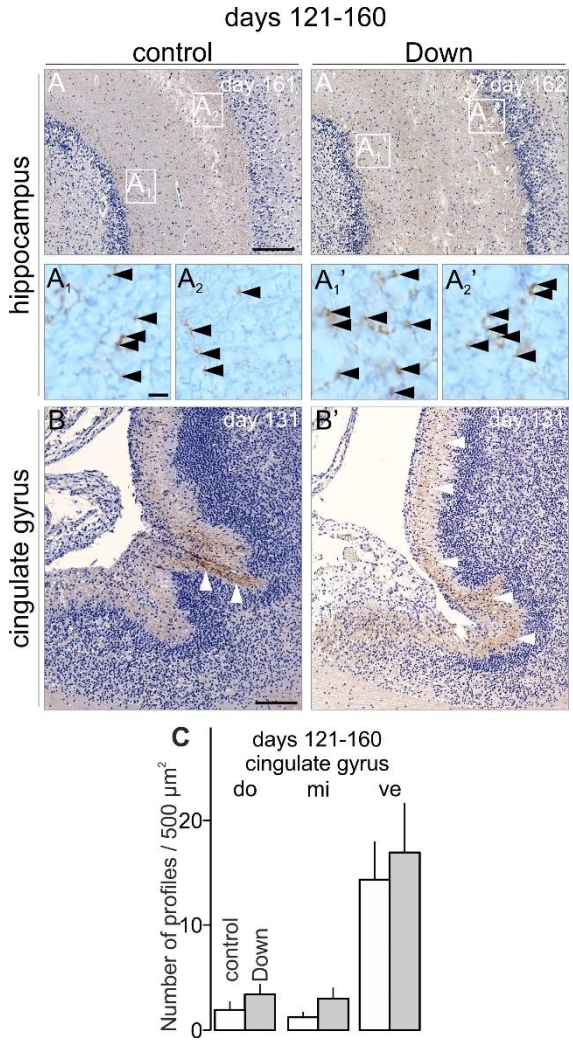

Figure 9. Axonal CB_1Rs in the hippocampus in Down's syndrome – days 121-160. A-A_2'. Thin CB_1R^+ fibres and varicosities in both the lacunosomolecular and the pyramidal layers of the hippocampus (*black arrowheads* in A_1, A_2, A_1', A_2' point to immunoreactive terminals). **B, B'.** CB_1R^+ fibres invaded the dorsal part of the cingulate

gyrus in Down's syndrome but not control fetal brains (*white arrowheads* point to immunoreactive fibres). **C.** No significant difference appeared in any of the investigated parts of the cingulate gyrus in Down's syndrome *vs.* control subjects between days 121-160. *Abbreviations*: do, dorsal; mi, middle; ve, ventral. *Scale bars* = 1 mm (A, B), 3 µm (A_1). (Published in *Neuropathology and Applied Neurobiology*, 2023).

4.3. Development of CB_1R expression during the 3rd trimester in control and Down's syndrome foetal brains

In contrast to the second trimester, no evident differences could be identified between Down's syndrome and age-matched control subjects during the last trimester of pregnancy. Both temporal and frontal cortices lacked CB_1R^+ profiles in the previously investigated areas in both control and Down's syndrome subjects (**Fig. 10 A-B_1'**, **Table 2**). Instead, CB_1R immunoreactivity appeared in the prospective layer V of the cingulate gyrus, with no difference between healthy and diseased brain development (**Fig. 11A-A_1'**). In the hippocampus, CB_1R^+ profiles populated all subfields of the hippocampal formation (**Table 3**), including the pyramidal and molecular layers of the Ammon's horn (**Fig. 11B-B_2'**), at approximately equivalent densities between Down's syndrome and age-matched samples (**Table 3**). Similarly, CB_1R^+ profiles appeared in the indusium griseum, the anterior extension of the hippocampal formation [116], of both control and Down's syndrome subjects (**Fig. 11C-C_1'**).

Cerebellum, in turn, showed a different pattern of CB_1R-immunoreactivity in its developing cortex; around day 240, its molecular layer contained a meshwork of fine-calibre CB_1R^+ processes in Down's syndrome but not in control brains (**Fig. 11D, D'**).

The above data gained from the second and third trimesters show a delayed appearance of CB_1R expression and suggest a delayed axonal development in Down's syndrome. This is normalized only in the last trimester of pregnancy where synaptogenesis proceeds. The impaired developmental CB_1R expression in mid-gestation and its only delayed normalization, however, could impact neuronal structure, function and plasticity later in the diseased offspring. To approach this assumption, we made use of a Down's syndrome transgenic mouse model [113] and performed *in vitro* neuropharmacology experiments to test the development and responsiveness of $Ts65Dn^{+/+}$ mice cortical neurons.

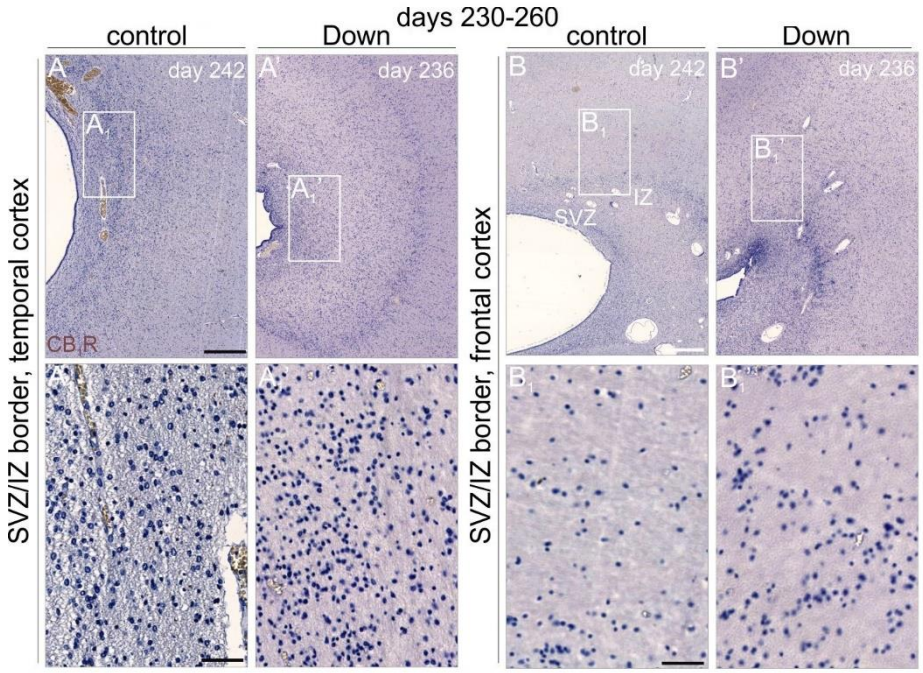

Figure 10. CB_1R expression in control and Down's syndrome subjects during the 3rd trimester – frontal and temporal cortices. A-A_1'. CB_1Rs were absent at the SVZ/IZ boundary in the temporal cortex of both control and Down's syndrome cases. **B-B_1'.** Similarly, CB_1R^+ processes did not appear in the similar region of the frontal cortex either. *Abbreviations*: CB_1R, cannabinoid receptor type 1; IZ, intermediate zone; SVZ, subventricular zone. *Scale bars* = 1 mm (A, B), 100 µm (A_1, B_1). (Published in *Neuropathology and Applied Neurobiology*, 2023).

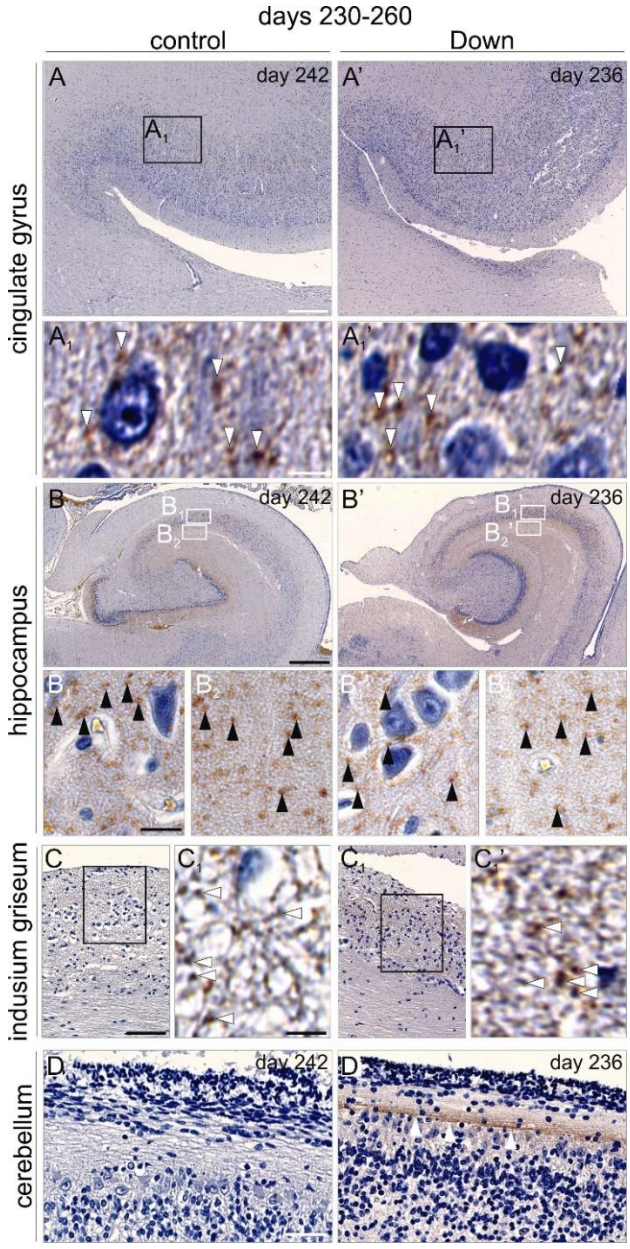

Figure 11. CB_1R expression in control and Down's syndrome subjects during the 3rd trimester – allocortex and cerebellum. A-A_1'. CB_1R^+ structures (*white arrowheads* in A_1, A_1') in the inner pyramidal layer of the cingulate gyrus. **B-B_2'** CB_1R^+ profiles in the strata pyramidale (*black arrowheads* in B_1, B_1') and radiatum (*black arrowheads* in B_2, B_2') of Ammon's horn. **C-C_1'.** CB_1R^+ structures in the indusium griseum. **D, D'.** CB_1R^+ processes were present in the cerebellar molecular layer in Down's syndrome (*white arrowheads* in D') but not in control subjects. *Scale bars* = 1 mm (A, B), 300 µm (C), 100 µm (D), 5 µm (A_1, B_1, C_1). (Published in *Neuropathology and Applied Neurobiology*, 2023).

Table 2. Semi-quantitative analysis of CB_1R-expressing fibres in the subventricular and intermediate zones of the developing neocortex in human foeti.

Control subjects			**Down syndrome subjects**		
Slide no. and age	*Temporal cortex*	*Frontal cortex*	*Slide no. and age*	*Temporal cortex*	*Frontal cortex*
days 98-120					
4-12-2 **day 98, f**	++	+	169-09-2 **day 99, nn**	0	0
240-11-2 **day 98, m**	++	+	156-11-3 **day 102, nn**	not on slide	0
56-11-2 **day 105, f**	not on slide	+	73-11-2 **day 109, nn**	0	+
33-11-3 **day 106, f**	not on slide	++	67-09-2 **day 111, f**	not on slide	0
178-10-1 **day 108, nn**	+++	+++	194-09-2 **day 112, nn**	0	0
104-11-2 **day 119, nn**	++	0	194-09-3 **day 112, nn**	0	0
			113-06-2 **day 112, m**	not on slide	0
			50-05-2 **day 116, f**	0	+
			171-07-1 **day 119, f**	0	not on slide
days 121-160					
131-11-2 **day 125, f**	not on slide	0	228-07-3 **day 128, f**	0	+
131-11-3 **day 125, f**	+	+	66-09-2 **day 130, f**	0	0
29-12-1 **day 131, m**	not on slide	++	4-09-2 **day 131, m**	not on slide	++
74-11-2 **day 133, nn**	0	+	4-09-4 **day 131, m**	+	+/++
151-11-2 **day 136, m**	0	0	90-08-2 **day 135, f**	++	+
151-11-3 **day 136, m**	++	+++	147-05-2 **day 138, m**	not on slide	+
184-10-2 **day 137, m**	0	0	95-10-1 **day 140, m**	+++	+++
39-11-2 **day 137, f**	0	0	118-07-1 I **day 145, m**	+	+
192-11-2 **day 146, m**	0	+	118-07-1 II **day 145, m**	0	++++
149-10-2 **day 148, f**	0	+	41-11-2 **day 151, m**	++++	++++
236-11-2 **day 149, m**	+	0	224-11-2 **day 155, f**	0	0
127-11-2 **day 154, m**	0	not on slide	36-11-3 **day 156, m**	+	0
216-11-2 **day 158, m**	0	0	119-04-2 I **day 157, m**	++	+
128-11-2 **day 159, m**	0	not on slide	119-04-2 II **day 157, m**	+++	+++
13-11-2 **day 161, f**	0	not on slide	60-05-2 **day 158, m**	0	0
199-10-2 **day 163, nn**	0	0	141-09-4 **day 161, f**	0	0
169-10-2 **day 165, m**	+	0	91-06-2 **day 162, m**	0	0
days 173-240					
207-10-1 **day 182, m**	0	0	47-02-1 **day 173, f**	0	0
216-09-4 **day 194, m**	0	0	239-08-4 **day 231, m**	0	not on slide
72-09-3 **day 197, f**	0	0	53-01-1 **day 235, m**	0	not on slide
54-10-2 **day 235, f**	0	0	53-01-2 **day 235, m**	not on slide	0
40-11-2 **day 242, f**	0	0	229-08-1 **day 236, m**	not on slide	0
40-11-3 **day 242, f**	0	not on slide	229-08-2a **day236, m**	0	0
			229-08-2b **day 236, m**	0	0

Table 3. Semi-quantitative analysis of CB_1R-expressing fibres in the hippocampal formation of human foeti. *Abbreviations:* Fim/for, fimbria / fornix; Pyr, pyramidal layer; Mol, molecular layer; Dent, dentate gyrus.

Control subjects					Down syndrome subjects				
Slide no. and age	*Fim/for*	*Pyr*	*Mol*	*Dent*	*Slide no. and age*	*Fim/for*	*Pyr*	*Mol*	*Dent*
days 98-120									
4-12-2 **day 98, f**	+++	+	0	not on slide	169-09-2 **day 99, nn**	0	0	not on slide	not on slide
240-11-2 **day 101, m**	++	0	0	0	156-11-3 **day 102, nn**	0	not on slide	not on slide	not on slide
56-11-2 **day 105, f**	+++	not on slide	not on slide	not on slide	73-11-2 **day 109, nn**	+	0	+	0
33-11-3 **day 106, f**	+/++	not on slide	not on slide	not on slide	194-09-2 **day 112, nn**	+	0	+	0
178-10-1 **day 108, nn**	+++	+	+++	+	194-09-3 **day 112, nn**	0	0	+	0
104-11-2 **day 119, nn**	+	+	++	+	113-06-2 **day 112, m**	0	not on slide	not on slide	not on slide
					50-05-2 **day 116, f**	+++	+	+++	+
					171-07-1 **day 119, f**	0	0	+	0
days 121-160									
131-11-2 **day125, f**	0	not on slide	not on slide	not on slide	61-12-1 **day 126, m**	0	+	++	+
131-11-3 **day 125, f**	0	+	++	+	228-07-3 **day 128, f**	+	not on slide	not on slide	not on slide
29-12-1 **day 131, m**	0	not on slide	not on slide	not on slide	66-09-2 **day 130, f**	0	0	++	0
74-11-2 **day 133, nn**	0	+	++	+	4-09-2 **day 131, m**	+	not on slide	not on slide	not on slide
151-11-2 **day 136, m**	0	0	++	+	4-09-4 **day 131, m**	++	+	+++	+
151-11-3 **day 136, m**	+++	++	++++	+++	90-08-2 **day 135, f**	+	+	+	0
39-11-2 **day 137, f**	+	++	+++	++	147-05-2 **day 138, m**	+	not on slide	not on slide	not on slide
192-11-2 **day 146, m**	+	+	++	++	95-10-1 **day 140, m**	++	++	+++	++
149-10-2 **day 148, f**	++	++	+++	+++	118-07-1 I **day 145, m**	+	++	+++	++
236-11-2 **day 149, m**	0	+	++	++	118-07-1 II **day 145, m**	+++	+	++	+
127-11-2 **day 154, m**	0	not on slide	not on slide	not on slide	41-11-2 **day 151, m**	++++	+++	++++	++++
216-11-2 **day 158, m**	+	0	+	+	224-11-2 **day 155, f**	0	++	++/+++	++
128-11-2 **day 159, m**	0	not on slide	not on slide	not on slide	36-11-3 **day 156, m**	0	+	++	+
13-11-2 **day 161, f**	0	+++	+++	+++	119-04-2 I **day 157, m**	+++	+++	++++	++++
199-11-2 **day 163, nn**	++	++	+++	++++	119-04-2 II **day 157, m**	+++	+++	++++	++++
169-10-2 **day 165, m**	0	+	+	+	60-05-2 **day 158, m**	0	+	++	not on slide
					141-09-4 **day 161, f**	0	0	0	0
					91-06-2 **day 162, m**	0	+	++	+++
days 173-240									
207-10-1 **day 182, m**	+	+/++	++	not on slide	47-02-1 **day 173, f**	+	++	+++	++
216-09-4 **day 194, m**	0	+	+	+	239-08-4 **day 231, m**	0	++++	+++	++++
72-09-3 **day 197, f**	+	+++	+++	+++	53-01-1 **day 235, m**	0	+++	++	+++
54-10-2 **day 235, f**	0	+	+++	not on slide	229-08-1 **day 236, m**	0	not on slide	not on slide	not on slide
40-11-2 **day 242, f**	0	++++	++++	++++	229-08-2a **day 236, m**	0	++++	+++	++++
40-11-3 **day 242, f**	0	++++	+++	++++	229-08-2b **day 236, m**	0	++++	+++	++++

4.4. The stimulation of CB_1Rs induces the degradation of the SCG10 protein and tubulin ageing in $Ts65Dn^{+/+}$ cortical neurons

Previous advances showed that the stimulation of CB_1Rs could impede the growth and maturation of neurites [55]. One possible intracellular cascade controlling this mechanism is an ERK/JNK1-dependent SCG10 degradation pathway, which promotes tubulin acetylation in neurites [55]; CB_1Rs can shape the binding of the SCG10 protein to tubulin dimers [56] and its degradation increases the stability of microtubules (referred to as 'ageing'). We hypothesized that neurons in Down's syndrome – at least in cortical neurons of the $Ts65Dn^{+/+}$ mouse model – could respond differently to CB_1R stimulation, especially since many duplicated genes in this mouse model affect kinase signalling and protein degradation [103].

SCG10 accumulated not only in the cell bodies, but selectively concentrated in axonal varicosities and growth cones in both $Ts65Dn^{+/+}$ and wild-type neurons (**Fig. 12A'-A_2, 12B-B_2**). $SCG10^+$ neurite segments located more proximal to somata in $Ts65Dn^{+/+}$, as compared to wild-type neurons (**Fig. 12E**; 76.41 ± 3.59 % [Ts65Dn] *vs*. 85.5 ± 2.2% [wild-type], as of total neurite length, $p = 0.02$), confirming differential protein localization under non-stimulated conditions. Exposure to WIN55,212-2 (500 nM) for 30 minutes triggered excess SCG10 degradation in $Ts65Dn^{+/+}$ neurons, particularly in their distal (motile) neurite segments (**Fig. 12C'-C_2**, **12D-D_2**, **12E**; 52.46 ± 3.85 % [Ts65Dn] *vs*. 90.29 ± 3.1 % [wild-type], of total neurite length, $p < 0.01$). Moreover, WIN55,212-2 treatment decreased the relative intensity of distalmost SCG10 immunoreactivity in neurites (as compared to somatic SCG10 intensity) in $Ts65Dn^{+/+}$ (12.78 ± 2.8% [WIN55,212-2] *vs*. 53.55 ± 7.03% [no treatment], scaled intensity values, $p < 0.01$) but not in wild-type neurons (**Fig. 12F**; 59.75 ± 11.35% [WIN55,212-2] *vs*. 43.06 ± 5.16% [no treatment], $p = 0.13$). Previous studies showed that increased accumulation of acetylated tubulin parallels excess SCG10 degradation [117]. Indeed, WIN55,212-2 treatment increased tubulin acetylation in $Ts65Dn^{+/+}$ but not in wild-type cortical neurons (**Fig. 12H, H'**). In summary, the above data suggest that cortical neurons of $Ts65Dn^{+/+}$ mice are hypersensitive to CB_1R's stimulation which results in slowed neuritogenesis during development.

4.5. Neurons from Ts65Dn$^{+/+}$ mice exhibit slowed CB_1R-dependent neuritogenesis in vitro

Previous physiological experiments showed the stimulation of CB_1Rs arrests neurite growth of principal neurons [118, 119], which can be overcome only by the short stimulation of the CB_1Rs. The differential expression and distribution of CB_1Rs in Down's syndrome foeti together with the increased sensitivity of the SCG10 pathway to CB_1R stimulation in Ts65Dn$^{+/+}$ mice suggests that disrupted CB_1R functionality, rather than altered localization, could underscore reduced neurite growth. Based on our SCG10 data, we exposed Ts65Dn$^{+/+}$ and wild-type cortical neurons to WIN55,212-2 for 30 minutes. After 24 hours, under control conditions, Ts65Dn$^{+/+}$ neurons grew significantly slower than their wild-type counterparts *in vitro* (**Fig. 12A-B$_2$**, **G**; 54.74 ± 3.56 µm [Ts65Dn] *vs.* 69.16 ± 4.33 µm [wild-type], $p = 0.02$). Notably, wild-type neurons had slightly, albeit non-significantly, longer neurites on DIV3 (**Fig. 12G**), which we interpreted as relative resistance to the low-dose WIN55,212-2 exposure (30 min). In contrast, WIN55,212-2 prevented neurite outgrowth in Ts65Dn$^{+/+}$ neurons (**Fig. 12C-D$_2$, G**; 46.3 ± 4.17 µm [Ts65Dn] *vs.* 82.62 ± 6.66 µm [wild-type], $p < 0.01$). These data suggest that neuritogenesis is *per se* slowed in Ts65Dn$^{+/+}$ neurons and parallels an enhanced sensitivity to agonist-induced CB_1R signalling.

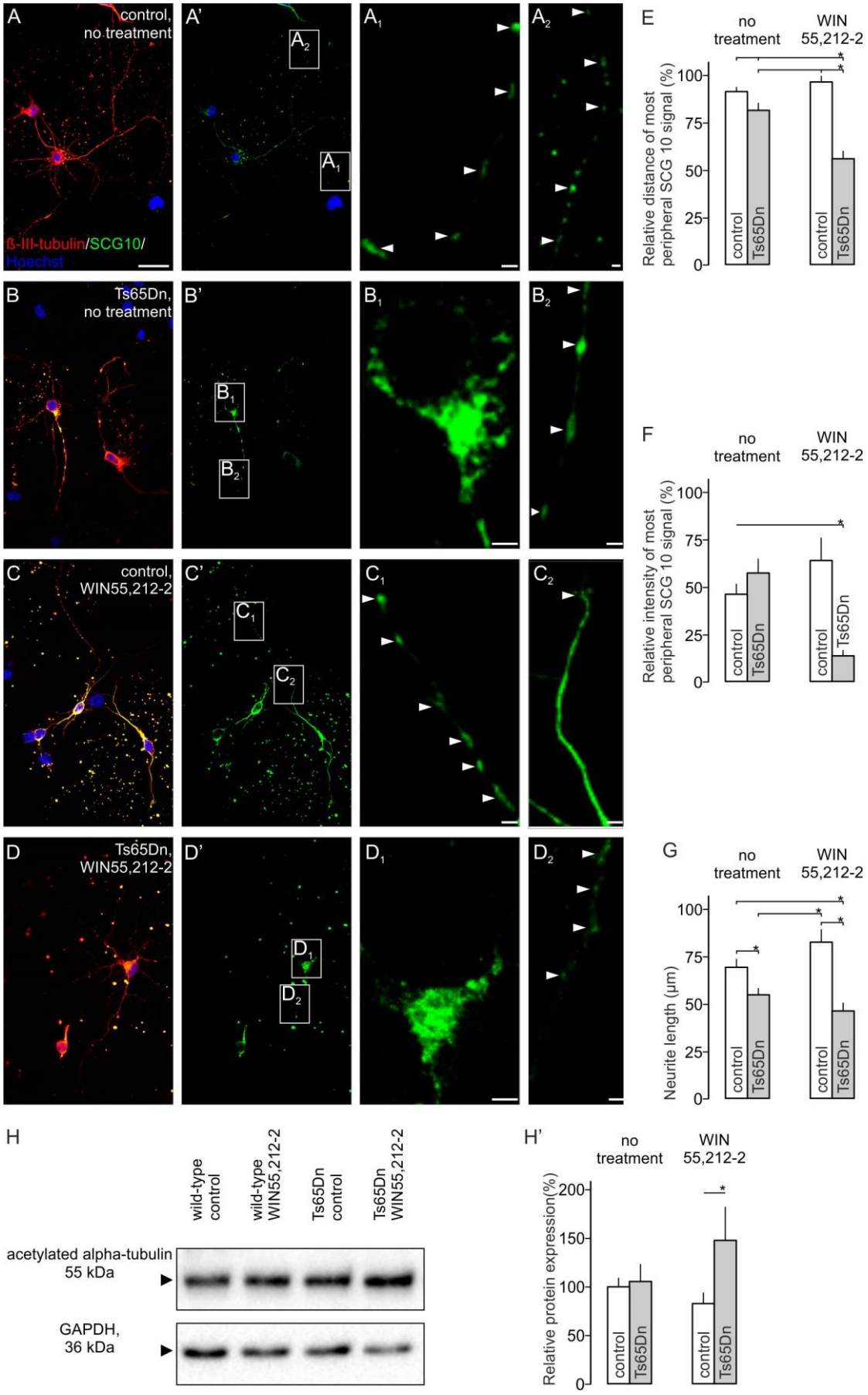
A
control,
no treatment
A'
A2
A1
A1
A2
ß-III-tubulin/SCG10/
Hoechst
B
Ts65Dn,
no treatment
B'
B1
B2
B1
B2
C
control,
WIN55,212-2
C'
C1
C2
C1
C2
D
Ts65Dn,
WIN55,212-2
D'
D1
D2
D1
D2
E
no
treatment
WIN
55,212-2
Relative distance of most
peripheral SCG 10 signal (%)
100
75
50
25
0
control
Ts65Dn
control
Ts65Dn
F
no
treatment
WIN
55,212-2
Relative intensity of most
peripheral SCG 10 signal (%)
100
75
50
25
0
control
Ts65Dn
control
Ts65Dn
G
no
treatment
WIN
55,212-2
Neurite length (µm)
100
75
50
25
0
control
Ts65Dn
control
Ts65Dn
H
wild-type
control
wild-type
WIN55,212-2
Ts65Dn
control
Ts65Dn
WIN55,212-2
acetylated alpha-tubulin
55 kDa
GAPDH,
36 kDa
H'
no
treatment
WIN
55,212-2
Relative protein expression(%)
200
150
100
50
0
control
Ts65Dn
control
Ts65Dn

Figure 12. Neurons from Ts65Dn$^{+/+}$ mice develop shorter neurites in a CB_1R-dependent fashion *in vitro*. A-A_2. Neocortical neurons of control littermate mice. Primary neuronal culture on P2. *Arrowheads* indicate SCG 10-immunoreactivity in a neurite. **B-B_2**. Neocortical neurons of Ts65Dn$^{+/+}$ mice. Primary neuronal culture on P2. Note the somatic accumulation of SCG10 in B_1. *Arrowheads* in B_2 indicate SCG10 immunoreactivity in a neurite. **C-C_2**. WIN55,212-2 increased SCG10 expression (*arrowheads* in C_1; arrowhead in C_2 points to neurite end-plate) in control cultures. **D-D_2**. WIN55,212-2 in primary neuronal cultures from Ts65Dn$^{+/+}$ mice reduced SCG10 immunoreactivity in neurites (*arrowheads*). **E.** WIN55,212-2 reduced the distance of peripheral SCG10 immunoreactivity. **F.** WIN55,212-2 reduced the intensity of peripheral SCG10 immunosignal. **G.** Neurons isolated from Ts65Dn$^{+/+}$ mice and cultured *in vitro* had shorter neurites. **H, H'.** WIN55,212-2 increased the expression of acetylated tubulin in neurons from Ts65Dn$^{+/+}$ but not wild-type littermate mice. *Abbreviations*: SCG10, superior cervical ganglion 10; GAPDH, glyceraldehyde 3-phosphate dehydrogenase. *Scale bars* = 20 µm (A), 3 µm (B_1,D_1) 2 µm (A_1,A_2,B_2,C_2,D_2). (Published in *Neuropathology and Applied Neurobiology*, 2023).

5. Discussion

The CB_1R and the ECS are increasingly recognized as fundamental signaling modules regulating multiple aspects of nervous system development [1, 70]. Based on the available data extracted from predominantly rodent models, cannabinoid signals influence brain morphogenesis through the control of neural progenitor proliferation, lineage commitment, neuronal migration, axonal growth and synaptogenesis [72, 75, 76, 78]. Accordingly, during development CB_1Rs are intricately interconnected with signaling pathways that modulate cell survival, cell differentation, cell structure and movement [52, 53, 55]. Albeit the number of studies investigating the precise expession and function of CB_1Rs in human brain development is limited, there is compelling evidence that functionally active CB_1Rs are expressed in human foetal brains since mid-gestation, and the distribution pattern of these receptors is different from the adult, specifically in certain white matter areas and proliferative zones [45, 79].

In our study, by combining high resolution light and confocal laser scanning microscopy we present a regional survey of CB_1R-expressing neurites covering the period of the late first trimester (week 14) until birth and propose that the regional distribution of CB_1Rs follows area-specific temporal scales. During the early second trimester, in healthy developing human foetal brains, we visualized numerous CB_1R^+ varicosity-containing immunoreactive processes, located at the SVZ-IZ boundary of all telencephalic areas including both the neo- and allocortex. These immunoreactive processes were typically positioned as if they were white matter pathways, and most likely corresponded to corticofugal axons emanating from projection neurons. This notion is in agreement with previous findings that long-range projection neurons are the primary source of CB_1Rs in the developing forebrain and that pathfinding decisions and fasciculation steps also rely on CB_1R-mediated signaling events [47, 55, 72]. As intrauterine development progressed, the number of CB_1R^+ varicosities in the aforementioned areas gradually decreased, and completely disappeared by the third trimester.

To the best of our knowledge, this is the first complete anatomical map of CB_1R expression in the developing human telencephalon. We believe that the knowledge of the exact timeline of CB_1R expression in select brain areas and layers will give useful support to investigate healthy and diseased development where sensitive time windows and specific brain domains with possible targeting are known. Evidently, marijuana

(*Cannabis sativa*) and its synthetic derivatives (designer drugs) are widely consumed with a peak between 15-30 years of age [2]. This includes the fertile period of women; actually, cannabinoids are often abused by pregnant women with a prevalence exceeding 10% in the United States [120]. References typically underline the teratological effects of early Δ^9-THC administration, although the available data linking prenatal cannabis exposure to congenital anomalies are weak [121, 122]. Regardless, Δ^9-THC can be harmful during any time of pregnancy, but a specific effect of exogenous cannabinoid administration during the later stages of pregnancy has not been accentuated. In general, cell biological effects can be identified during early ontogenesis [123] – drug administration in later stages can be rather ambiguously linked to select malformation or dysgenesis; the possible connection with adverse neurobehavioural outcome is more pronounced [124]. Our present anatomical CB_1R expression diagram helps to identify those periods where the foetal brain is especially sensitive to exogenous cannabinoids.

Unfortunately, we could not draw conclusions on the precise subcellular compartmentalization of CB_1Rs due to suboptimal post-mortem delay and tissue preservation which did not allow an ultrastructural analysis. Therefore, we employed the term 'varicosities', a morphological descriptor purely considering the shape of CB_1R^+ structures. Previous studies examining the rodent and primate neocortex revealed CB_1R expression in the somata of radially migrating immature neurons [81]. While we can not exclude the somatic localization and presence of CB_1R-containing intracellular vesicles in our samples, our imaging data support the conclusion that in certain time windows disproportionately many CB_1Rs reside in neurites to efficiently regulate neuritogenesis in the developing human cortex.

Down's syndrome, the leading chromosomal cause of intellectual disability, can be interpreted as a complex neurodevelopmental disorder characterized by impaired neurogenesis, astrogliosis and inhibiting interneuron predominance [94-97]. Dysfunctional morphogenesis is also reflected by the decreased number of dendritic spines and synaptosomal structures [100]. Moreover, based on experimental data obtained from DS rodent models and cell systems, neuronal migration is slower [104, 109], the development of cortical white matter is delayed [104, 107] and the growth of individual axons is defective [108-110]. The vast majority of the developmental observations made on human brain tissue came from the analysis of foetal brains from the second trimester.

Accordingly, these pathological changes shall originate from morphogenetic events during the first/early second trimester.

In our study, we demonstrate that the temporal dynamics of CB_1R expression is distinct in DS: during the early phase of brain development (first/early second trimester), the appearance of CB_1R^+ processes is delayed (by at least a month), but stays disproportionately high even at foetal periods when CB_1R expression in typically developing brains becomes reduced (late second trimester). We hypothesize that these pathogenic changes could provoke an imbalance of neurogenesis, radial cell migration and synaptogenesis, resulting in the cortical delamination and errant synaptic connectivity seen in DS [98]. We did not detect a morphological difference of CB_1R^+ profiles in DS, supporting that not compartmentalization but the time factor is a primary determinant of altered eCB signaling. In support of this theory, a recent study on the dynamics of $GABA_A$ receptor subunit expression *in utero* highlighted that temporal modifications of ionotropic receptor expression that gate the GABA-mediated control of cell proliferation, migration and differentiation are also delayed in DS [125].

Naturally, examining the distribution of CB_1Rs does not equal the study of the entire ECS, which consists of additional receptors, endogenous ligands and their respective metabolic apparatus. Nonetheless, we are confident in our results, as human neuropathology studies on congenital neurological and psychiatric disorders (e.g, epilepsy, fragile X syndrome, schizophrenia) underscore that CB_1R distribution changes faithfully reflect the involvement and even the impairment of the ECS in disease pathogenesis [126-128].

In developing neurons, CB_1Rs are able to shape both major polymers that compose the cytoskeleton. The CB_1R-dependent reconfiguration of the highly plastic filamentous actin network is primarily mediated by Rho monomer G proteins and Rho-associated protein kinases [52], while the regulation of the more stable microtubule network involves members of the mitogen-activated protein kinase family [55]. In particular, CB_1R activation induces JNK1 phosphorylation, which in turn leads to the phosphorylation of the microtubule destabilizing factor SCG10, designating it for proteosomal degradation [54]. SCG10 degradation limits the rate of dynamic microtubule reorganization (a prerequisite of axonal growth advance), and coincides with the accumulation of acetylated tubulin, a marker for increased microtubule stability (termed 'ageing'). This signaling cascade was previously shown to be crucial in the Δ^9-THC-induced neural

circuit wiring deficits upon *in utero* cannabis exposure [55]. Disruption of SCG10 signaling is associated with devastating neurological conditions, such as amyotrophic lateral sclerosis (ALS) [129]. Interestingly, reduced SCG10 mRNA expression was also reported in neurospheres derived from foetuses with DS [110].

Based on these observations and our human neuropathological data, we performed *in vitro* neuropharmacology on immature Ts65Dn$^{+/+}$ and wild-type neurons, focusing on the differences of SCG10 availability in response to CB_1R stimulation. In addition to differential SCG10 protein localization under non-stimulated conditions, Ts65Dn$^{+/+}$ neurons were found to be more sensitive to CB_1R stimulation than their wild-type counterparts, mirrored by the decreased SCG10 immunoreactivity in neurites and increased tubulin acetylation upon CB_1R agonist exposure. Furthermore, we showed that Ts65Dn$^{+/+}$ neurons display slowed CB_1R-dependent neuritogenesis. These findings are in line with previous results that reported diminished axon growth in developing hippocampal neurons from Ts65Dn$^{+/+}$ mice and held this phenomenon responsible for the reduced hippocampal commissure volume in these animals [108].

Consequently, we present that DS is associated with not only delayed CB_1R expression, but increased CB_1R responsiveness as well. This concept is supported by data showing that CB_1R function is increased in the hippocampus of adult Ts65Dn$^{+/+}$ mice and its pharmacological inhibition restores synaptic plasticity and memory processes [113]. Our study, however, implies that increased CB_1R responsiveness is present since the early life of Ts65Dn$^{+/+}$ neurons, at least *in vitro*, and provokes axonal growth errors that could potentially contribute to the neurodevelopmental phenotypes seen in DS. Moreover, we propose CB_1R hypersensitivity - aberrant SCG10 degradation - increased concentration of acetylated tubulin - excess microtubule stability as a possible molecular cascade underlying slowed brain development in foeti with DS.

Maternal alcohol and cocaine abuse are acknowledged as the most devastating agents for the foetal brain. Among others, this reflects in a measurable reduction of head – and consequently brain – size which makes mothers recognize the harmful effects of these drugs [130]. Cannabis use during pregnancy, in turn, does not result in overt anatomical alterations right after birth which makes mothers believe that cannabinoids are harmless for their offspring. Longitudinal studies evidently proved, however, that prenatal exposure to exogenous cannabinoids profoundly impact brain development, leading to

long-term neurobehavioural disturbances especially in executive functions [2, 131, 132]. In light of our results, the effects of maternal cannabis use in mothers who give birth to children with DS – where deficits are prevailing in this cognitive domain – remains frighteningly enigmatic. Babies born with DS carry evident anatomical and behavioural signs postnatally and our knowledge about the superimposed worsening effect of foetal cannabis exposure is rather limited. Nevertheless, according to community-wide genotoxicity studies based on drug exposure data from the National Survey of Drug Use and Health 2003-2017 and congenital anomaly data from National Birth Defects Prevention Network, prenatal exposure to Δ^9-THC, cannabigerol and cannabichromene appears to be causally associated with an increased risk for DS [133]. Hence, it is plausible to assume that maternal cannabis abuse during pregnancy could aggravate the genetic penetrance and clinical manifestation of this devastating disorder.

6. Conclusions

During our immunohistochemical analysis of healthy developing human foetal brains, we explored the transient expression of CB_1Rs on developing white matter tracts – in accordance with previous observations on developing rodent brains –, underscoring the participation of the ECS in the formation of proper neuronal circuitries. We delivered the first complete neuroanatomical diagram of CB_1Rs in the developing human telencephalon. By comparing with age-matched foetal brains with DS, we found that in trisomy 21 this transient receptor expression is delayed by at least a month during the second trimester of pregnancy. *In vitro* neuropharmacology on cortical neurons derived from neonatal Ts65Dn$^{+/+}$ transgenic mice showed that CB_1R stimulation leads to excess SCG10 degradation and microtubule stabilisation. This leads to reduced neurite outgrowth, which reflects a neuronal hypersensitivity to CB_1R excitation in this widely used mouse model of DS. Taken together, our results imply that the neuroarchitectural impairments in DS include the delayed development and aberrant functions of the ECS, with a profound impact on eCBs modulating axonal wiring.

7. Summary

Proper brain development depends on multiple chemotropic guidance systems whose action in critical time windows can affect neuroblast proliferation, migration and differentiation. In addition to its well-characterized neuromodulatory function at mature synapses, the endocannabinoid system (ECS) has emerged as a fundamental signaling module controlling numerous morphogenetic processes during the formation of the central nervous system. Endocannabinoid (eCB) signals through cannabinoid receptor type 1 (CB_1R) influence the number, placement and connectivity of cortical neurons in many vertebrates. Despite the growing knowledge about the physiological rules of eCB action during foetal brain development, little is known about the neuroanatomy and involvement of the ECS in the pathogenesis of developmental brain disorders.

In our study, we focused on the leading genetic cause of intellectual disability, Down's syndrome (DS), as the CB_1R is a fine-tuner of several neurodevelopmental events that are pathological in this disorder. By using standard immunohistochemistry and high-resolution digitalised light microscopy, we systematically mapped CB_1R expression and distribution in human foetal brains with normal development and with DS, spanning the period from the 14^{th} gestational week until birth. CB_1R^+ processes appeared as fine-calibre meshworks in most investigated brain areas, and were first detected at the border of the subventricular and intermediate zones of the cortical plate in the early second trimester, corresponding to developing telencephalic fiber tracts. In control foeti, the amount of these CB_1R^+ fibres gradually decreased in the second, and completely disappeared by the third trimester, whereas in foeti with DS we found the delayed appearance and persistent maintenance of CB_1R^+ axons during the second trimester. *In vitro* neuropharmacology on cortical neurons from neonatal $Ts65Dn^{+/+}$ mice carrying an additional copy of ~90 conserved protein-coding gene orthologues of the human chromosome 21 showed increased CB_1R responsiveness, which was reflected in excess microtubule stabilisation and slowed CB_1R dependent neuritogenesis. Our results indicate that impaired brain morphogenesis in DS is associated with the temporal and functional deterioration of the ECS, particularly affecting the establishment of proper axonal connectivity.

8. References

1. Harkany, T., K. Mackie, and P. Doherty, *Wiring and firing neuronal networks: endocannabinoids take center stage.* Curr Opin Neurobiol, 2008. **18**(3): p. 338-45.
2. Alpar, A., V. Di Marzo, and T. Harkany, *At the Tip of an Iceberg: Prenatal Marijuana and Its Possible Relation to Neuropsychiatric Outcome in the Offspring.* Biol Psychiatry, 2016. **79**(7): p. e33-45.
3. Cristino, L., T. Bisogno, and V. Di Marzo, *Cannabinoids and the expanded endocannabinoid system in neurological disorders.* Nat Rev Neurol, 2020. **16**(1): p. 9-29.
4. Mechoulam, R., *Marihuana chemistry.* Science, 1970. **168**(3936): p. 1159-66.
5. Lu, H.C. and K. Mackie, *Review of the Endocannabinoid System.* Biol Psychiatry Cogn Neurosci Neuroimaging, 2021. **6**(6): p. 607-615.
6. Harkany, T., M. Guzman, I. Galve-Roperh, P. Berghuis, L.A. Devi, and K. Mackie, *The emerging functions of endocannabinoid signaling during CNS development.* Trends Pharmacol Sci, 2007. **28**(2): p. 83-92.
7. Devane, W.A., L. Hanus, A. Breuer, R.G. Pertwee, L.A. Stevenson, G. Griffin, D. Gibson, A. Mandelbaum, A. Etinger, and R. Mechoulam, *Isolation and structure of a brain constituent that binds to the cannabinoid receptor.* Science, 1992. **258**(5090): p. 1946-9.
8. Mechoulam, R., S. Ben-Shabat, L. Hanus, M. Ligumsky, N.E. Kaminski, A.R. Schatz, A. Gopher, S. Almog, B.R. Martin, D.R. Compton, and et al., *Identification of an endogenous 2-monoglyceride, present in canine gut, that binds to cannabinoid receptors.* Biochem Pharmacol, 1995. **50**(1): p. 83-90.
9. Di Marzo, V., L. De Petrocellis, T. Sugiura, and K. Waku, *Potential biosynthetic connections between the two cannabimimetic eicosanoids, anandamide and 2-arachidonoyl-glycerol, in mouse neuroblastoma cells.* Biochem Biophys Res Commun, 1996. **227**(1): p. 281-8.
10. Grabiec, U. and F. Dehghani, *N-Arachidonoyl Dopamine: A Novel Endocannabinoid and Endovanilloid with Widespread Physiological and Pharmacological Activities.* Cannabis Cannabinoid Res, 2017. **2**(1): p. 183-196.

11. Wei, F., L. Zhao, and Y. Jing, *Signaling molecules targeting cannabinoid receptors: Hemopressin and related peptides.* Neuropeptides, 2020. **79**: p. 101998.
12. Stella, N., P. Schweitzer, and D. Piomelli, *A second endogenous cannabinoid that modulates long-term potentiation.* Nature, 1997. **388**(6644): p. 773-8.
13. Mock, E.D., B. Gagestein, and M. van der Stelt, *Anandamide and other N-acylethanolamines: A class of signaling lipids with therapeutic opportunities.* Prog Lipid Res, 2023. **89**: p. 101194.
14. Katona, I. and T.F. Freund, *Endocannabinoid signaling as a synaptic circuit breaker in neurological disease.* Nat Med, 2008. **14**(9): p. 923-30.
15. Bisogno, T., N. Sepe, D. Melck, S. Maurelli, L. De Petrocellis, and V. Di Marzo, *Biosynthesis, release and degradation of the novel endogenous cannabimimetic metabolite 2-arachidonoylglycerol in mouse neuroblastoma cells.* Biochem J, 1997. **322 (Pt 2)**(Pt 2): p. 671-7.
16. Bisogno, T., F. Howell, G. Williams, A. Minassi, M.G. Cascio, A. Ligresti, I. Matias, A. Schiano-Moriello, P. Paul, E.J. Williams, U. Gangadharan, C. Hobbs, V. Di Marzo, and P. Doherty, *Cloning of the first sn1-DAG lipases points to the spatial and temporal regulation of endocannabinoid signaling in the brain.* J Cell Biol, 2003. **163**(3): p. 463-8.
17. Simon, G.M. and B.F. Cravatt, *Endocannabinoid biosynthesis proceeding through glycerophospho-N-acyl ethanolamine and a role for alpha/beta-hydrolase 4 in this pathway.* J Biol Chem, 2006. **281**(36): p. 26465-72.
18. Buczynski, M.W. and L.H. Parsons, *Quantification of brain endocannabinoid levels: methods, interpretations and pitfalls.* Br J Pharmacol, 2010. **160**(3): p. 423-42.
19. Berrendero, F., N. Sepe, J.A. Ramos, V. Di Marzo, and J.J. Fernandez-Ruiz, *Analysis of cannabinoid receptor binding and mRNA expression and endogenous cannabinoid contents in the developing rat brain during late gestation and early postnatal period.* Synapse, 1999. **33**(3): p. 181-91.
20. Kaczocha, M. and S. Haj-Dahmane, *Mechanisms of endocannabinoid transport in the brain.* Br J Pharmacol, 2022. **179**(17): p. 4300-4310.

21. Albarran, E., Y. Sun, Y. Liu, K. Raju, A. Dong, Y. Li, S. Wang, T.C. Sudhof, and J.B. Ding, *Postsynaptic synucleins mediate endocannabinoid signaling.* Nat Neurosci, 2023. **26**(6): p. 997-1007.
22. Keimpema, E., K. Barabas, Y.M. Morozov, G. Tortoriello, M. Torii, G. Cameron, Y. Yanagawa, M. Watanabe, K. Mackie, and T. Harkany, *Differential subcellular recruitment of monoacylglycerol lipase generates spatial specificity of 2-arachidonoyl glycerol signaling during axonal pathfinding.* J Neurosci, 2010. **30**(42): p. 13992-4007.
23. Keimpema, E., K. Mackie, and T. Harkany, *Molecular model of cannabis sensitivity in developing neuronal circuits.* Trends Pharmacol Sci, 2011. **32**(9): p. 551-61.
24. Blankman, J.L., G.M. Simon, and B.F. Cravatt, *A comprehensive profile of brain enzymes that hydrolyze the endocannabinoid 2-arachidonoylglycerol.* Chem Biol, 2007. **14**(12): p. 1347-56.
25. Rouzer, C.A. and L.J. Marnett, *Endocannabinoid oxygenation by cyclooxygenases, lipoxygenases, and cytochromes P450: cross-talk between the eicosanoid and endocannabinoid signaling pathways.* Chem Rev, 2011. **111**(10): p. 5899-921.
26. Breivogel, C.S. and L.J. Sim-Selley, *Basic neuroanatomy and neuropharmacology of cannabinoids.* Int Rev Psychiatry, 2009. **21**(2): p. 113-21.
27. Howlett, A.C., Evans, D.M., Houston, D.B., *The Cannabinoid Receptor*, in *Marihuana/Cannabinoids: Neurobiology and Neurophysiology*, A.B. L. Murphy, Editor. 1992, CRC Press: Boca Raton. p. 35-72.
28. Yang, H., J. Zhou, and C. Lehmann, *GPR55 - a putative "type 3" cannabinoid receptor in inflammation.* J Basic Clin Physiol Pharmacol, 2016. **27**(3): p. 297-302.
29. Kano, M., T. Ohno-Shosaku, Y. Hashimotodani, M. Uchigashima, and M. Watanabe, *Endocannabinoid-mediated control of synaptic transmission.* Physiol Rev, 2009. **89**(1): p. 309-80.
30. Gouvea, E.S., A.F.F. Santos, V.K. Ota, V. Mrad, A. Gadelha, R.A. Bressan, Q. Cordeiro, and S.I. Belangero, *The role of the CNR1 gene in schizophrenia: a*

systematic review including unpublished data. Braz J Psychiatry, 2017. **39**(2): p. 160-171.

31. Chavarria-Siles, I., J. Contreras-Rojas, E. Hare, C. Walss-Bass, P. Quezada, A. Dassori, S. Contreras, R. Medina, M. Ramirez, R. Salazar, H. Raventos, and M.A. Escamilla, *Cannabinoid receptor 1 gene (CNR1) and susceptibility to a quantitative phenotype for hebephrenic schizophrenia.* Am J Med Genet B Neuropsychiatr Genet, 2008. **147**(3): p. 279-84.
32. Ponce, G., J. Hoenicka, G. Rubio, I. Ampuero, M.A. Jimenez-Arriero, R. Rodriguez-Jimenez, T. Palomo, and J.A. Ramos, *Association between cannabinoid receptor gene (CNR1) and childhood attention deficit/hyperactivity disorder in Spanish male alcoholic patients.* Mol Psychiatry, 2003. **8**(5): p. 466-7.
33. Katona, I., *Endocannabinoid receptors: CNS localization of the CB(1) cannabinoid receptor.* Curr Top Behav Neurosci, 2009. **1**: p. 65-86.
34. Herkenham, M., A.B. Lynn, M.D. Little, M.R. Johnson, L.S. Melvin, B.R. de Costa, and K.C. Rice, *Cannabinoid receptor localization in brain.* Proc Natl Acad Sci U S A, 1990. **87**(5): p. 1932-6.
35. Moldrich, G. and T. Wenger, *Localization of the CB1 cannabinoid receptor in the rat brain. An immunohistochemical study.* Peptides, 2000. **21**(11): p. 1735-42.
36. Marsicano, G. and B. Lutz, *Expression of the cannabinoid receptor CB1 in distinct neuronal subpopulations in the adult mouse forebrain.* Eur J Neurosci, 1999. **11**(12): p. 4213-25.
37. Bodor, A.L., I. Katona, G. Nyiri, K. Mackie, C. Ledent, N. Hajos, and T.F. Freund, *Endocannabinoid signaling in rat somatosensory cortex: laminar differences and involvement of specific interneuron types.* J Neurosci, 2005. **25**(29): p. 6845-56.
38. Katona, I., B. Sperlagh, Z. Magloczky, E. Santha, A. Kofalvi, S. Czirjak, K. Mackie, E.S. Vizi, and T.F. Freund, *GABAergic interneurons are the targets of cannabinoid actions in the human hippocampus.* Neuroscience, 2000. **100**(4): p. 797-804.
39. Katona, I., G.M. Urban, M. Wallace, C. Ledent, K.M. Jung, D. Piomelli, K. Mackie, and T.F. Freund, *Molecular composition of the endocannabinoid system at glutamatergic synapses.* J Neurosci, 2006. **26**(21): p. 5628-37.

40. Herkenham, M., B.G. Groen, A.B. Lynn, B.R. De Costa, and E.K. Richfield, *Neuronal localization of cannabinoid receptors and second messengers in mutant mouse cerebellum.* Brain Res, 1991. **552**(2): p. 301-10.
41. Hu, S.S. and K. Mackie, *Distribution of the Endocannabinoid System in the Central Nervous System.* Handb Exp Pharmacol, 2015. **231**: p. 59-93.
42. Breivogel, C.S., L.J. Sim, and S.R. Childers, *Regional differences in cannabinoid receptor/G-protein coupling in rat brain.* J Pharmacol Exp Ther, 1997. **282**(3): p. 1632-42.
43. Hillard, C.J., M. Beatka, and J. Sarvaideo, *Endocannabinoid Signaling and the Hypothalamic-Pituitary-Adrenal Axis.* Compr Physiol, 2016. **7**(1): p. 1-15.
44. Parizek, A., J. Suchopar, Z. Lastuvka, M. Alblova, M. Hill, and M. Duskova, *The Endocannabinoid System and Its Relationship to Human Reproduction.* Physiol Res, 2023. **72**(S4): p. S365-S380.
45. Mato, S., E. Del Olmo, and A. Pazos, *Ontogenetic development of cannabinoid receptor expression and signal transduction functionality in the human brain.* Eur J Neurosci, 2003. **17**(9): p. 1747-54.
46. Romero, J., E. Garcia-Palomero, F. Berrendero, L. Garcia-Gil, M.L. Hernandez, J.A. Ramos, and J.J. Fernandez-Ruiz, *Atypical location of cannabinoid receptors in white matter areas during rat brain development.* Synapse, 1997. **26**(3): p. 317-23.
47. Vitalis, T., J. Laine, A. Simon, A. Roland, C. Leterrier, and Z. Lenkei, *The type 1 cannabinoid receptor is highly expressed in embryonic cortical projection neurons and negatively regulates neurite growth in vitro.* Eur J Neurosci, 2008. **28**(9): p. 1705-18.
48. Castillo, P.E., T.J. Younts, A.E. Chavez, and Y. Hashimotodani, *Endocannabinoid signaling and synaptic function.* Neuron, 2012. **76**(1): p. 70-81.
49. Zou, S. and U. Kumar, *Cannabinoid Receptors and the Endocannabinoid System: Signaling and Function in the Central Nervous System.* Int J Mol Sci, 2018. **19**(3).
50. Glass, M. and C.C. Felder, *Concurrent stimulation of cannabinoid CB1 and dopamine D2 receptors augments cAMP accumulation in striatal neurons: evidence for a Gs linkage to the CB1 receptor.* J Neurosci, 1997. **17**(14): p. 5327-33.

51. Navarrete, M. and A. Araque, *Endocannabinoids mediate neuron-astrocyte communication.* Neuron, 2008. **57**(6): p. 883-93.

52. Roland, A.B., A. Ricobaraza, D. Carrel, B.M. Jordan, F. Rico, A. Simon, M. Humbert-Claude, J. Ferrier, M.H. McFadden, S. Scheuring, and Z. Lenkei, *Cannabinoid-induced actomyosin contractility shapes neuronal morphology and growth.* Elife, 2014. **3**: p. e03159.

53. Turu, G. and L. Hunyady, *Signal transduction of the CB1 cannabinoid receptor.* J Mol Endocrinol, 2010. **44**(2): p. 75-85.

54. Shin, J.E., B.R. Miller, E. Babetto, Y. Cho, Y. Sasaki, S. Qayum, E.V. Russler, V. Cavalli, J. Milbrandt, and A. DiAntonio, *SCG10 is a JNK target in the axonal degeneration pathway.* Proc Natl Acad Sci U S A, 2012. **109**(52): p. E3696-705.

55. Tortoriello, G., C.V. Morris, A. Alpar, J. Fuzik, S.L. Shirran, D. Calvigioni, E. Keimpema, C.H. Botting, K. Reinecke, T. Herdegen, M. Courtney, Y.L. Hurd, and T. Harkany, *Miswiring the brain: Delta9-tetrahydrocannabinol disrupts cortical development by inducing an SCG10/stathmin-2 degradation pathway.* EMBO J, 2014. **33**(7): p. 668-85.

56. Riederer, B.M., V. Pellier, B. Antonsson, G. Di Paolo, S.A. Stimpson, R. Lutjens, S. Catsicas, and G. Grenningloh, *Regulation of microtubule dynamics by the neuronal growth-associated protein SCG10.* Proc Natl Acad Sci U S A, 1997. **94**(2): p. 741-5.

57. Maison, P., D.J. Walker, F.S. Walsh, G. Williams, and P. Doherty, *BDNF regulates neuronal sensitivity to endocannabinoids.* Neurosci Lett, 2009. **467**(2): p. 90-4.

58. Aso, E., A. Ozaita, E.M. Valdizan, C. Ledent, A. Pazos, R. Maldonado, and O. Valverde, *BDNF impairment in the hippocampus is related to enhanced despair behavior in CB1 knockout mice.* J Neurochem, 2008. **105**(2): p. 565-72.

59. Berghuis, P., M.B. Dobszay, X. Wang, S. Spano, F. Ledda, K.M. Sousa, G. Schulte, P. Ernfors, K. Mackie, G. Paratcha, Y.L. Hurd, and T. Harkany, *Endocannabinoids regulate interneuron migration and morphogenesis by transactivating the TrkB receptor.* Proc Natl Acad Sci U S A, 2005. **102**(52): p. 19115-20.

60. Williams, E.J., F.S. Walsh, and P. Doherty, *The FGF receptor uses the endocannabinoid signaling system to couple to an axonal growth response.* J Cell Biol, 2003. **160**(4): p. 481-6.
61. Argaw, A., G. Duff, N. Zabouri, B. Cecyre, N. Chaine, H. Cherif, N. Tea, B. Lutz, M. Ptito, and J.F. Bouchard, *Concerted action of CB1 cannabinoid receptor and deleted in colorectal cancer in axon guidance.* J Neurosci, 2011. **31**(4): p. 1489-99.
62. Alpar, A., G. Tortoriello, D. Calvigioni, M.J. Niphakis, I. Milenkovic, J. Bakker, G.A. Cameron, J. Hanics, C.V. Morris, J. Fuzik, G.G. Kovacs, B.F. Cravatt, J.G. Parnavelas, W.D. Andrews, Y.L. Hurd, E. Keimpema, and T. Harkany, *Endocannabinoids modulate cortical development by configuring Slit2/Robo1 signalling.* Nat Commun, 2014. **5**: p. 4421.
63. Paria, B.C. and S.K. Dey, *Ligand-receptor signaling with endocannabinoids in preimplantation embryo development and implantation.* Chem Phys Lipids, 2000. **108**(1-2): p. 211-20.
64. Matsuda, L.A., S.J. Lolait, M.J. Brownstein, A.C. Young, and T.I. Bonner, *Structure of a cannabinoid receptor and functional expression of the cloned cDNA.* Nature, 1990. **346**(6284): p. 561-4.
65. Maccarrone, M., I. Bab, T. Biro, G.A. Cabral, S.K. Dey, V. Di Marzo, J.C. Konje, G. Kunos, R. Mechoulam, P. Pacher, K.A. Sharkey, and A. Zimmer, *Endocannabinoid signaling at the periphery: 50 years after THC.* Trends Pharmacol Sci, 2015. **36**(5): p. 277-96.
66. Maejima, T., T. Ohno-Shosaku, and M. Kano, *Endogenous cannabinoid as a retrograde messenger from depolarized postsynaptic neurons to presynaptic terminals.* Neurosci Res, 2001. **40**(3): p. 205-10.
67. Chevaleyre, V., K.A. Takahashi, and P.E. Castillo, *Endocannabinoid-mediated synaptic plasticity in the CNS.* Annu Rev Neurosci, 2006. **29**: p. 37-76.
68. Marinelli, S., S. Pacioni, A. Cannich, G. Marsicano, and A. Bacci, *Self-modulation of neocortical pyramidal neurons by endocannabinoids.* Nat Neurosci, 2009. **12**(12): p. 1488-90.
69. Marinelli, S., S. Pacioni, T. Bisogno, V. Di Marzo, D.A. Prince, J.R. Huguenard, and A. Bacci, *The endocannabinoid 2-arachidonoylglycerol is responsible for the*

slow self-inhibition in neocortical interneurons. J Neurosci, 2008. **28**(50): p. 13532-41.

70. Harkany, T. and V. Cinquina, *Physiological Rules of Endocannabinoid Action During Fetal and Neonatal Brain Development.* Cannabis Cannabinoid Res, 2021. **6**(5): p. 381-388.
71. Aguado, T., K. Monory, J. Palazuelos, N. Stella, B. Cravatt, B. Lutz, G. Marsicano, Z. Kokaia, M. Guzman, and I. Galve-Roperh, *The endocannabinoid system drives neural progenitor proliferation.* FASEB J, 2005. **19**(12): p. 1704-6.
72. Mulder, J., T. Aguado, E. Keimpema, K. Barabas, C.J. Ballester Rosado, L. Nguyen, K. Monory, G. Marsicano, V. Di Marzo, Y.L. Hurd, F. Guillemot, K. Mackie, B. Lutz, M. Guzman, H.C. Lu, I. Galve-Roperh, and T. Harkany, *Endocannabinoid signaling controls pyramidal cell specification and long-range axon patterning.* Proc Natl Acad Sci U S A, 2008. **105**(25): p. 8760-5.
73. Jiang, W., Y. Zhang, L. Xiao, J. Van Cleemput, S.P. Ji, G. Bai, and X. Zhang, *Cannabinoids promote embryonic and adult hippocampus neurogenesis and produce anxiolytic- and antidepressant-like effects.* J Clin Invest, 2005. **115**(11): p. 3104-16.
74. Aguado, T., J. Palazuelos, K. Monory, N. Stella, B. Cravatt, B. Lutz, G. Marsicano, Z. Kokaia, M. Guzman, and I. Galve-Roperh, *The endocannabinoid system promotes astroglial differentiation by acting on neural progenitor cells.* J Neurosci, 2006. **26**(5): p. 1551-61.
75. Maccarrone, M., M. Guzman, K. Mackie, P. Doherty, and T. Harkany, *Programming of neural cells by (endo)cannabinoids: from physiological rules to emerging therapies.* Nat Rev Neurosci, 2014. **15**(12): p. 786-801.
76. Diaz-Alonso, J., A. de Salas-Quiroga, J. Paraiso-Luna, D. Garcia-Rincon, P.P. Garcez, M. Parsons, C. Andradas, C. Sanchez, F. Guillemot, M. Guzman, and I. Galve-Roperh, *Loss of Cannabinoid CB1 Receptors Induces Cortical Migration Malformations and Increases Seizure Susceptibility.* Cereb Cortex, 2017. **27**(11): p. 5303-5317.
77. Berghuis, P., A.M. Rajnicek, Y.M. Morozov, R.A. Ross, J. Mulder, G.M. Urban, K. Monory, G. Marsicano, M. Matteoli, A. Canty, A.J. Irving, I. Katona, Y. Yanagawa, P. Rakic, B. Lutz, K. Mackie, and T. Harkany, *Hardwiring the brain:*

endocannabinoids shape neuronal connectivity. Science, 2007. **316**(5828): p. 1212-6.

78. Wu, C.S., J. Zhu, J. Wager-Miller, S. Wang, D. O'Leary, K. Monory, B. Lutz, K. Mackie, and H.C. Lu, *Requirement of cannabinoid CB(1) receptors in cortical pyramidal neurons for appropriate development of corticothalamic and thalamocortical projections.* Eur J Neurosci, 2010. **32**(5): p. 693-706.
79. Zurolo, E., A.M. Iyer, W.G. Spliet, P.C. Van Rijen, D. Troost, J.A. Gorter, and E. Aronica, *CB1 and CB2 cannabinoid receptor expression during development and in epileptogenic developmental pathologies.* Neuroscience, 2010. **170**(1): p. 28-41.
80. Goncalves, M.B., P. Suetterlin, P. Yip, F. Molina-Holgado, D.J. Walker, M.J. Oudin, M.P. Zentar, S. Pollard, R.J. Yanez-Munoz, G. Williams, F.S. Walsh, M.N. Pangalos, and P. Doherty, *A diacylglycerol lipase-CB2 cannabinoid pathway regulates adult subventricular zone neurogenesis in an age-dependent manner.* Mol Cell Neurosci, 2008. **38**(4): p. 526-36.
81. Morozov, Y.M., K. Mackie, and P. Rakic, *Cannabinoid Type 1 Receptor is Undetectable in Rodent and Primate Cerebral Neural Stem Cells but Participates in Radial Neuronal Migration.* Int J Mol Sci, 2020. **21**(22).
82. Purves D, A.G., Fitzpatrick D, et al., editors., *Neuroscience. 2nd edition*. 2001, Sunderland (MA): Sinauer Associates.
83. O'Donnell, M., R.K. Chance, and G.J. Bashaw, *Axon growth and guidance: receptor regulation and signal transduction.* Annu Rev Neurosci, 2009. **32**: p. 383-412.
84. Keimpema, E., G. Tortoriello, A. Alpar, S. Capsoni, I. Arisi, D. Calvigioni, S.S. Hu, A. Cattaneo, P. Doherty, K. Mackie, and T. Harkany, *Nerve growth factor scales endocannabinoid signaling by regulating monoacylglycerol lipase turnover in developing cholinergic neurons.* Proc Natl Acad Sci U S A, 2013. **110**(5): p. 1935-40.
85. Cristino, L. and V. Di Marzo, *Fetal cannabinoid receptors and the "dis-joint-ed" brain.* EMBO J, 2014. **33**(7): p. 665-7.

86. de Graaf, G., F. Buckley, and B.G. Skotko, *Estimates of the live births, natural losses, and elective terminations with Down syndrome in the United States.* Am J Med Genet A, 2015. **167A**(4): p. 756-67.
87. Haydar, T.F. and R.H. Reeves, *Trisomy 21 and early brain development.* Trends Neurosci, 2012. **35**(2): p. 81-91.
88. Klein, J.A. and T.F. Haydar, *Neurodevelopment in Down syndrome: Concordance in humans and models.* Front Cell Neurosci, 2022. **16**: p. 941855.
89. Altuna, M., S. Gimenez, and J. Fortea, *Epilepsy in Down Syndrome: A Highly Prevalent Comorbidity.* J Clin Med, 2021. **10**(13).
90. Raz, N., I.J. Torres, S.D. Briggs, W.D. Spencer, A.E. Thornton, W.J. Loken, F.M. Gunning, J.D. McQuain, N.R. Driesen, and J.D. Acker, *Selective neuroanatomic abnormalities in Down's syndrome and their cognitive correlates: evidence from MRI morphometry.* Neurology, 1995. **45**(2): p. 356-66.
91. Pinter, J.D., S. Eliez, J.E. Schmitt, G.T. Capone, and A.L. Reiss, *Neuroanatomy of Down's syndrome: a high-resolution MRI study.* Am J Psychiatry, 2001. **158**(10): p. 1659-65.
92. Wisniewski, K.E., *Down syndrome children often have brain with maturation delay, retardation of growth, and cortical dysgenesis.* Am J Med Genet Suppl, 1990. **7**: p. 274-81.
93. Schmidt-Sidor, B., K.E. Wisniewski, T.H. Shepard, and E.A. Sersen, *Brain growth in Down syndrome subjects 15 to 22 weeks of gestational age and birth to 60 months.* Clin Neuropathol, 1990. **9**(4): p. 181-90.
94. Contestabile, A., T. Fila, C. Ceccarelli, P. Bonasoni, L. Bonapace, D. Santini, R. Bartesaghi, and E. Ciani, *Cell cycle alteration and decreased cell proliferation in the hippocampal dentate gyrus and in the neocortical germinal matrix of fetuses with Down syndrome and in Ts65Dn mice.* Hippocampus, 2007. **17**(8): p. 665-78.
95. Larsen, K.B., H. Laursen, N. Graem, G.B. Samuelsen, N. Bogdanovic, and B. Pakkenberg, *Reduced cell number in the neocortical part of the human fetal brain in Down syndrome.* Ann Anat, 2008. **190**(5): p. 421-7.
96. Guidi, S., A. Giacomini, F. Stagni, M. Emili, B. Uguagliati, M.P. Bonasoni, and R. Bartesaghi, *Abnormal development of the inferior temporal region in fetuses with Down syndrome.* Brain Pathol, 2018. **28**(6): p. 986-998.

97. Zdaniuk, G., T. Wierzba-Bobrowicz, G.M. Szpak, and T. Stepien, *Astroglia disturbances during development of the central nervous system in fetuses with Down's syndrome.* Folia Neuropathol, 2011. **49**(2): p. 109-14.

98. Golden, J.A. and B.T. Hyman, *Development of the superior temporal neocortex is anomalous in trisomy 21.* J Neuropathol Exp Neurol, 1994. **53**(5): p. 513-20.

99. Benavides-Piccione, R., I. Ballesteros-Yanez, M.M. de Lagran, G. Elston, X. Estivill, C. Fillat, J. Defelipe, and M. Dierssen, *On dendrites in Down syndrome and DS murine models: a spiny way to learn.* Prog Neurobiol, 2004. **74**(2): p. 111-26.

100. Weitzdoerfer, R., M. Dierssen, M. Fountoulakis, and G. Lubec, *Fetal life in Down syndrome starts with normal neuronal density but impaired dendritic spines and synaptosomal structure.* J Neural Transm Suppl, 2001(61): p. 59-70.

101. Guidi, S., P. Bonasoni, C. Ceccarelli, D. Santini, F. Gualtieri, E. Ciani, and R. Bartesaghi, *Neurogenesis impairment and increased cell death reduce total neuron number in the hippocampal region of fetuses with Down syndrome.* Brain Pathol, 2008. **18**(2): p. 180-97.

102. Guidi, S., E. Ciani, P. Bonasoni, D. Santini, and R. Bartesaghi, *Widespread proliferation impairment and hypocellularity in the cerebellum of fetuses with down syndrome.* Brain Pathol, 2011. **21**(4): p. 361-73.

103. Aziz, N.M., F. Guedj, J.L.A. Pennings, J.L. Olmos-Serrano, A. Siegel, T.F. Haydar, and D.W. Bianchi, *Lifespan analysis of brain development, gene expression and behavioral phenotypes in the Ts1Cje, Ts65Dn and Dp(16)1/Yey mouse models of Down syndrome.* Dis Model Mech, 2018. **11**(6).

104. Chakrabarti, L., Z. Galdzicki, and T.F. Haydar, *Defects in embryonic neurogenesis and initial synapse formation in the forebrain of the Ts65Dn mouse model of Down syndrome.* J Neurosci, 2007. **27**(43): p. 11483-95.

105. Chakrabarti, L., T.K. Best, N.P. Cramer, R.S. Carney, J.T. Isaac, Z. Galdzicki, and T.F. Haydar, *Olig1 and Olig2 triplication causes developmental brain defects in Down syndrome.* Nat Neurosci, 2010. **13**(8): p. 927-34.

106. Fernandez, F., W. Morishita, E. Zuniga, J. Nguyen, M. Blank, R.C. Malenka, and C.C. Garner, *Pharmacotherapy for cognitive impairment in a mouse model of Down syndrome.* Nat Neurosci, 2007. **10**(4): p. 411-3.

107. Cheng, A., T.F. Haydar, P.J. Yarowsky, and B.K. Krueger, *Concurrent generation of subplate and cortical plate neurons in developing trisomy 16 mouse cortex.* Dev Neurosci, 2004. **26**(2-4): p. 255-65.

108. Jain, S., C.A. Watts, W.C.J. Chung, and K. Welshhans, *Neurodevelopmental wiring deficits in the Ts65Dn mouse model of Down syndrome.* Neurosci Lett, 2020. **714**: p. 134569.

109. Huo, H.Q., Z.Y. Qu, F. Yuan, L. Ma, L. Yao, M. Xu, Y. Hu, J. Ji, A. Bhattacharyya, S.C. Zhang, and Y. Liu, *Modeling Down Syndrome with Patient iPSCs Reveals Cellular and Migration Deficits of GABAergic Neurons.* Stem Cell Reports, 2018. **10**(4): p. 1251-1266.

110. Bahn, S., M. Mimmack, M. Ryan, M.A. Caldwell, E. Jauniaux, M. Starkey, C.N. Svendsen, and P. Emson, *Neuronal target genes of the neuron-restrictive silencer factor in neurospheres derived from fetuses with Down's syndrome: a gene expression study.* Lancet, 2002. **359**(9303): p. 310-5.

111. Vázquez-Oliver, A., *Long-term decreased cannabinoid type-1 receptor activity restores specific neurological phenotypes in the Ts65Dn mouse model of Down syndrome.* Neuroscience, 2021. **Preprint**.

112. Di Franco, N., G. Drutel, V. Roullot-Lacarriere, F. Julio-Kalajzic, V. Lalanne, A. Grel, T. Leste-Lasserre, I. Matias, A. Cannich, D. Gonzales, V. Simon, D. Cota, G. Marsicano, P.V. Piazza, M. Vallee, and J.M. Revest, *Differential expression of the neuronal CB1 cannabinoid receptor in the hippocampus of male Ts65Dn Down syndrome mouse model.* Mol Cell Neurosci, 2022. **119**: p. 103705.

113. Navarro-Romero, A., A. Vazquez-Oliver, M. Gomis-Gonzalez, C. Garzon-Montesinos, R. Falcon-Moya, A. Pastor, E. Martin-Garcia, N. Pizarro, A. Busquets-Garcia, J.M. Revest, P.V. Piazza, F. Bosch, M. Dierssen, R. de la Torre, A. Rodriguez-Moreno, R. Maldonado, and A. Ozaita, *Cannabinoid type-1 receptor blockade restores neurological phenotypes in two models for Down syndrome.* Neurobiol Dis, 2019. **125**: p. 92-106.

114. Pinter, A., Z. Hevesi, P. Zahola, A. Alpar, and J. Hanics, *Chondroitin sulfate proteoglycan-5 forms perisynaptic matrix assemblies in the adult rat cortex.* Cell Signal, 2020. **74**: p. 109710.

115. Bradford, M.M., *A rapid and sensitive method for the quantitation of microgram quantities of protein utilizing the principle of protein-dye binding.* Anal Biochem, 1976. **72**: p. 248-54.

116. Fuzik, J., S. Rehman, F. Girach, A.G. Miklosi, S. Korchynska, G. Arque, R.A. Romanov, J. Hanics, L. Wagner, K. Meletis, Y. Yanagawa, G.G. Kovacs, A. Alpar, T.G.M. Hokfelt, and T. Harkany, *Brain-wide genetic mapping identifies the indusium griseum as a prenatal target of pharmacologically unrelated psychostimulants.* Proc Natl Acad Sci U S A, 2019. **116**(51): p. 25958-25967.

117. Maruta, H., K. Greer, and J.L. Rosenbaum, *The acetylation of alpha-tubulin and its relationship to the assembly and disassembly of microtubules.* J Cell Biol, 1986. **103**(2): p. 571-9.

118. Jordan, J.D., J.C. He, N.J. Eungdamrong, I. Gomes, W. Ali, T. Nguyen, T.G. Bivona, M.R. Philips, L.A. Devi, and R. Iyengar, *Cannabinoid receptor-induced neurite outgrowth is mediated by Rap1 activation through G(alpha)o/i-triggered proteasomal degradation of Rap1GAPII.* J Biol Chem, 2005. **280**(12): p. 11413-21.

119. He, J.C., I. Gomes, T. Nguyen, G. Jayaram, P.T. Ram, L.A. Devi, and R. Iyengar, *The G alpha(o/i)-coupled cannabinoid receptor-mediated neurite outgrowth involves Rap regulation of Src and Stat3.* J Biol Chem, 2005. **280**(39): p. 33426-34.

120. *Results from the 2010 National Survey on Drug Use and Health: Summary of National Findings*. 2011, Substance Abuse and Mental Health Services Administration: Rockville, MD.

121. van Gelder, M.M., J. Reefhuis, A.R. Caton, M.M. Werler, C.M. Druschel, N. Roeleveld, and S. National Birth Defects Prevention, *Maternal periconceptional illicit drug use and the risk of congenital malformations.* Epidemiology, 2009. **20**(1): p. 60-6.

122. Wu, C.S., C.P. Jew, and H.C. Lu, *Lasting impacts of prenatal cannabis exposure and the role of endogenous cannabinoids in the developing brain.* Future Neurol, 2011. **6**(4): p. 459-480.

123. Khare, M., A.H. Taylor, J.C. Konje, and S.C. Bell, *Delta9-tetrahydrocannabinol inhibits cytotrophoblast cell proliferation and modulates gene transcription.* Mol Hum Reprod, 2006. **12**(5): p. 321-33.

124. Campolongo, P., V. Trezza, M. Palmery, L. Trabace, and V. Cuomo, *Developmental exposure to cannabinoids causes subtle and enduring neurofunctional alterations.* Int Rev Neurobiol, 2009. **85**: p. 117-33.

125. Milenkovic, I., T. Stojanovic, E. Aronica, L. Fulop, Z. Bozso, Z. Mate, Y. Yanagawa, H. Adle-Biassette, G. Lubec, G. Szabo, T. Harkany, G.G. Kovacs, and E. Keimpema, *GABA(A) receptor subunit deregulation in the hippocampus of human foetuses with Down syndrome.* Brain Struct Funct, 2018. **223**(3): p. 1501-1518.

126. Ludanyi, A., L. Eross, S. Czirjak, J. Vajda, P. Halasz, M. Watanabe, M. Palkovits, Z. Magloczky, T.F. Freund, and I. Katona, *Downregulation of the CB1 cannabinoid receptor and related molecular elements of the endocannabinoid system in epileptic human hippocampus.* J Neurosci, 2008. **28**(12): p. 2976-90.

127. Martin, B.S. and M.M. Huntsman, *Pathological plasticity in fragile X syndrome.* Neural Plast, 2012. **2012**: p. 275630.

128. Murray, R.M., A. Englund, A. Abi-Dargham, D.A. Lewis, M. Di Forti, C. Davies, M. Sherif, P. McGuire, and D.C. D'Souza, *Cannabis-associated psychosis: Neural substrate and clinical impact.* Neuropharmacology, 2017. **124**: p. 89-104.

129. Melamed, Z., J. Lopez-Erauskin, M.W. Baughn, O. Zhang, K. Drenner, Y. Sun, F. Freyermuth, M.A. McMahon, M.S. Beccari, J.W. Artates, T. Ohkubo, M. Rodriguez, N. Lin, D. Wu, C.F. Bennett, F. Rigo, S. Da Cruz, J. Ravits, C. Lagier-Tourenne, and D.W. Cleveland, *Premature polyadenylation-mediated loss of stathmin-2 is a hallmark of TDP-43-dependent neurodegeneration.* Nat Neurosci, 2019. **22**(2): p. 180-190.

130. Lumeng, J.C., H.J. Cabral, K. Gannon, T. Heeren, and D.A. Frank, *Pre-natal exposures to cocaine and alcohol and physical growth patterns to age 8 years.* Neurotoxicol Teratol, 2007. **29**(4): p. 446-57.

131. Fried, P.A. and A.M. Smith, *A literature review of the consequences of prenatal marihuana exposure. An emerging theme of a deficiency in aspects of executive function.* Neurotoxicol Teratol, 2001. **23**(1): p. 1-11.

132. Trezza, V., V. Cuomo, and L.J. Vanderschuren, *Cannabis and the developing brain: insights from behavior.* Eur J Pharmacol, 2008. **585**(2-3): p. 441-52.
133. Reece, A.S. and G.K. Hulse, *Epidemiological overview of multidimensional chromosomal and genome toxicity of cannabis exposure in congenital anomalies and cancer development.* Sci Rep, 2021. **11**(1): p. 13892.

9. Bibliography of the candidate's publications

9.1. Publication related to the thesis

Patthy Á, Hanics J, Zachar G, Kovács GG, Harkany T, Alpár A. Regional redistribution of CB1 cannabinoid receptors in human foetal brains with Down's syndrome and their functional modifications in Ts65Dn$^{+/+}$ mice. Neuropathol Appl Neurobiol. 2023 Feb;49(1):e12887. doi: 10.1111/nan.12887. PMID: 36716771.

9.2. Posters related to the thesis

Patthy Á, Alpár A. Kannabinoid receptor expresszió magzati agyvelőben és változásai Down-kórban. Annual conference of the Hungarian Anatomical Society, Budapest, 2021

Patthy Á, Kovács GG, Harkany T, Alpár A. Cannabinoid receptor type 1 expression in the fetal cortex and its alterations in Down syndrome. International Neuroscience Meeting, Budapest, 2022

Patthy Á, Hanics J, Zachar G, Kovács GG, Harkany T, Alpár A. Regional redistribution of CB1 cannabinoid receptors in human fetal brains with Down's syndrome, and their functional modifications in Ts65Dn$^{+/+}$ mice. Joint Meeting of the Hungarian Neuroscience Society and the Austrian Neuroscience Association, Budapest, 2023

9.3. Presentation related to the thesis

Patthy Á, Alpár A. 1-es típusú kannabinoid receptor expresszió magzati agyvelőben és változásai Down-kórban. Semmelweis University Students' Scientific Conference, Budapest, 2022

9.4. Publication not related to the thesis

Patthy Á, Murai J, Hanics J, Pintér A, Zahola P, Hökfelt TGM, Harkany T, Alpár A. Neuropathology of the Brainstem to Mechanistically Understand and to Treat Alzheimer's Disease. J Clin Med. 2021 Apr 7;10(8):1555. doi: 10.3390/jcm10081555. PMID: 33917176; PMCID: PMC8067882.

10. Acknowledgements

First, I would like to express my deepest gratitude to my supervisor and mentor Professor Dr. Alán Alpár, who persistently and patiently supported my work with his guidance and constructive advice. Without the constant motivation and encouragement provided by him, this thesis would not have been possible. I am proud to record that I had the opportunity to work with an exceptionally erudite, experienced and humble professor like him.

I owe a debt of gratitude to the members of the Research Group of Experimental Neuroanatomy and Developmental Biology – Dr. János Hanics, Andrea Németh –, and Dr. Gergely Zachar for their substantial help in carrying out the experimental work.

I am grateful to Professor Dr. Gábor G. Kovács and the associates of the Institute of Neurology at the Medical University of Vienna for providing us the great number of human samples that laid the foundation for our research.

I would like to thank Professor Dr. Tibor Harkany the conceivement of the study and the fruitful consultations, and Professor Dr. Ken Mackie the gift of the anti-CB_1R antibody.

Last but not least, I am indebted to my family and friends who provided an inspiring and supportive environment, and whose unwavering belief in my abilites fueled my perseverance.

Received: 10 May 2022 | Revised: 24 January 2023 | Accepted: 25 January 2023

DOI: 10.1111/nan.12887

ORIGINAL ARTICLE

Neuropathology and Applied Neurobiology
JOURNAL OF THE BRITISH NEUROPATHOLOGICAL SOCIETY

WILEY

Regional redistribution of CB1 cannabinoid receptors in human foetal brains with Down's syndrome and their functional modifications in Ts65Dn$^{+/+}$ mice

Ágoston Patthy[1] | János Hanics[1,2] | Gergely Zachar[1] | Gábor G. Kovács[3,4] | Tibor Harkany[5,6] | Alán Alpár[1,2]

[1]Department of Anatomy, Semmelweis University, Budapest, Hungary

[2]SE NAP Research Group of Experimental Neuroanatomy and Developmental Biology, Semmelweis University, Budapest, Hungary

[3]Institute of Neurology, Medical University of Vienna, Vienna, Austria

[4]Department of Laboratory Medicine and Pathobiology and Tanz Centre for Research in Neurodegenerative Disease, University of Toronto, Toronto, Canada

[5]Department of Molecular Neurosciences, Center for Brain Research, Medical University of Vienna, Vienna, Austria

[6]Department of Neuroscience, Biomedicum, Karolinska Institutet, Solna, Sweden

Correspondence
Alán Alpár, H-1085 Budapest, Tűzoltó utca 58, Budapest, Hungary.
Email: alpar.alan@med.semmelweis-univ.hu

Funding information
This work was supported by the National Brain Research Program of Hungary (2017-1.2.1-NKP-2017-00002 and NAP2022-I-1/2022 to A.A.); the Excellence Program for Higher Education of Hungary (TKP-EGA-25, A.A.); the Swedish Medical Research Council (2018-02838 to T.H.); Novo Nordisk Foundation (NNF20OC0063667 to T.H.); the NKFIH UNKP-22-23 and the FK 131966 grants (to G.Z.); Hjärnfonden (FO2019-0277 to T.H.); and the European Research Council (FOODFORLIFE, 2020-AdG-101021016, and SECRET-DOCK, 2022-PoC2-101082277 to T.H.).

Abstract

Aims: The endocannabinoid system with its type 1 cannabinoid receptor (CB_1R) expressed in postmitotic neuroblasts is a critical chemotropic guidance module with its actions cascading across neurogenic commitment, neuronal polarisation and synaptogenesis in vertebrates. Here, we present the systematic analysis of regional CB_1R expression in the developing human brain from gestational week 14 until birth. In parallel, we diagrammed differences in CB_1R development in Down syndrome foetuses and identified altered CB_1R signalling.

Methods: Foetal brains with normal development or with Down's syndrome were analysed using standard immunohistochemistry, digitalised light microscopy and image analysis (NanoZoomer). CB_1R function was investigated by in vitro neuropharmacology from neonatal Ts65Dn transgenic mice brains carrying an additional copy of ~90 conserved protein-coding gene orthologues of the human chromosome 21.

Results: We detected a meshwork of fine-calibre, often varicose processes between the subventricular and intermediate zones of the cortical plate in the late first trimester, when telencephalic fibre tracts develop. The density of CB_1Rs gradually decreased during the second and third trimesters in the neocortex. In contrast, CB_1R density was maintained, or even increased, in the hippocampus. We found the onset of CB_1R expression being delayed by ≥1 month in age-matched foetal brains with Down's syndrome. In vitro, CB_1R excitation induced excess microtubule stabilisation and, consequently, reduced neurite outgrowth.

Conclusions: We suggest that neuroarchitectural impairments in Down's syndrome brains involve the delayed development and errant functions of the endocannabinoid system, with a particular impact on endocannabinoids modulating axonal wiring.

KEYWORDS
cannabinoid receptor, developmental delay, endocannabinoid system, genetic brain disease, neurodevelopmental disorder, trisomy

INTRODUCTION

The temporal and spatial interaction of chemotropic guidance systems shapes brain development by controlling many aspects of intercellular communication. Amongst these signalling modules, the endocannabinoid system is recognised as one of the most abundant units, which is present in virtually all synapses. Endocannabinoid signalling attracted significant interest recently because of its medical relevance and sensitivity to plant-derived and synthetic drugs [1, 2]. Notably, both the localization and function of the enzymatic machinery controlling endocannabinoid bioavailability and of both the typical and atypical cannabinoid receptors differ between foetal and adult brains [3–6]. Both 2-arachidonoglycerol (2-AG) [7] and anandamide (AEA) [8], the major endocannabinoid ligands, participate in the retrograde control of synaptic plasticity at mature synapses by acting at type 1 cannabinoid receptors (CB_1Rs) postnatally [4–6]. In contrast, the endocannabinoid family of small signal lipids serves as one of the guidance systems to define synapse localisation and selection during brain development. Herein, endocannabinoids can act in an autocrine/cell-autonomous fashion when controlling neural progenitor proliferation through non-CB_1R-mediated mechanisms [9–12]. Indeed, CB_1R expression is seen as a feature of neurogenic commitment in vertebrates [13], with a marked increase in CB_1R expression and responsiveness once neuroblasts leave their respective progenitor zones [14, 15]. Subsequently, endocannabinoids modulate directional motility for both neurons (cell migration) and their navigating neurites (neuronal polarisation and pathfinding) [16, 17], at least in the cerebral cortex. In doing so, endocannabinoid engagement of CB_1Rs can alter cytoskeletal dynamics in growth cones and neurites [18], alone or in interplay with other signalling systems [19]. Endocannabinoids so far have been suggested to act by volumetric diffusion (although they are released by postsynaptic vesicular exocytosis, in a process that requires synucleins [20]) because signal lipids can likely spread along and within biological membranes. Endocannabinoid signals could thus have a substantial impact, particularly during intrauterine development, when neuronal polarisation and morphogenesis rest on a >1,000-fold expansion of the membrane surface in each neuroblast and when the brain is yet devoid of astroglial and/or oligodendroglial limiting cellular barriers [17]. Despite the incomplete glial map of the antenatal brain, diffusible lipids can instead be spatially confined by recruitment of the enzymatic machinery that controls their availability. For 2-AG, the differential distribution of *sn*-1-diacylglycerol lipases (DAGLα) and monoacylglycerol lipase (MAGL) along growing neurites is one such example to maintain unidirectional lipid signalling [16, 17]. Once the ground plan of the neuronal connectome is complete, endocannabinoid signalling between glia and neurons starts to refine neuronal metabolism and synaptic neurotransmission [19].

Within the family of 'cannabinoid receptors' [21, 22], the CB_1R predominates in the nervous system of both rodents [14] and humans [23]. Because of its abundant expression, neocortical development is thought to rely on CB_1Rs-mediated endocannabinoid signalling. Upon synthesis and *trans*-Golgi maturation in neuronal somata [12], CB_1Rs are rapidly transported on small vesicles along corticofugal axons [24].

Key points

- This study gives a regional distribution pattern of cannabinoid receptor type 1 expression in the human foetal brain.
- In Down's syndrome, receptor expression is delayed by at least a month.
- CB_1R activation induces excess microtubule stabilisation in cortical neurons of Ts65Dn Down's syndrome model transgenic mice.

The preferential axonal distribution of CB_1Rs can thus steer directional growth decisions [14, 19]. Even before developmental processes are complete, CB_1Rs accumulate in varicose foci in nascent axons, thus marking prospective terminal and/or *en passant* synaptic boutons [25, 26]. This subcellular distribution of CB_1Rs is thus poised to uninterruptedly traverse from growth to the retrograde control of emergent synaptic activity [27, 28]. CB_1R activation during foetal life triggers either mTOR [14, 29] or Erk, PI3K/Akt and c-Jun kinase signalling [30]. For the c-Jun cascade, the rate of c-Jun N-terminal kinase (JNK1) phosphorylation/dephosphorylation represents a major determinant of cytoskeletal instability. This is because JNK1 exerts a direct effect on the availability of SCG10/stathmin-2 by triggering its proteasomal degradation by phosphorylation. SCG10/stathmin-2 itself controls tubulin availability for cytoskeletal reorganisation [18], including during neuritogenesis.

Despite recent progress [31–33], we know little about whether errant endocannabinoid signalling contributes to the pathogenesis of developmental brain disorders or if its changes are instead secondary to the evolving pattern of structural synaptic deficits. The best-known congenital neurological disorders with endocannabinoid involvement are fragile X syndrome [34] and epilepsy [35]. Synaptic impairment in fragile X syndrome, a genetic disorder caused by a mutant form of the *FMR1* gene, is attenuated by non-CB_1R-acting cannabidiol (ZYN002) [36]. Alternatively, the efficacy of CB_1R antagonism to reverse synaptic deficits in a mouse model of fragile X syndrome offers a therapeutic perspective [37]. The developmental significance of manipulating endocannabinoid signalling is illustrated by the ability of CB_1R antagonists to shift the excitation/inhibition balance in cortical neurocircuits, thus inducing epileptiform discharges in infants. Conversely, enhanced signalling at CB_1Rs dampens network activity, at least in animal models [25].

Here, we focused on Down's syndrome, or trisomy 21, a major genetic cause of intellectual disability with a probability of about 1-in-700-to-1,000 live births [38]. Epilepsy is a highly prevalent comorbidity of Down's syndrome [39]. At the cellular level, Down's syndrome is characterised by altered cortical lamination and decreased synaptic neurotransmission, the latter being due to the malformation of dendrites, including dendritic spines, which are the structural targets of excitatory synapses [40, 41]. Previously, down-regulation of repressor

element-1 silencing transcription factor (REST)-regulated genes was identified in foetuses with Down's syndrome [42]. Amongst these, *STMN2* (the gene coding the SCG10 protein) was the topmost affected target. This finding is exciting for developmental neurobiologists because it allows us to link SCG10 to upstream CB_1R activity at synapses across the foetal brain [18]. Significantly, SCG10 protein expression in the developing brain is restricted to neuronal contingents that transit from a migratory towards a differentiated/polarised state and are actively engaged in neuritogenesis [43]. Therefore, we first systematically mapped CB_1R distribution in foetal brains with Down's syndrome and age-matched controls. Second, we tested a mechanistic link between CB_1R–SCG10 activity-impaired neuritogenesis in foetuses of Ts65Dn$^{+/+}$ mice, which carry an extra copy of a large part of the mouse chromosome 16, resulting in trisomy of around 90 conserved protein-coding gene orthologues to the human chromosome 21 [44–46]. Our findings reveal a temporal mismatch in antenatal CB_1R expression in Down's syndrome vs. age-matched controls, particularly in telencephalic axonal tracts, and implicate excess CB_1R-to-SCG10 signalling as a mechanism limiting neuritogenesis.

MATERIALS AND METHODS

Neuropathology: Human foetal tissues, their preparation, histochemistry and quantification

To map CB_1R distribution, $n = 13$ male and $n = 14$ female foetal brains with normal development (between gestational weeks 14 and 40) were selected from the Brain Bank of the Institute of Neurology, Medical University of Vienna, Austria. We investigated another $n = 3$ brains for which sex was unknown. Foetal brain tissue was obtained from spontaneous or medically induced abortions. Only cases without genetic disorders, head injury or neurological complications were included as controls. These cases showed neither chromosomal aberrations nor *post-mortem* autolysis. Neuropathological examination excluded major central nervous system malformations, severe hypoxic/ischemic encephalopathy, intraventricular haemorrhage, hydrocephalus, meningitis or ventriculitis. Another $n = 10$ male, $n = 8$ female and $n = 5$ foetal brains with unknown sex but all with Down's syndrome were included in this study. Tissues were obtained and used in compliance with the Declaration of Helsinki and following institutional guidelines. Brain analysis was performed according to an approval for histopathology by the Human Ethical Committee of the Medical University of Vienna (No. 104/2009).

Three-micrometre-thick tissue sections of formalin-fixed, paraffin-embedded tissue blocks were mounted on pre-coated glass slides (StarFrost). Shortly after deparaffinisation and rehydration, the sections were pre-treated in low-pH EnVision FLEX antigen retrieval solution at 98°C for 20 min (PTLink; Dako) and subsequently incubated with a polyclonal anti-CB_1R antibody made in rabbit (gift from Ken Mackie, 1:1,000, [16]). A biotinylated anti-rabbit secondary antibody produced in donkey (K5007, ThermoFisher) and the DAKO EnVision detection kit including peroxidase/3,3-diaminobenzidine-tetrahydrochloride (DAB; Agilent) were used to visualise antibody binding. Immunolabelling of the medulla oblongata, which harbours the corticospinal and corticobulbar tracts known to contain CB_1Rs in mammals [47], served as a positive control to validate the specificity of the anti-CB_1R^+ antibody (Figure 1A). Sections were counterstained with haematoxylin, dehydrated in an ascending gradient of ethanol, cleared with xylene and coverslipped with Consil-Mount (Shandon; ThermoFisher) (Figure 1B). Representative images containing the area of interest were automatically captured on a slide-scanner (Nikon) and exported from stored images using the NanoZoomer 2.0 plug-in (Hamamatsu). A semi-quantitative analysis of CB_1R^+ varicosities was made with the relative density of these structures classified as 0, +, + +, +++ or ++++. CB_1R^+ varicosities were counted in regions of

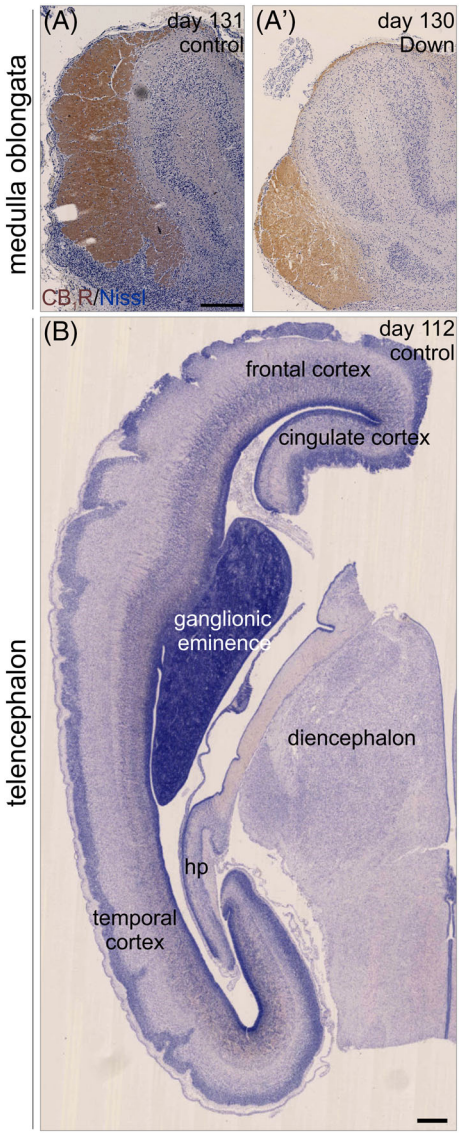

FIGURE 1 (A, A') CB_1R^+ pyramidal tract axons in the medulla oblongata of control and Down's syndrome subjects. (B) Overview of a foetal forebrain section indicating the regions studied. Abbreviations: CB_1R, cannabinoid receptor type 1; ctrl, control; hp, hippocampus. Scale bars = 1 mm

interest and normalised to equivalent surface areas (500 μm^2, $n = 10$/area/section) using the NanoZoomer 2.0 toolbox (Figure S1).

For confocal laser scanning microscopy, human samples were deparaffinated, rehydrated, washed in phosphate buffer (0.1 M PB; pH 7.4) and pre-treated with 0.3% Triton X-100 (Sigma; in 0.1 M PB) at 22–24°C for 2 h to enhance antibody penetration [18, 48] (Table S1). To suppress non-specific immunoreactivity, we incubated the tissue specimens in a mixture of 5% (wt/vol) normal donkey serum (NDS; Jackson ImmunoResearch), 2% (wt/vol) BSA (Sigma) and 0.3% Triton X-100 in 0.1 M PB at 22–24°C for another 1.5 h. Sections were then exposed to a mixture of mouse anti-NeuN and rabbit anti-CB_1R antibodies (Table S1) diluted in 0.1 M PB, to which 0.1% NDS and 0.3% Triton X-100 had been added, at 4°C for 16–72 h. Immunoreactivities were revealed by carbocyanine (Cy) 3- or 5-tagged secondary antibodies raised in donkey (1:200; Jackson) and applied at 22–24°C for 2 h. Nuclei were counterstained with Hoechst 33,421 (1:10,000; Sigma). Sections were dehydrated in an ascending gradient of ethanol, cleared with xylene and coverslipped with DePeX (ACM, Fluka). Images were captured on an LSM780 confocal laser-scanning microscope (Zeiss) with optical zoom ranging from 1–3X when using a 40X (Plan-Apochromat 40X/1.40) objective and the pinhole set to 0.5–0.7 μm ('optical thickness').

Experimental neurobiology: Dissociated cortical cultures of neonatal mice

On postnatal day 2 (P2), whole neocortices were dissected out from wild-type and littermate Ts65Dn$^{+/+}$ mice, the most common model of Down's syndrome [44–46]. Tissues were enzymatically dissociated and plated at a density of 200,000 cells/well in six-well plates for Western blotting. On day 2 in vitro (DIV), neurons were stimulated by WIN55,212-2 (500 nM, Tocris) for 30 min (control cultures received no vehicle treatment; we did not include WIN55,212-3 either because our earlier studies did not reveal any drug effect at 500 nM [49]) and lyzed immediately afterwards (see below).

Alternatively, primary neurons were seeded at a density of 50,000 cells/well on poly-D-lysine-coated coverslips in 24-well plates and maintained in DMEM/F12 (1:1) containing B27 supplement [2% (vol/-vol)], L-glutamine (2mM), penicillin (100 U/ml) and streptomycin (100 μg/ml) (all from Invitrogen). Neurons were challenged with WIN55,212-2 (500 nM) for 30 min on DIV2 and kept alive for another 24 h in maintenance medium (DMEM/F12/B27). Subsequently, cells on coverslips were immersion-fixed in ice-cold 4% paraformaldehyde in 0.05 M PB for morphometry. The rationale of this experiment was to test if Ts650Dn$^{+/+}$ neurons could overcome WIN55,212-2-induced growth arrest, as is known for wild-type neurons [18, 24, 49].

Western blotting

Neurons were collected and homogenised by sonication in TNE buffer containing 0.5% Triton X-100 (Sigma), 1% octyl-β-D-glucopyranoside (Calbiochem), 5mM NaF, 100 μM Na_3VO_4 and a mixture of protease inhibitors (Complete™; Roche). Cell debris and nuclei were pelleted by centrifugation (800×g at 4°C for 10 min). Protein concentration was determined by Bradford's colourimetric method [50]. Samples were diluted to a final protein concentration of 2 μg/μl, denatured in 5× Laemmli buffer and analysed by SDS-PAGE on 8% or 10% (vol/-vol) resolving gels. After transfer onto Immobilon-FL PVDF membranes (Millipore), membrane-bound protein samples were blocked in 3% (wt/vol) BSA and 0.5% Tween-20 diluted in TRIS-buffered saline (for 1.5 h) and exposed to primary antibodies (Table S1) at 4°C overnight. Appropriate combinations of horseradish peroxidase (HRP)-conjugated secondary antibodies from goat, rabbit or mouse hosts (Jackson; 1:10,000; 2 h) were used for signal detection. Image acquisition and analysis were performed on a Bio-Rad XRS$^+$ imaging platform.

Immunocytochemistry

Coverslips were rinsed in 0.1 M PB (pH 7.4) and pre-treated with 0.3% Triton X-100 (Sigma; in PB) at 22–24°C for 1 h to enhance the penetration of primary antibodies [18, 48] (Table S1). Non-specific immunoreactivity was suppressed by incubating our specimens in a mixture of 5% (wt/vol) NDS (Jackson), 2% (wt/vol) BSA (Sigma) and 0.3% Triton X-100 in 0.1 M PB at 22–24°C for another 1 h. Coverslips were then exposed to mouse anti-β-III-tubulin and rabbit anti-SCG10 primary antibodies (Table S1) diluted in 0.1 M PB, to which 0.1% NDS and 0.3% Triton X-100 had been added, at 4°C for 16–72 h. Immunoreactivities were revealed by carbocyanine (Cy) 2- or 3-tagged secondary antibodies raised in donkey (1:200; Jackson) and applied at 22–24°C for 2 h. Nuclei were routinely counterstained by Hoechst 33,421 (1:10,000; Sigma). Coverslips were drop-dried and mounted onto fluorescence-free glass slides with glycerol/gelatin (GG-1; Sigma). Images were captured on an LSM780 confocal laser-scanning microscope (Zeiss) with optical zoom ranging from 1–3X when using a 40X (Plan-Apochromat 40X/1.40) objective and the pinhole set to 0.5–0.7 μm ('optical thickness'). Emission spectra for the dyes were limited to 450–480 nm (Hoechst 33,421), 505–530 nm (Cy2) and 560–610 nm (Cy3).

Statistics

Data were expressed as means ± s.e.m. Morphological parameters were statistically compared between control ($n = 3$) and Down's syndrome ($n = 3$) subjects in equivalent age groups using two-tailed, paired Student's t tests with gestational age being the intrinsic variable for pairing (GraphPad Prism). A two-tailed Student's t test for independent samples was used to test pharmacological and genetic variables in vitro. A p value of <0.05 was taken as indicative of statistical differences. Multi-panel figures were assembled in CorelDraw X7 (Corel Corp.). The cohort available allowed us to investigate sex-specific differences only between gestational days 121–160. Applying

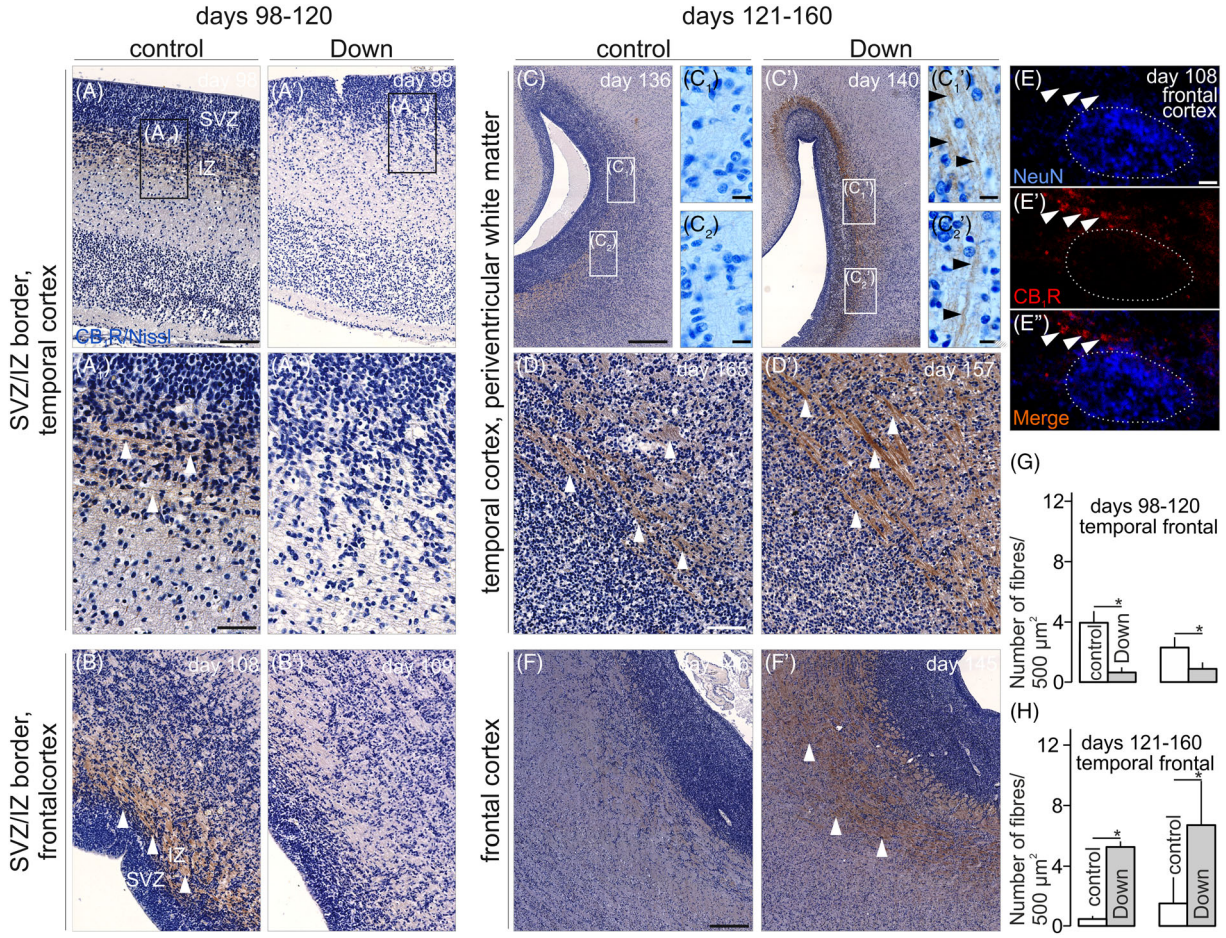

FIGURE 2 Axonal CB_1Rs in the neocortex in Down syndrome. Panels A-B′ and C-E′ show specimens between days 98–120 and 121–160, respectively. (A–A_1′) CB_1R^+ fibres in the SVZ/IZ zone of the temporal cortex in control but not in Down's syndrome subjects (*arrowheads* point to CB_1R^+ axons). (B, B′) CB_1R^+ fibres in the SVZ/IZ zone of the frontal cortex in control but not in Down syndrome subjects (*arrowheads*). (C–D′) Between days 121 and 160, CB_1R^+ processes dominated in Down's syndrome vs. control subjects in the periventricular temporal cortex (*white arrowheads* in D and D′). (E–E″) Extrasomatic CB_1R^+ profiles (*white arrowheads*). (F, F′) CB_1R^+ axonal bundles in Down's syndrome but not in control brains (*white arrowheads* in F′). (G) The density of CB_1R^+ fibres was lower in temporal and frontal cortices of subjects with Down's syndrome between days 98 and 120, as compared to age-matched controls. (H) CB_1R^+ density of subjects with Down's syndrome exceeded that of control subjects in the temporal and in frontal cortex between days 121 and 160. Abbreviations: CB_1R, cannabinoid receptor type 1; ctrl, control. Scale bar = 1 mm (C, F), 300 µm (A, D), 100 µm (A_1) and 3 µm (C_1)

the five unit scales (0, +, ++, +++, ++++; see first paragraph of this section), we used ordinal logistic regression models to investigate the interaction between Down's syndrome status and sex.

RESULTS

Neuropathology

CB_1R^+ processes and varicosities appeared as fine-calibre meshworks in most brain areas. Here, we first determined their distribution in cortical areas, hippocampal subfields and the cerebellum across the three trimesters of pregnancy. Our principal finding is the delayed appearance and persistent maintenance of CB_1R^+ fibres in foetuses with Down's syndrome as late as the fourth month of pregnancy, which contrasts the early and transient presence of CB_1R^+ axons coincident with their active growth processes in control foetuses.

Disrupted temporal dynamics of CB_1R expression in Down's syndrome in the second trimester

In control subjects, a dense bundle of CB_1R^+ fibres at the boundary between the cortical subventricular (SVZ) and intermediate zones (IZ) was detected, being particularly notable in the temporal cortex, between days 98 and 120 (Figure 2A, A_1). In contrast, less and weakly immunoreactive fibres were only visible in age-matched Down's syndrome samples in the corresponding regions (Figure 2A′, A_1′, G; Table 1). We came across similar differences when assessing the frontal cortex at the same intrauterine age (Figure 2B, B′, G; Table 1).

TABLE 1 Semi-quantitative analysis of CB_1R-expressing fibres in the subventricular and intermediate zones of the developing neocortex in human foetuses

Control subjects			Down syndrome subjects		
Slide No. and age	**Temporal cortex**	**Frontal cortex**	**Slide No. and age**	**Temporal cortex**	**Frontal cortex**
Days 98–120					
4-12-2 day 98, f	++	+	169-09-2 day 99, nn	0	0
240-11-2 day 98, m	++	+	156-11-3 day 102, nn	Not on slide	0
56-11-2 day 105, f	Not on slide	+	73-11-2 day 109, nn	0	+
33-11-3 day 106, f	Not on slide	++	67-09-2 day 111, f	Not on slide	0
178-10-1 day 108, nn	+++	+++	194-09-2 day 112, nn	0	0
104-11-2 day 119, nn	++	0	194-09-3 day 112, nn	0	0
			113-06-2 day 112, m	Not on slide	0
			50-05-2 day 116, f	0	+
			171-07-1 day 119, f	0	Not on slide
Days 121–160					
131-11-2 day 125, f	Not on slide	0	228-07-3 day 128, f	0	+
131-11-3 day 125, f	+	+	66-09-2 day 130, f	0	0
29-12-1 day 131, m	Not on slide	++	4-09-2 day 131, m	Not on slide	++
74-11-2 day 133, nn	0	+	4-09-4 day 131, m	+	+/++
151-11-2 day 136, m	0	0	90-08-2 day 135, f	++	+
151-11-3 day 136, m	++	+++	147-05-2 day 138, m	Not on slide	+
184-10-2 day 137, m	0	0	95-10-1 day 140, m	+++	+++
39-11-2 day 137, f	0	0	118-07-1 I day 145, m	+	+
192-11-2 day 146, m	0	+	118-07-1 II day 145, m	0	++++
149-10-2 day 148, f	0	+	41-11-2 day 151, m	++++	++++
236-11-2 day 149, m	+	0	224-11-2 day 155, f	0	0
127-11-2 day 154, m	0	Not on slide	36-11-3 day 156, m	+	0
216-11-2 day 158, m	0	0	119-04-2 I day 157, m	++	+
128-11-2 day 159, m	0	Not on slide	119-04-2 II day 157, m	+++	+++
Days 173–240					
207-10-1 day 182, m	0	0	47-02-1 day 173, f	0	0
216-09-4 day 194, m	0	0	239-08-4 day 231, m	0	Not on slide
72-09-3 day 197, f	0	0	53-01-1 day 235, m	0	Not on slide
54-10-2 day 235, f	0	0	53-01-2 day 235, m	Not on slide	0
40-11-2 day 242, f	0	0	229-08-1 day 236, m	Not on slide	0
40-11-3 day 242, f	0	Not on slide	229-08-2a day236, m	0	0
			229-08-2b day 236, m	0	0

Cortical differences appeared throughout the areas irrespective of their 'phylogenetic age': Although axons and dendrites were difficult to distinguish, allocortical hippocampi were also rich in fine CB_1R^+ immunoreactive fibres in control subjects during the fourth month of gestation, which contrasted those in Down's syndrome (Figure 3A–A_1'; Table 2). Likewise, processes coursing in the fornix, which likely correspond to hippocampal efferent axons emanating from the subiculum, were CB_1R^+ in control but not in Down's syndrome cases (Figure 3A, A′). Conversely, CB_1R^+ axons invaded the cingulate gyrus (even its dorsal part) in Down's syndrome but not in control foetuses (Figure 3B, B′,E).

Between gestational days 121–160, CB_1Rs were redistributed with remarkable alterations in Down's syndrome foetuses: In the temporal cortex, CB_1R^+ processes first appeared adjacent to the cortical proliferative zone (at the SVZ/IZ boundary) around day 140. This contrasted the weakening expression of CB_1Rs in controls (Figure 2C,C′; Table 1). At this stage, we identified CB_1R^+ fibres at a higher density in Down's syndrome and considered them as ectopic and likely transient, relative to controls (Figure 2C_1–C'_2,H; Table 1). CB_1R^+ immunoreactivity of periventricular processes in Down's syndrome remained greater than those in age-matched controls, at least until day 160 (Figure 2D,D′; Table 2). CB_1R^+ processes

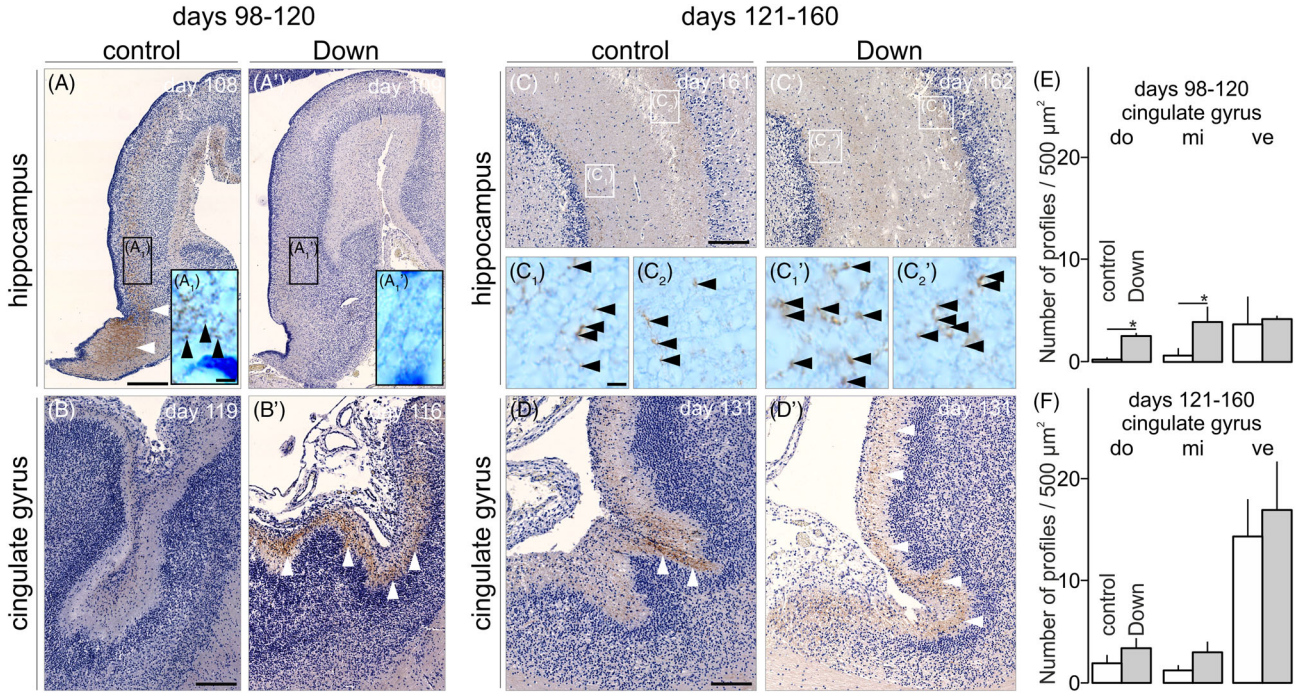

FIGURE 3 Axonal CB_1Rs in the hippocampus in Down's syndrome. Panels A–B′ and C–E' show specimens between days 98–120 and 121–160, respectively. (A–A_1′) In control subjects, hippocampal CB_1R^+ fibres appear in the Ammon's horn (*black arrowheads* in A_1) and in the fornix (*white arrowheads* in A). Poor immunolabelling was noted in Down's syndrome subjects. (B, B′) In the cingulate gyrus, CB_1R^+ fibres appeared in Down's syndrome (*white arrowheads* in E′) but not in control subjects. (C–C_2′) Thin CB_1R^+ fibres and varicosities in both the lacunosomolecular and the pyramidal layers of the hippocampus (*black arrowheads* in C_1, C_2, C_1′ and C_2′ point to immunoreactive terminals). (D, D′) CB_1R^+ fibres invaded the dorsal part of the cingulate gyrus in Down's syndrome but not control foetal brains (*white arrowheads* point to immunoreactive fibres). (E) In the ventral and middle parts of the cingulate gyrus, CB_1R^+ fibre density was higher in Down's syndrome relative to control between days 98 and 120. (F) No significant difference appeared in any of the investigated parts of the cingulate gyrus in Down's syndrome vs. control subjects between days 121 and 160. Abbreviations: CB_1R, cannabinoid receptor type 1; ctrl, control. Scale bars = 1 mm (A–C); 3 µm (A_1, C_1)

often carried pearl-lace-like swellings, which we considered as nascent varicosities instead of mature synapses. We did not detect CB_1R immunoreactivity overlapping with NeuN; instead, we typically observed CB_1R^+ varicosities amongst or around $NeuN^+$ perikarya (Figure 2E–E″), supporting their axonal identity. CB_1R expression and distribution in the frontal cortex did not differ from those in temporal areas (Figure 2F,F′,H; Table 1). In the control hippocampi, CB_1R^+ varicose structures were first seen in the Ammon's horn around day 160 (Figure 3C,C_1,C_2; Table 2) and occurred more often in all developing suprapyramidal layers, including the strata radiatum and lacunosomoleculare, in Down's syndrome cases (Figure 3C,C_1′, C_2′; Table 2). In the cingulate gyrus of control samples, CB_1R^+ fibres were first detected by day 130. However, the immunoreactivity in the equivalent structure of Down's syndrome cases had again greater labelling (Figure 3D,D′,F).

The sex of the embryos had no significant effect on the CB_1R^+ label intensity either in neocortex or in allocortex (temporal cortex: W = 2.05, p = 0.153; frontal cortex: W = 2.81, p = 0.094; fimbriae/fornix: $W_{3,149}$ = 0.002, p = 0.962; pyramidal layer of the hippocampus: W = 2.36, p = 0.127; molecular layer of the hippocampus: W = 0.435, p = 0.509; dentate gyrus: W = 0.83, p = 0.362).

Differences in CB_1R expression during the 3rd trimester

Next, we focused on differences between Down's syndrome and age-matched control subjects during the last trimester of pregnancy. CB_1R^+ processes were not detected in the temporal and frontal cortices of either control or Down's syndrome subjects (Figure 4A–B_1′; Table 1). Instead, CB_1R immunoreactivity appeared in the prospective layer V of the cingulate gyrus, but without a disease-related difference (Figure 4C–C_1′). In the hippocampus, CB_1R^+ profiles populated all subfields of the hippocampal formation (Table 2), including the strata pyramidale and moleculare of the Ammon's horn (Figure 4D–D_2′), at equivalent densities between Down's syndrome and age-matched cases (Table 2). Likewise, CB_1R^+ profiles decorated the indusium griseum, the anterior extension of the hippocampal formation [51], of both control and Down's syndrome subjects (Figure 4F–F_1′).

A notable difference was found in the cerebellar cortex; its molecular layer contained a meshwork of fine-calibre CB_1R^+ processes in Down's syndrome but not in control brains around day 240 (Figure 4E,E′), a difference that existed since gestational days 130–140 (data not shown).

TABLE 2 Semi-quantitative analysis of CB_1R-expressing fibres in the hippocampal formation of human foetuses

Control subjects					Down syndrome subjects				
Slide No. and age	**Fim/for**	**Pyr**	**Mol**	**Dent**	**Slide No. and age**	**Fim/for**	**Pyr**	**Mol**	**Dent**
Days 98–120									
4-12-2 day 98, f	+++	+	0	Not on slide	169-09-2 day 99, nn	0	0	Not on slide	Not on slide
240-11-2 day 101, m	++	0	0	0	156-11-3 day 102, nn	0	Not on slide	Not on slide	Not on slide
56-11-2 day 105, f	+++	Not on slide	Not on slide	Not on slide	73-11-2 day 109, nn	+	0	+	0
33-11-3 day 106, f	+/++	Not on slide	Not on slide	Not on slide	194-09-2 day 112, nn	+	0	+	0
178-10-1 day 108, nn	+++	+	+++	+	194-09-3 day 112, nn	0	0	+	0
104-11-2 day 119, nn	+	+	++	+	113-06-2 day 112, m	0	Not on slide	Not on slide	Not on slide
					50-05-2 day 116, f	+++	+	+++	+
					171-07-1 day 119, f	0	0	+	0
Days 121–160									
131-11-2 day125, f	0	Not on slide	Not on slide	Not on slide	61-12-1 day 126, m	0	+	++	+
131-11-3 day 125, f	0	+	++	+	228-07-3 day 128, f	+	Not on slide	Not on slide	Not on slide
29-12-1 day 131, m	0	Not on slide	Not on slide	Not on slide	66-09-2 day 130, f	0	0	++	0
74-11-2 day 133, nn	0	+	++	+	4-09-2 day 131, m	+	Not on slide	Not on slide	Not on slide
151-11-2 day 136, m	0	0	++	+	4-09-4 day 131, m	++	+	+++	+
151-11-3 day 136, m	+++	++	++++	+++	90-08-2 day 135, f	+	+	+	0
39-11-2 day 137, f	+	++	+++	++	147-05-2 day 138, m	+	Not on slide	Not on slide	Not on slide
192-11-2 day 146, m	+	+	++	++	95-10-1 day 140, m	++	++	+++	++
149-10-2 day 148, f	++	++	+++	+++	118-07-1 I day 145, m	+	++	+++	++
236-11-2 day 149, m	0	+	++	++	118-07-1 II day 145, m	+++	+	++	+
127-11-2 day 154, m	0	Not on slide	Not on slide	Not on slide	41-11-2 day 151, m	++++	+++	++++	++++
216-11-2 day 158, m	+	0	+	+	224-11-2 day 155, f	0	++	++/+++	++
128-11-2 day 159, m	0	Not on slide	Not on slide	Not on slide	36-11-3 day 156, m	0	+	++	+
					119-04-2 I day 157, m	+++	+++	++++	++++
					119-04-2 II day 157, m	+++	+++	++++	++++
					60-05-2 day 158, m	0	+	++	Not on slide

(Continues)

TABLE 2 (Continued)

Control subjects					Down syndrome subjects				
Slide No. and age	**Fim/for**	**Pyr**	**Mol**	**Dent**	**Slide No. and age**	**Fim/for**	**Pyr**	**Mol**	**Dent**
Days 173–240									
207-10-1 day 182, m	+	+/++	++	Not on slide	47-02-1 day 173, f	+	++	+++	++
216-09-4 day 194, m	0	+	+	+	239-08-4 day 231, m	0	++++	+++	++++
72-09-3 day 197, f	+	+++	+++	+++	53-01-1 day 235, m	0	+++	++	+++
54-10-2 day 235, f	0	+	+++	Not on slide	229-08-1 day 236, m	0	Not on slide	Not on slide	Not on slide
40-11-2 day 242, f	0	++++	++++	++++	229-08-2a day 236, m	0	++++	+++	++++
40-11-3 day 242, f	0	++++	+++	++++	229-08-2b day 236, m	0	++++	+++	++++

In sum, our data on human neurodevelopment suggest that CB_1R expression marks delayed axonal development in Down's syndrome, which is mostly overcome by the third trimester when synaptogenesis dominates. Nevertheless, the impaired positioning of CB_1Rs during mid-gestation could imprint long-lasting modifications on neuronal structure and function, thus adversely impacting synaptic plasticity in affected offspring. To experimentally test this hypothesis, we resorted to CB_1R pharmacology in Ts65Dn$^{+/+}$ mice (vs. littermate controls), which represent a tractable genetic model of Down's syndrome [45].

CB_1R stimulation induces SCG10 degradation and tubulin ageing in Ts65Dn$^{+/+}$ neurons

CB_1R stimulation impairs neuritogenesis by inducing an Erk/Jnk1-dependent SCG10 degradation pathway, which coincidentally increases the presence of acetylated tubulin in shortened neurites [18]. This is because SCG10 binds tubulin dimers in a CB_1R-dependent fashion [43] and its degradation increases microtubule stability (termed 'ageing') [18]. Here, we tested the hypothesis that Ts65Dn$^{+/+}$ neurons could have differential responses to agonist stimulation of CB_1Rs, particularly since many duplicated genes in this mouse model affect kinase signalling and protein degradation.

SCG10 accumulated in the perikarya of cultured neurons, with a selective concentration in axonal varicosities, as well as the growth cone in both Ts65Dn$^{+/+}$ and wild-type neurons (Figure 5A′–A_2,B–B_2). SCG10^{+} neurite segments were more proximal to the somata on the Ts65Dn$^{+/+}$ background, as compared to wild-type neurons (Figure 5E; 76.41 ± 3.59% [Ts65Dn] vs. 85.5 ± 2.2% [wild-type], as of total neurite length, $p = 0.02$), confirming differential protein localization under non-stimulated conditions. When exposing neurons to WIN55,212-2 (500 nM) for 30 min [18], we found Ts65Dn$^{+/+}$ neurons to show excess SCG10 degradation, particularly in their distal (motile) neurite segments (Figure 5C′–C_2,D–D_2,E; 52.46 ± 3.85% [Ts65Dn] vs. 90.29 ± 3.1% [wild-type], of total neurite length, $p < 0.01$). Moreover, WIN55,212-2 decreased the relative intensity of distal-most SCG10 immunoreactivity in neurites (as compared to somatic SCG10 intensity) in Ts65Dn$^{+/+}$ (12.78 ± 2.8% [WIN55,212–2] vs. 53.55 ± 7.03% [no treatment], scaled intensity values, $p < 0.01$) but not in wild-type neurons (Figure 5F; 59.75 ± 11.35% [WIN55,212-2] vs. 43.06 ± 5.16% [no treatment], $p = 0.13$). The increased accumulation of acetylated tubulin is often used as a surrogate of excess SCG10 degradation [52]. Indeed, WIN55,212-2 treatment increased tubulin acetylation in Ts65Dn$^{+/+}$ but not control neurons (Figure 5H,H′). Thus, our data suggest neuronal hypersensitivity to CB_1R's stimulation in Ts65Dn$^{+/+}$ mice, whose developmental consequence is slowed neuritogenesis.

Neurons from Ts65Dn mice exhibit slowed CB_1R-dependent neuritogenesis in vitro

The general physiological paradigm for CB_1R-mediated growth responses is that CB_1R stimulation stalls neurite growth in primary cells [53, 54], which can be overcome if agonist stimulation of the CB_1Rs is only brief. The differential expression and distribution of CB_1Rs in Down's syndrome together with the increased sensitivity of the SCG10 pathway to CB_1R stimulation in Ts65Dn$^{+/+}$ mice suggest that disrupted CB_1R functionality, rather than altered localization, could underscore slowed neurite growth. Therefore, and relying on our SCG10 data (see above), we challenged Ts65Dn-derived and wild-type cortical neurons with WIN55,212-2 for 30 min and allowed them to grow for another day. Under control conditions, Ts65Dn$^{+/+}$ neurons grew significantly slower than their wild-type counterparts in vitro (Figure 5A–B_2,G; 54.74 ± 3.56 μm [Ts65Dn] vs. 69.16 ± 4.33 μm [wild-type], $p = 0.02$). Notably, wild-type neurons had slightly, albeit non-significantly, longer neurites on DIV3 (Figure 5G), which we interpreted as relative resistance to the low-dose WIN55,212-2 exposure (30 min). In contrast, WIN55,212-2 occluded neurite outgrowth in Ts65Dn$^{+/+}$ neurons (Figure 5C–D_2,G; 46.3 ± 4.17 μm [Ts65Dn] vs. 82.62 ± 6.66 μm [wild-type], $p < 0.01$). These data suggest that neuritogenesis is per se slowed in Ts65Dn$^{+/+}$

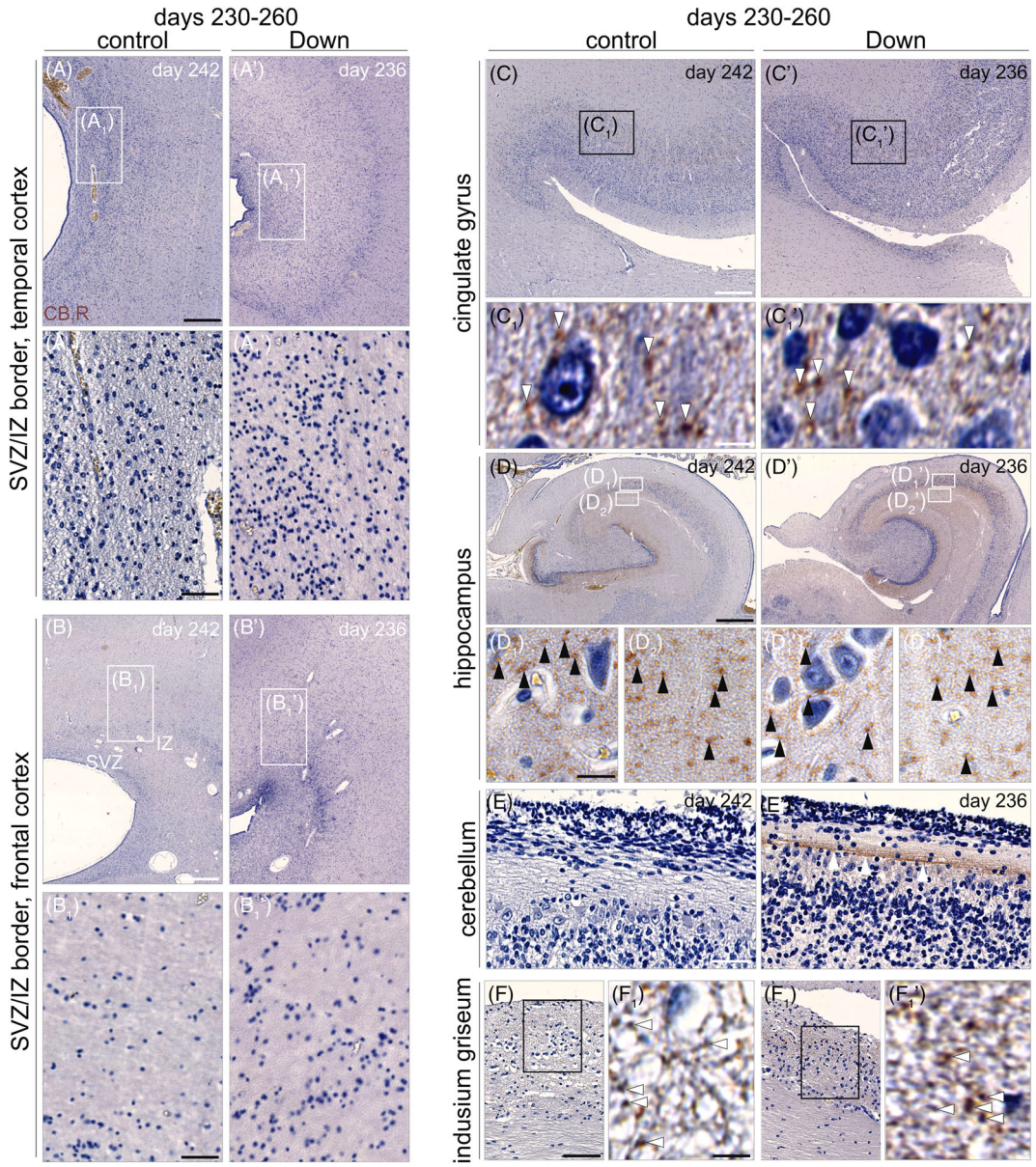

FIGURE 4 CB_1R expression in control and Down's syndrome subjects during the 3rd trimester. (A–A_1') CB_1Rs were absent at the SVZ/IZ boundary in the temporal cortex of both control and Down's syndrome cases. (B–B_1') Similarly, CB_1R^+ processes did not appear in the frontal cortex either. (C–C_1') CB_1R^+ structures (*white arrowheads* in C_1, C_1') in the inner pyramidal layer of the cingulate gyrus. (D–D_2') CB_1R^+ profiles in the strata pyramidale (*black arrowheads* in D_1, D_1') and radiatum (*black arrowheads* in D_2, D_2') of Ammon's horn. (E, E′) CB_1R^+ processes were present in the cerebellar molecular layer in Down's syndrome (*white arrowheads* in E′) but not in control subjects. (F–F_1') CB_1R^+ structures in the indusium griseum. Abbreviations: CB_1R, cannabinoid receptor type; ctrl, control; IZ, intermediate zone; SVZ, subventricular zone. Scale bars = 1 mm (A–D), 300 μm (F); 100 μm (A_1, B_1, E); 5 μm (C_1, D_1, F_1)

neurons and coincides with enhanced sensitivity to agonist-induced CB_1R signalling.

DISCUSSION

Previous studies reported *CNR1*/CB_1R mRNA expression in limbic cortices of the human foetal brains from mid-gestation (weeks 18-22) [55] and proposed vulnerability to exogenous cannabinoids [2]. Autoradiography of foetal brains (19–40 weeks of gestation) demonstrated that CB_1Rs are functional and their expression increases progressively until adulthood [56]. Here, we provide a regional survey of CB_1R-expressing neurites at the light microscopy level spanning the period of the late first trimester (week 14) until birth. We demonstrate that the regional distribution of CB_1Rs follows area-specific temporal scales. Our study employed high-resolution light-and confocal laser scanning microscopy. Unfortunately, the often lengthy *post-mortem* delay and the conditions of

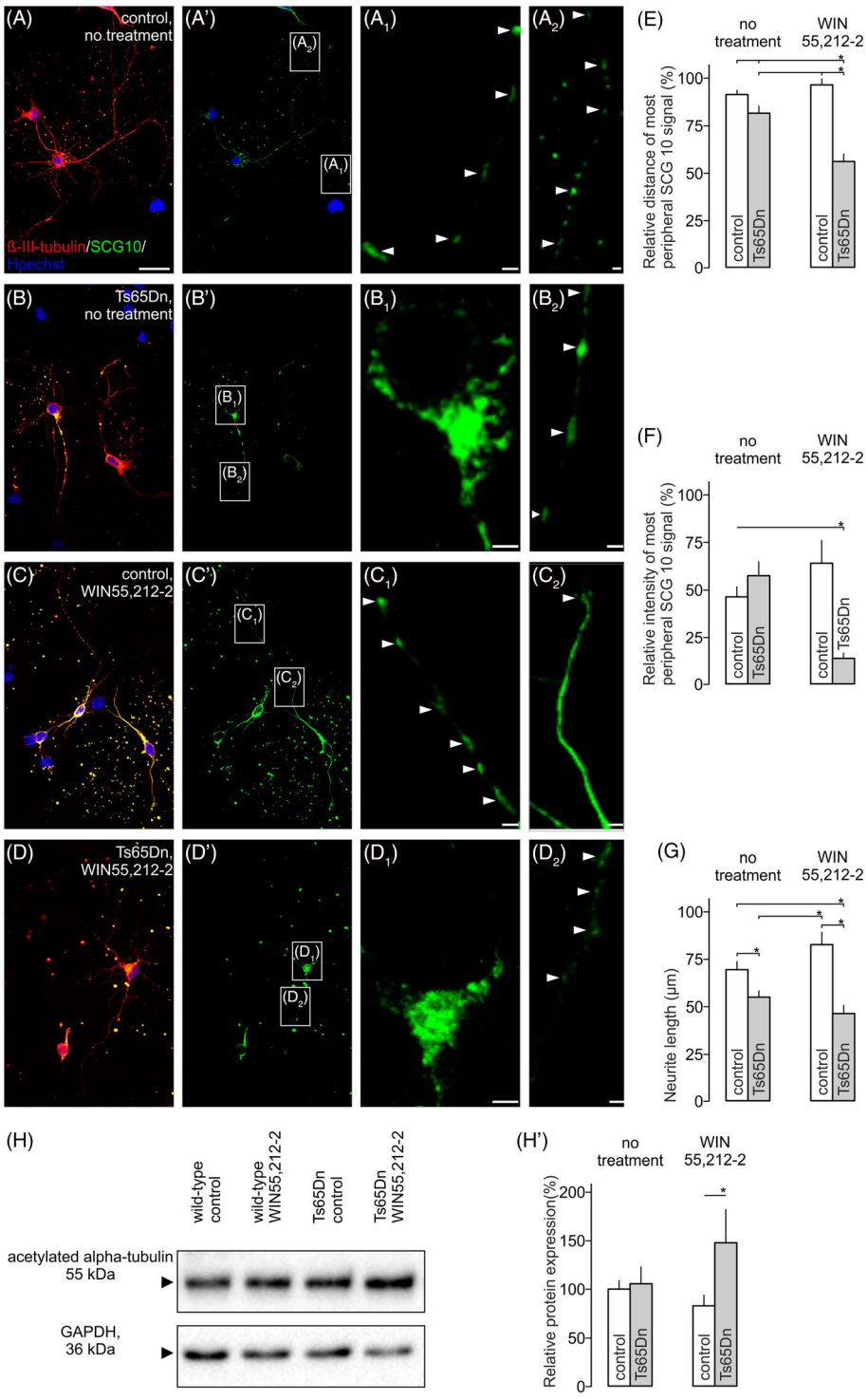

FIGURE 5 Neurons from Ts65Dn$^{+/+}$ mice develop shorter neurites in a CB_1R-dependent fashion in vitro. (A–A_2) Neocortical neurons of control littermate mice. Primary neuronal culture on P2. Arrowheads indicate SCG 10-immunoreactivity in a neurite. (B–B_2) Neocortical neurons of Ts65Dn$^{+/+}$ mice. Primary neuronal culture on P2. Note the somatic accumulation of SCG10 in B_1. Arrowheads in B_2 indicate SCG10 immunoreactivity in a neurite. (C–C_2) WIN55,212-2 increased SCG10 expression (*arrowheads* in C_1; arrowhead in C_2 points to neurite end) in control cultures. (D–D_2) WIN55,212-2 in primary neuronal cultures from Ts65Dn$^{+/+}$ mice reduced SCG10 immunoreactivity in neurites (*arrowheads*). (E) WIN55,212-2 reduced the distance of peripheral SCG10 immunoreactivity. (F) WIN55,212-2 reduced the intensity of peripheral SCG10 immunosignal. (G) Neurons isolated from Ts65Dn$^{+/+}$ mice and cultured in vitro had shorter neurites. (H, H′) WIN55,212-2 increased the expression of acetylated tubulin in neurons from Ts65Dn$^{+/+}$ but not wild-type littermate mice. Abbreviation: ctrl, control. Scale bars = 20 µm (A); 3 µm (B_1, D_1); 2 µm (A_1, A_2, B_2, C_2, D_2)

tissue preservation did not allow for ultrastructural analysis. Therefore, we have not drawn conclusions on, e.g., the subcellular compartmentalization of CB_1Rs, and the number, level of structural maturation, neurochemical identity or the ability of vesicular exocytosis of putative CB_1R^+ synapses. Instead, we referred to 'varicosities', a morphological descriptor purely considering the shape of CB_1R^+ structures. Nevertheless, ultrastructural data from the rodent and primate neocortex revealed CB_1R expression in the somata of neurons radially migrating across the cortical plate [12]. The expression of CB_1R at the early neuroblast phase is relevant to (endo-)cannabinoid-induced nucleokinesis [57], a key step of directional chemotaxis. While we can neither confirm nor exclude the somatic localization and presence of CB_1R-containing intracellular vesicles in the cortex of human foetuses, our imaging data support the conclusion that disproportionately many CB_1Rs reside in neurites to efficiently modulate neuritogenesis.

In contrast to the adult pattern, long-range projection neurons (e.g., cortical pyramidal cells) are the primary source of CB_1Rs in the developing forebrain [14, 58], a finding that corroborates model studies showing that pathfinding decisions and fasciculation steps also rely on CB_1R-mediated signalling events [18, 24, 59]. Due to their vast number and diverse subtypes (including associative, commissural and projection), CB_1R^+ axons were visualised throughout the developing human foetal forebrain. The immunoreactive processes, which were typically positioned as if they were white matter pathways, harboured CB_1R^+ varicosities. Varicose structures were numerous at the SVZ–IZ boundary of all telencephalic areas [60], including both the neocortex and allocortex.

Down's syndrome is characterised by reduced neurogenesis [61, 62], an imbalance of the projection neuron/interneuron ratio, and astrogliosis [63]. The reduced number of dendritic spines and synaptosomal structures reflect defunct morphogenesis [64]. Most of these observations are based on results described in foetal brains from the second trimester. Likely, these changes shall originate from morphogenetic events during the first/early second trimester. Here, we show that the temporal dynamics of CB_1R expression is distinct in Down's syndrome: The appearance of CB_1Rs is delayed, particularly during the early phase of brain development (first/second trimesters), and stays disproportionately high also at foetal periods when CB_1R expression in controls becomes reduced. These pathogenic changes could provoke an imbalance of neurogenesis, radial cell migration [12] and morphogenesis leading to cortical delamination in Down's syndrome. We could not identify a morphological difference of CB_1R^+ profiles in Down's syndrome, supporting that the time factor, but not compartmentalization, is a principal determinant of altered endocannabinoid signalling.

Testing the distribution of CB_1Rs does not equal the study of the entire endocannabinoid system, which includes enzymes, receptor-interacting proteins (like CRIP1a [65]) and putative transporters. Nevertheless, we are confident in our data because human neuropathology studies in congenital neurological and psychiatric conditions (e.g., epilepsy [66, 67], schizophrenia [68], fragile X syndrome [69] and attention-deficit spectrum disorder [70]) highlight that changes in CB_1R distribution faithfully capture the involvement, as well as impairment of the endocannabinoid system in disease pathogenesis. Moreover, a recent study on temporal changes in the expression of $GABA_A$ receptor subunits in utero highlighted that temporal modifications of ionotropic receptor expression that directly gate synaptic neurotransmission are delayed in Down's syndrome [71]. This finding also linked foetal changes in synaptogenesis to excess β-amyloid load in Down's syndrome brains. Therefore, we suggest that altered CB_1R expression might be both a surrogate for impaired neuronal migration/specification and causal to errant synaptic connectivity and plasticity in this devastating disorder.

We propose that Down's syndrome is associated with not only delayed CB_1R expression but also increased CB_1R responsiveness. This hypothesis is based on our in vitro neuropharmacology data from $Ts65Dn^{+/+}$ neurons, which were found to be more sensitive to CB_1R stimulation than their wild-type counterparts. These findings are supported by data showing that CB_1R expression and function are increased in the hippocampus of adult $Ts65Dn^{+/+}$ mice and its pharmacological inhibition restores synaptic plasticity, memory processes and neurogenesis [45]. The novelty of our study derives from showing that increased CB_1R responsiveness persists throughout the lifetime of $Ts65Dn^{+/+}$ neurons, at least in vitro, and is due, at least in part, to the accelerated breakdown of SCG10/stathmin-2, a key component of the microtubule elongation and proofreading machinery in neurites [43]. Of note, reduced *Stmn2*/SCG10 mRNA expression was also reported in neurospheres derived from foetuses with Down's syndrome [42]. Indeed, an increased concentration of acetylated tubulin, a post-translational modification indicative of excess microtubule stability and slowed turnover (i.e., 'ageing') [52], is poised to link CB_1R hypersensitivity-aberrant SCG10 degradation-increased tubulin stability-slowed brain development in foetuses with Down's syndrome [18].

Community-wide genotoxicity studies from the National Survey of Drug Use and Health (2003–2017) and the National Birth Defects Prevention Network demonstrated elevated rates of Down's syndrome in infants prenatally exposed to THC, cannabigerol and cannabichromene, and this association fulfilled formal quantitative criteria of causality [72]. Therefore, we suggest that maternal cannabinoid use during pregnancy could aggravate the genetic penetrance and clinical manifestation of Down's syndrome.

AUTHOR CONTRIBUTIONS

A.A. and T.H. conceived the study. J.H., T.H., G.K. and A.A. designed the experiments. A.A. and T.H. procured the funding. A.P., J.H. and G.Z. performed the experiments and analysed the data. All authors contributed to writing the manuscript and approved its submitted version.

ACKNOWLEDGEMENTS

We thank Dr. Erik Keimpema (Medical University of Vienna, Austria) for helpful discussions and Dr. Ken Mackie (Indiana University, USA) for his gift of the anti-CB_1R antibody.

CONFLICT OF INTEREST STATEMENT

The authors declare no conflict of interest. GK is an executive editor of *Neuropathology and Applied Neurobiology*. The Editors of *Neuropathology and Applied Neurobiology* are committed to peer-review integrity and upholding the highest standards of review. As such, this article was peer-reviewed by independent, anonymous expert referees, and the authors (including GK) had no role in either the editorial decision or the handling of the paper.

DATA AVAILABILITY STATEMENT

The data that support the findings of this study are available from the corresponding author upon reasonable request.

ETHICS STATEMENT

This study was performed according to the Declaration of Helsinki. Analysis was performed according to an approval for histopathology

by the Human Ethical Committee of the Medical University of Vienna (No. 104/2009).

ORCID

Gábor G. Kovács https://orcid.org/0000-0003-3841-5511

PEER REVIEW

The peer review history for this article is available at https://publons.com/publon/10.1111/nan.12887.

REFERENCES

1. Alexandre J, Carmo H, Carvalho F, Silva JP. Synthetic cannabinoids and their impact on neurodevelopmental processes. *Addict Biol*. 2020;25(2):e12824. doi:10.1111/adb.12824
2. Alpar A, di Marzo V, Harkany T. At the tip of an iceberg: prenatal marijuana and its possible relation to neuropsychiatric outcome in the offspring. *Biol Psychiatry*. 2016;79(7):e33-e45. doi:10.1016/j.biopsych.2015.09.009
3. Harkany T, Guzman M, Galve-Roperh I, Berghuis P, Devi LA, Mackie K. The emerging functions of endocannabinoid signaling during CNS development. *Trends Pharmacol Sci*. 2007;28(2):83-92. doi:10.1016/j.tips.2006.12.004
4. Katona I, Sperlágh B, Maglóczky Z, et al. GABAergic interneurons are the targets of cannabinoid actions in the human hippocampus. *Neuroscience*. 2000;100(4):797-804. doi:10.1016/S0306-4522(00)00286-4
5. Katona I, Sperlágh B, Sík A, et al. Presynaptically located CB1 cannabinoid receptors regulate GABA release from axon terminals of specific hippocampal interneurons. *J Neurosci*. 1999;19(11):4544-4558. doi:10.1523/JNEUROSCI.19-11-04544.1999
6. Katona I, Urbán GM, Wallace M, et al. Molecular composition of the endocannabinoid system at glutamatergic synapses. *J Neurosci*. 2006;26(21):5628-5637. doi:10.1523/JNEUROSCI.0309-06.2006
7. Tanimura A, Yamazaki M, Hashimotodani Y, et al. The endocannabinoid 2-arachidonoylglycerol produced by diacylglycerol lipase alpha mediates retrograde suppression of synaptic transmission. *Neuron*. 2010;65(3):320-327. doi:10.1016/j.neuron.2010.01.021
8. Devane WA, Hanus L, Breuer A, et al. Isolation and structure of a brain constituent that binds to the cannabinoid receptor. *Science*. 1992;258(5090):1946-1949. doi:10.1126/science.1470919
9. Walker DJ, Suetterlin P, Reisenberg M, Williams G, Doherty P. Down-regulation of diacylglycerol lipase-alpha during neural stem cell differentiation: identification of elements that regulate transcription. *J Neurosci Res*. 2010;88(4):735-745. doi:10.1002/jnr.22251
10. Diaz-Alonso J, Guzman M, Galve-Roperh I. Endocannabinoids via CB(1) receptors act as neurogenic niche cues during cortical development. *Philos Trans R Soc Lond B Biol Sci*. 2012;367(1607):3229-3241. doi:10.1098/rstb.2011.0385
11. Galve-Roperh I, Chiurchiu V, Diaz-Alonso J, Bari M, Guzman M, Maccarrone M. Cannabinoid receptor signaling in progenitor/stem cell proliferation and differentiation. *Prog Lipid Res*. 2013;52(4):633-650. doi:10.1016/j.plipres.2013.05.004
12. Morozov YM, Mackie K, Rakic P. Cannabinoid type 1 receptor is undetectable in rodent and primate cerebral neural stem cells but participates in radial neuronal migration. *Int J Mol Sci*. 2020;21(22):8657. doi:10.3390/ijms21228657
13. Begbie J, Doherty P, Graham A. Cannabinoid receptor, CB1, expression follows neuronal differentiation in the early chick embryo. *J Anat*. 2004;205(3):213-218. doi:10.1111/j.0021-8782.2004.00325.x
14. Mulder J, Aguado T, Keimpema E, et al. Endocannabinoid signaling controls pyramidal cell specification and long-range axon patterning. *Proc Natl Acad Sci U S a*. 2008;105(25):8760-8765. doi:10.1073/pnas.0803545105
15. Sonego M, Gajendra S, Parsons M, et al. Fascin regulates the migration of subventricular zone-derived neuroblasts in the postnatal brain. *J Neurosci*. 2013;33(30):12171-12185. doi:10.1523/JNEUROSCI.0653-13.2013
16. Keimpema E, Barabas K, Morozov YM, et al. Differential subcellular recruitment of monoacylglycerol lipase generates spatial specificity of 2-arachidonoyl glycerol signaling during axonal pathfinding. *J Neurosci*. 2010;30(42):13992-14007. doi:10.1523/JNEUROSCI.2126-10.2010
17. Keimpema E, Alpar A, Howell F, et al. Diacylglycerol lipase alpha manipulation reveals developmental roles for intercellular endocannabinoid signaling. *Sci Rep*. 2013;3(1):2093. doi:10.1038/srep02093
18. Tortoriello G, Morris CV, Alpár A, et al. Miswiring the brain: Δ9-tetrahydrocannabinol disrupts cortical development by inducing an SCG10/stathmin-2 degradation pathway. *EMBO j*. 2014;33(7):668-685. doi:10.1002/embj.201386035
19. Alpár A, Tortoriello G, Calvigioni D, et al. Endocannabinoids modulate cortical development by configuring Slit2/Robo1 signalling. *Nat Commun*. 2014;5:54421. doi:10.1038/ncomms5421
20. Albarran E, Sun Y, Liu Y, et al. Postsynaptic synucleins mediate vesicular exocytosis of endocannabinoids. *bioRxiv*. 2021;2021. doi:10.1101/2021.10.04.462870
21. Maccarrone M, Guzman M, Mackie K, Doherty P, Harkany T. Programming of neural cells by (endo)cannabinoids: from physiological rules to emerging therapies. *Nat Rev Neurosci*. 2014;15(12):786-801. doi:10.1038/nrn3846
22. Estrada JA, Contreras I. Endocannabinoid receptors in the CNS: potential drug targets for the prevention and treatment of neurologic and psychiatric disorders. *Curr Neuropharmacol*. 2020;18(8):769-787. doi:10.2174/1570159X18666200217140255
23. Herkenham M, Lynn AB, Little MD, et al. Cannabinoid receptor localization in brain. *Proc Natl Acad Sci U S a*. 1990;87(5):1932-1936. doi:10.1073/pnas.87.5.1932
24. Berghuis P, Rajnicek AM, Morozov YM, et al. Hardwiring the brain: endocannabinoids shape neuronal connectivity. *Science*. 2007;316(5828):1212-1216. doi:10.1126/science.1137406
25. Bernard C, Milh M, Morozov YM, Ben-Ari Y, Freund TF, Gozlan H. Altering cannabinoid signaling during development disrupts neuronal activity. *Proc Natl Acad Sci U S a*. 2005;102(26):9388-9393. doi:10.1073/pnas.0409641102
26. Morozov YM, Freund TF. Post-natal development of type 1 cannabinoid receptor immunoreactivity in the rat hippocampus. *Eur J Neurosci*. 2003;18(5):1213-1222. doi:10.1046/j.1460-9568.2003.02852.x
27. Alger BE. Retrograde signaling in the regulation of synaptic transmission: focus on endocannabinoids. *Prog Neurobiol*. 2002;68(4):247-286. doi:10.1016/S0301-0082(02)00080-1
28. Monory K, Polack M, Remus A, Lutz B, Korte M. Cannabinoid CB1 receptor calibrates excitatory synaptic balance in the mouse hippocampus. *J Neurosci*. 2015;35(9):3842-3850. doi:10.1523/JNEUROSCI.3167-14.2015
29. Diaz-Alonso J, Aguado T, Wu CS, et al. The CB(1) cannabinoid receptor drives corticospinal motor neuron differentiation through the Ctip2/Satb2 transcriptional regulation axis. *J Neurosci*. 2012;32(47):16651-16665. doi:10.1523/JNEUROSCI.0681-12.2012
30. Bromberg KD, Ma'ayan A, Neves SR, Iyengar R. Design logic of a cannabinoid receptor signaling network that triggers neurite outgrowth. *Science*. 2008;320(5878):903-909. doi:10.1126/science.1152662
31. Calvigioni D, Hurd YL, Harkany T, Keimpema E. Neuronal substrates and functional consequences of prenatal cannabis exposure. *Eur Child Adolesc Psychiatry*. 2014;23(10):931-941. doi:10.1007/s00787-014-0550-y

32. Nardou R, Ferrari DC, Ben-Ari Y. Mechanisms and effects of seizures in the immature brain. *Semin Fetal Neonatal Med*. 2013;18(4):175-184. doi:10.1016/j.siny.2013.02.003
33. Scheyer AF, Melis M, Trezza V, Manzoni OJJ. Consequences of perinatal cannabis exposure. *Trends Neurosci*. 2019;42(12):871-884. doi:10.1016/j.tins.2019.08.010
34. Neuhofer D, Henstridge CM, Dudok B, et al. Functional and structural deficits at accumbens synapses in a mouse model of fragile X. *Front Cell Neurosci*. 2015;9:100. doi:10.3389/fncel.2015.00100
35. Soltesz I, Alger BE, Kano M, et al. Weeding out bad waves: towards selective cannabinoid circuit control in epilepsy. *Nat Rev Neurosci*. 2015;16(5):264-277. doi:10.1038/nrn3937
36. Heussler H, Cohen J, Silove N, et al. A phase 1/2, open-label assessment of the safety, tolerability, and efficacy of transdermal cannabidiol (ZYN002) for the treatment of pediatric fragile X syndrome. *J Neurodev Disord*. 2019;11(1):16. doi:10.1186/s11689-019-9277-x
37. Gomis-Gonzalez M, Busquets-Garcia A, Matute C, Maldonado R, Mato S, Ozaita A. Possible therapeutic doses of cannabinoid type 1 receptor antagonist reverses key alterations in fragile X syndrome mouse model. *Genes (Basel)*. 2016;7(9). doi:10.3390/genes7090056
38. Dierssen M. Down syndrome: the brain in trisomic mode. *Nat Rev Neurosci*. 2012;13(12):844-858. doi:10.1038/nrn3314
39. Altuna M, Gimenez S, Fortea J. Epilepsy in down syndrome: a highly prevalent comorbidity. *J Clin Med*. 2021;10(13):2776. doi:10.3390/jcm10132776
40. Ross MH, Galaburda AM, Kemper TL. Down's syndrome: is there a decreased population of neurons? *Neurology*. 1984;34(7):909-916. doi:10.1212/wnl.34.7.909
41. Golden JA, Hyman BT. Development of the superior temporal neocortex is anomalous in trisomy 21. *J Neuropathol Exp Neurol*. 1994;53(5):513-520. doi:10.1097/00005072-199409000-00011
42. Bahn S, Mimmack M, Ryan M, et al. Neuronal target genes of the neuron-restrictive silencer factor in neurospheres derived from fetuses with Down's syndrome: a gene expression study. *Lancet*. 2002;359(9303):310-315. doi:10.1016/S0140-6736(02)07497-4
43. Riederer BM, Pellier V, Antonsson B, et al. Regulation of microtubule dynamics by the neuronal growth-associated protein SCG10. *Proc Natl Acad Sci U S a*. 1997;94(2):741-745. doi:10.1073/pnas.94.2.741
44. Reeves RH, Irving NG, Moran TH, et al. A mouse model for Down syndrome exhibits learning and behaviour deficits. *Nat Genet*. 1995;11(2):177-184. doi:10.1038/ng1095-177
45. Navarro-Romero A, Vazquez-Oliver A, Gomis-Gonzalez M, et al. Cannabinoid type-1 receptor blockade restores neurological phenotypes in two models for Down syndrome. *Neurobiol Dis*. 2019;125:92-106. doi:10.1016/j.nbd.2019.01.014
46. Aziz NM, Guedj F, Pennings JLA, et al. Lifespan analysis of brain development, gene expression and behavioral phenotypes in the Ts1Cje, Ts65Dn and Dp(16)1/Yey mouse models of Down syndrome. *Dis Model Mech*. 2018;11(6). doi:10.1242/dmm.031013
47. Diaz-Alonso J, de Salas-Quiroga A, Paraiso-Luna J, et al. Loss of cannabinoid CB1 receptors induces cortical migration malformations and increases seizure susceptibility. *Cereb Cortex*. 2017;27(11):5303-5317. doi:10.1093/cercor/bhw309
48. Pinter A, Hevesi Z, Zahola P, Alpar A, Hanics J. Chondroitin sulfate proteoglycan-5 forms perisynaptic matrix assemblies in the adult rat cortex. *Cell Signal*. 2020;74:109710. doi:10.1016/j.cellsig.2020.109710
49. Keimpema E, Tortoriello G, Alpar A, et al. Nerve growth factor scales endocannabinoid signaling by regulating monoacylglycerol lipase turnover in developing cholinergic neurons. *Proc Natl Acad Sci U S A*. 2013;110(5):1935-1940. doi:10.1073/pnas.1212563110
50. Bradford MM. A rapid and sensitive method for the quantitation of microgram quantities of protein utilizing the principle of protein-dye binding. *Anal Biochem*. 1976;(72):248-254. doi:10.1016/0003-2697(76)90527-3
51. Fuzik J, Rehman S, Girach F, et al. Brain-wide genetic mapping identifies the indusium griseum as a prenatal target of pharmacologically unrelated psychostimulants. *Proc Natl Acad Sci U S a*. 2019;116(51):25958-25967. doi:10.1073/pnas.1904006116
52. Maruta H, Greer K, Rosenbaum JL. The acetylation of alpha-tubulin and its relationship to the assembly and disassembly of microtubules. *J Cell Biol*. 1986;103(2):571-579. doi:10.1083/jcb.103.2.571
53. Jordan JD, He JC, Eungdamrong NJ, et al. Cannabinoid receptor-induced neurite outgrowth is mediated by Rap1 activation through G (alpha)o/i-triggered proteasomal degradation of Rap1GAPII. *J Biol Chem*. 2005;280(12):11413-11421. doi:10.1074/jbc.M411521200
54. He JC, Gomes I, Nguyen T, et al. The G alpha(o/i)-coupled cannabinoid receptor-mediated neurite outgrowth involves Rap regulation of Src and Stat3. *J Biol Chem*. 2005;280(39):33426-33434. doi:10.1074/jbc.M502812200
55. Wang X, Dow-Edwards D, Keller E, Hurd YL. Preferential limbic expression of the cannabinoid receptor mRNA in the human fetal brain. *Neuroscience*. 2003;118(3):681-694. doi:10.1016/S0306-4522(03)00020-4
56. Mato S, del Olmo E, Pazos A. Ontogenetic development of cannabinoid receptor expression and signal transduction functionality in the human brain. *Eur J Neurosci*. 2003;17(9):1747-1754. doi:10.1046/j.1460-9568.2003.02599.x
57. Oudin MJ, Gajendra S, Williams G, Hobbs C, Lalli G, Doherty P. Endocannabinoids regulate the migration of subventricular zone-derived neuroblasts in the postnatal brain. *J Neurosci*. 2011;31(11):4000-4011. doi:10.1523/JNEUROSCI.5483-10.2011
58. Vitalis T, Laine J, Simon A, Roland A, Leterrier C, Lenkei Z. The type 1 cannabinoid receptor is highly expressed in embryonic cortical projection neurons and negatively regulates neurite growth in vitro. *Eur J Neurosci*. 2008;28(9):1705-1718. doi:10.1111/j.1460-9568.2008.06484.x
59. Keimpema E, di Marzo V, Harkany T. Biological basis of cannabinoid medicines. *Science*. 2021;374(6574):1449-1450. doi:10.1126/science.abf6099
60. Molnar Z, Clowry GJ, Sestan N, et al. New insights into the development of the human cerebral cortex. *J Anat*. 2019;235(3):432-451. doi:10.1111/joa.13055
61. Contestabile A, Fila T, Ceccarelli C, et al. Cell cycle alteration and decreased cell proliferation in the hippocampal dentate gyrus and in the neocortical germinal matrix of fetuses with Down syndrome and in Ts65Dn mice. *Hippocampus*. 2007;17(8):665-678. doi:10.1002/hipo.20308
62. Larsen KB, Laursen H, Graem N, Samuelsen GB, Bogdanovic N, Pakkenberg B. Reduced cell number in the neocortical part of the human fetal brain in Down syndrome. *Ann Anat*. 2008;190(5):421-427. doi:10.1016/j.aanat.2008.05.007
63. Stagni F, Giacomini A, Emili M, et al. Subicular hypotrophy in fetuses with Down syndrome and in the Ts65Dn model of Down syndrome. *Brain Pathol*. 2019;29(3):366-379. doi:10.1111/bpa.12663
64. Weitzdoerfer R, Dierssen M, Fountoulakis M, Lubec G. Fetal life in Down syndrome starts with normal neuronal density but impaired dendritic spines and synaptosomal structure. *J Neural Transm Suppl*. 2001;61(61):59-70. doi:10.1007/978-3-7091-6262-0_5
65. Guggenhuber S, Alpar A, Chen R, et al. Cannabinoid receptor-interacting protein Crip1a modulates CB1 receptor signaling in mouse hippocampus. *Brain Struct Funct*. 2016;221(4):2061-2074. doi:10.1007/s00429-015-1027-6
66. Katona I, Freund TF. Endocannabinoid signaling as a synaptic circuit breaker in neurological disease. *Nat Med*. 2008;14(9):923-930. doi:10.1038/nm.f.1869
67. Ludányi A, Erőss L, Czirják S, et al. Downregulation of the CB1 cannabinoid receptor and related molecular elements of the endocannabinoid system in epileptic human hippocampus. *J Neurosci*. 2008;28(12):2976-2990. doi:10.1523/JNEUROSCI.4465-07.2008

68. Murray RM, Englund A, Abi-Dargham A, et al. Cannabis-associated psychosis: neural substrate and clinical impact. *Neuropharmacology*. 2017;124:89-104. doi:10.1016/j.neuropharm.2017.06.018
69. Martin BS, Huntsman MM. Pathological plasticity in fragile X syndrome. *Neural Plast*. 2012;2012:275630. doi:10.1155/2012/275630
70. de Pol M, Kolla NJ. Endocannabinoid markers in autism spectrum disorder: a scoping review of human studies. *Psychiatry Res*. 2021;306:114256. doi:10.1016/j.psychres.2021.114256
71. Milenkovic I, Stojanovic T, Aronica E, et al. GABAA receptor subunit deregulation in the hippocampus of human foetuses with Down syndrome. *Brain Struct Funct*. 2018;223(3):1501-1518. doi:10.1007/s00429-017-1563-3
72. Reece AS, Hulse GK. Epidemiological overview of multidimensional chromosomal and genome toxicity of cannabis exposure in congenital anomalies and cancer development. *Sci Rep*. 2021;11(1):13892. doi:10.1038/s41598-021-93411-5

SUPPORTING INFORMATION

Additional supporting information can be found online in the Supporting Information section at the end of this article.

How to cite this article: Patthy Á, Hanics J, Zachar G, Kovács GG, Harkany T, Alpár A. Regional redistribution of CB1 cannabinoid receptors in human foetal brains with Down's syndrome and their functional modifications in Ts65Dn$^{+/+}$ mice. *Neuropathol Appl Neurobiol*. 2023;49(1):e12887. doi:10.1111/nan.12887